In compliance with the
Canadian Privacy Legislation
some supporting forms
may have been removed from
this dissertation.

While these forms may be included
in the document page count,
their removal does not represent
any loss of content from the dissertation.

Comparison of Methods for Estimating Molecular Weight Distributions of Linear Polymers from Rheological Data.

By

Miguel Baqueiro Avila

Department of Chemical Engineering
McGill University, Montreal
May 2003

A thesis submitted to the Faculty of Graduate Studies and Research in partial fulfillment of the requirements of the degree of Master of Engineering

© Miguel Baqueiro Avila 2003

National Library
of Canada

Acquisitions and
Bibliographic Services

395 Wellington Street
Ottawa ON K1A 0N4
Canada

Bibliothèque nationale
du Canada

Acquisisitons et
services bibliographiques

395, rue Wellington
Ottawa ON K1A 0N4
Canada

Your file Votre référence
ISBN: 0-612-88343-4
Our file Notre référence
ISBN: 0-612-88343-4

The author has granted a non-exclusive licence allowing the National Library of Canada to reproduce, loan, distribute or sell copies of this thesis in microform, paper or electronic formats.

The author retains ownership of the copyright in this thesis. Neither the thesis nor substantial extracts from it may be printed or otherwise reproduced without the author's permission.

L'auteur a accordé une licence non exclusive permettant à la Bibliothèque nationale du Canada de reproduire, prêter, distribuer ou vendre des copies de cette thèse sous la forme de microfiche/film, de reproduction sur papier ou sur format électronique.

L'auteur conserve la propriété du droit d'auteur qui protège cette thèse. Ni la thèse ni des extraits substantiels de celle-ci ne doivent être imprimés ou aturement reproduits sans son autorisation.

Canadä

ABSTRACT

In recent years there have been many reports of methods for inferring the molecular weight distribution (MWD) of linear polymers from either viscosity data or dynamic data. This subject is of great interest in the polymer industry, since MWD affects the processing and final properties of polymers, and gel permeation chromatography (GPC), normally used for determining MWD, has several limitations. There are two main types of method for inferring the MWD from rheological data. The first one involves empirical transformations that lead directly to a MWD, whereas the second type involves the inversion of an integral that gives the relaxation modulus $G(t)$ of a polydisperse polymer in terms of its MWD. A comparison of the reliabilities of these methods for use with samples having a wide variety of polydispersities is lacking, especially for materials with high polydispersities. This study presents a comparison of the MWD predictions of four of these techniques in terms of their performance with groups of HDPEs, LLDPEs and polypropylenes having polydispersities from two to six and various molecular weights. It was found that the viscosity transform (as modified by Wood-Adams) and a modified time-dependent diffusion reptation model proposed by des Cloizeaux (TDD-DR model) are, to a certain extent, satisfactory methods for use with polymers having moderate to high polydispersities, whereas the modulus transform is reliable only for narrow distributions.

RÉSUMÉ

Au cours des dernières années il y a eu plusieurs travaux sur des méthodes pour la détermination de la distribution de masse moléculaire (DMM) de polymères à chaînes linéaires à partir de données de viscosité complexe ou bien de données dynamiques. Ce sujet comporte un grand intérêt pour l'industrie des polymères puisque la DMM affecte directement les étapes de transformation ainsi que les propriétés finales des polymères, et aussi parce que la chromatographie par permeation de gel (CPG), normalement utilisée pour cet objective, comprend plusieurs limitations. Il y a deux types de méthodes pour déduire la DMM à partir de données rhéologiques. La première implique des transformations empiriques qui donnent directement une DMM, tandis que la deuxième implique l'inversion d'une intégrale qui donne le module de relaxation *G(t)* d'un polymère polydisperse en function de sa DMM. Il manque encore une comparaison entre ces méthodes en utilisant les même polymères, afin d'analyser leur performance à hautes polydispersités. Nous présentons cette comparaison de prédictions de DMM en se servant de quatre techniques différentes afin d'évaluer leurs performances pour des séries de polyéthylène haute densité linéaires, polyéthylènes basse densité à chaînes linéaires, et deux polypropylènes avec plusieurs degrés de polydispersité (entre 2 et 6) et poids moléculaire. Nous avons trouvé que la méthode de transformation de viscosité complexe par Shaw (modifiée par Wood-Adams) et le modèle de double reptation et diffusion dépendante du temps propose par des Cloizeaux (TDD-DR) sont, jusqu'à un certain mesure, des méthodes satisfaisantes quand il s'agit de polymères qui possèdent des polydispersités modérées à élevées, tandis que la méthode de transformation du module développée par Tuminello et McGrory et n'est fiable que pour des distributions plutôt étroites.

Acknowledgements

I would like to thank Professor John Dealy for his supervision and for giving me the opportunity to work with him during this project. I also would like to thank Professor Wood-Adams for her unconditional help and assistance and for supplying me with dynamic data for my calculations. I am also grateful to The Dow Chemical Company for supplying the gel permeation chromatography data for the polymers studied in this work.

The support of the rheology group at McGill was also of great help for me, and I would like to thank each and every one of them for offering me their help every time I needed it and for sharing their knowledge in this field with me.

Finally, I would like to thank The National Council of Science and Technology in Mexico (CONACYT) for sponsoring this work.

Table of Contents

Abstract i

Résumé ii

Acknowledgements iii

Table of Contents iv

List of Figures vi

List of Tables viii

Table of Nomenclature ix

1. Introduction 1

    1.1 Molecular Weight Averages and Molecular Weight Distributions 1

    1.2 Linear Viscoelastic Properties of Polymers 3

    1.3 MWD Determination from GPC and from Rheology 5

    1.4 Linear Polyethylenes 7

    1.5 Polypropylene 8

2. Overview of Rheological Methods for Determining MWD 9

    2.1 Empirical Transformations 9

        2.1.1 Viscosity Methods 9

        2.1.2 Empirical Correlations based on the Elastic Modulus 13

    2.2 Modulus Methods 14

        2.2.1 Double Reptation 14

3. Objective of this study 17

4. Experimental Aspects 18

  - 4.1 Experimental Materials 18
  - 4.2 Experimental Methods 18

5. Calculation of Molecular Weight Distributions 20
  - 5.1 Modified Viscosity Transform Method 20
  - 5.2 Modified Modulus Transform 22
  - 5.3 Wasserman's Discrete MWD Method 25
  - 5.4 TDD-DR model using a DGEX function 26
    - 5.4.1 DGEX function and Minimization Technique 27

6. Results and Discussion 30
  - 6.1 Narrow distributions and typical values of M_w 31
  - 6.2 Polymers with high and low molecular weight 40
  - 6.3 Polymers with broad MWD 44

7. Conclusions 57

References 58

Appendix A. Relaxation Functions for Modulus Models 62

Appendix B. Linear Viscoelastic Data 63

Appendix C Gel Permeation Chromatography Data 73

List of Figures

Figure 1.1 MWD for a typical polydisperse polymer 2

Figure 1.2 Dynamic Data for a HDPE at 170°C 5

Figure 1.3 Gel permeation chromatography column 6

Figure 2.1 Viscosity curve for a monodisperse polymer 10

Figure 5.1a G'' fitting for HDL1 to find G_N^0 from Eq.5.11 24

Figure 5.1b G'' fitting for HDL1 to find G_N^0 using a pseudo-Voigt model 24

Figure 6.1 GPC and Viscosity Transform MWD for HDL1 31

Figure 6.2 GPC and Modulus Transform MWD for HDL1 32

Figure 6.3 GPC and Wasserman's MWD for HDL1 32

Figure 6.4 GPC and Viscosity Transform MWD for LDL1 33

Figure 6.5 GPC and Modulus Transform MWD for LDL1 33

Figure 6.6 GPC and Wasserman's MWD for LDL1 34

Figure 6.7 GPC and TDD-DR MWD for HDL1 35

Figure 6.8 Experimental and Predicted Dynamic Data using the TDD-DR model for HDL1 at 150 °C 35

Figure 6.9 Evolution of function evaluations during Nelder-Mead iterations for HDL1 36

Figure 6.10 GPC and TDD-DR MWD for LDL1 37

Figure 6.11 Experimental and Predicted Dynamic Data using the TDD-DR model for LDL1 at 130 °C 37

Figure 6.12 Evolution of the TDD-DR MWD predictions for HDL1 starting from optimized DGEX parameters 39

Figure 6.13 Evolution of the TDD-DR MWD predictions for HDL1 without optimization of initial DGEX parameters 39

Figure 6.14 GPC and Viscosity Transform MWD for HDL2 40

Figure 6.15 GPC and Modulus Transform MWD for HDL2 40

Figure 6.16 GPC and Wasserman's MWD for HDL2 41

Figure 6.17 GPC and TDD-DR MWD for HDL2 41

Figure 6.18 GPC, Viscosity and Modulus Transform MWD for HDL4 42

Figure 6.19 GPC and Wasserman's MWD for HDL4 42

Figure 6.20 GPC and TDD-DR MWD for HDL4 43

Figure 6.21 GPC and Viscosity Transform MWD for LLDPE1 44

Figure 6.22 GPC and Viscosity Transform MWD for LLDPE2 45

Figure 6.23 GPC and Modulus Transform MWD for LLDPE1 45

Figure 6.24 GPC and Modulus Transform MWD for LLDPE2 46

Figure 6.25 GPC and Wasserman's MWD for LLDPE1 46

Figure 6.26 GPC and Wasserman's MWD for LLDPE2 47

Figure 6.27 GPC and TDD-DR MWD for LLDPE1 47

Figure 6.28 Experimental and Predicted Dynamic Data for LLDPE1 at 150 °C using the TDD-DR model 48

Figure 6.29 GPC and TDD-DR MWD for LLDPE2 48

Figure 6.30 Experimental and Predicted Dynamic Data for LLDPE2 at 150 °C using the TDD-DR model 49

Figure 6.31 GPC and Viscosity Transform MWD for PP1 50

Figure 6.32 GPC and Viscosity Transform MWD for PP2 50

Figure 6.33 GPC and Modulus Transform MWD for PP1 51

Figure 6.34 GPC and Modulus Transform MWD for PP2 51

Figure 6.35 GPC and Wasserman's MWD for PP1 52

Figure 6.36 GPC and Wasserman's MWD for PP2 52

Figure 6.37 GPC and TDD-DR MWD for PP1 53

Figure 6.38 GPC and TDD-DR MWD for PP2 53

Figure 6.39 Experimental and Predicted Dynamic Data for PP1 using the TDD-DR model at 180 °C 54

Figure 6.40 Experimental and Predicted Dynamic Data for PP2 using the TDD-DR model at 180 °C 55

Figure 6.41 Evolution of function evaluations during Nelder-Mead iterations for PP2 55

List of Tables

Table 4.1 Characteristics of the polymers studied from GPC 18

Table 6.1 Parameters of materials studied 30

Table 6.2 Plateau Modulus and Sigmoid function parameters 34

Table 6.3 DGEX parameters and Relative Errors on Dynamic Moduli for HDL1 and LDL1 38

Table 6.4 M_w/M_n values for HDL1 and LDL1 38

Table 6.5 M_w/M_n for HDL2 and HDL4 43

Table 6.6 DGEX parameters and Relative Errors on Dynamic Moduli for HDL2 and HDL4 44

Table 6.7 DGEX parameters and Relative Errors on Dynamic Moduli for LLDPE1 and LLDPE2 49

Table 6.8 M_w/M_n for LLDPE1 and LLDPE2 49

Table 6.9 DGEX parameters and Relative Errors on Dynamic Moduli for PP1 and PP2 54

Table 6.10 M_w/M_n for PP1 and PP2 54

Table of Nomenclature

α	exponent in dependence of zero-shear viscosity on molecular weight
β	double reptation exponent
δ	phase shift angle
γ	strain
γ_o	strain amplitude
$\dot{\gamma}$	strain rate
$\dot{\gamma}_s$	critical shear rate for a monodisperse polymer
$\dot{\gamma}_c$	critical shear rate for a polydisperse polymer
η	viscosity
η_o	zero-shear viscosity
$\eta^*(\omega)$	complex viscosity
λ	relaxation time
σ	stress
σ_o	stress amplitude
ν	negative of the power law slope in viscosity curve
$\tau_{rept}(M)$	reptation relaxation time
ω	Frequency
ω_C	critical frequency

F(t,M)	kernel relaxation function
$F_{mono}(t,M)$	relaxation function for a monodisperse polymer
$F_{sr}(t,M)$	simple reptation relaxation function
$G(t)$	relaxation function
$G'(\omega)$	storage modulus
$G''(\omega)$	loss modulus
G_N^o	plateau modulus
$G^*(\omega)$	complex modulus
$H(\lambda)$	relaxation spectrum
K	coefficient in dependence of zero-shear viscosity on molecular weight
K_{TDD}	constant in reptation time dependence in molecular weight
M	molecular weight
M_c	critical molecular weight
M_e	molecular weight between entanglements
M_n	number average molecular weight
M_w	weight average molecular weight
m	reduced molecular weight
PI	polydispersity index
t	time
$w(M)$	weight fraction molecular weight distribution
$w(\log M)$	differential molecular weight distribution
$W(M)$	cumulative molecular weight distribution
$w_{GEX}(\log M)$	GEX molecular weight distribution

1. INTRODUCTION

1.1 Molecular Weight Averages and Molecular Weight Distributions

It is well known that polymers are large molecules made of many repeating units and that a given polymer sample consists of molecules of various sizes and weights. The existence of a fairly broad molecular weight distribution (MWD) in all commercial polymers results from the statistical way polymerization processes occur. Various average molecular weights are used to describe the molecular weight distribution.

If a polymer sample is a mixture of chains having weight fractions w_i and molecular weights M_i, the weight average molecular weight M_w of the sample is defined as:

$$M_w = \frac{\sum M_i w_i}{\sum w_i} \tag{1.1}$$

The number average molecular weight M_n is calculated by counting every molecule in the same way, regardless of its mass. It is thus obtained by dividing the mass of the sample by the number of molecules it contains.

$$M_n = \frac{\sum M_i n_i}{\sum n_i} \tag{1.2}$$

In this equation n_i is the number fraction of molecules having a molecular weight M_i. The number fraction is related to the weight fraction w_i by the expression $n_i = w_i/M_i$, so this average can also be expressed in terms of weight fractions:

$$\frac{1}{M_n} = \sum \frac{w_i}{M_i} \tag{1.3}$$

Since heavier molecules contribute more to M_w that light ones, M_w is always greater than M_n except for a hypothetical monodisperse polymer, in which these two averages are equal. The polydispersity index PI is defined as the ratio of these two averages and it is thus equal to one for a monodisperse polymer and is always greater than one in a polydisperse polymer. This index describes how broad a distribution is and can be as high as 10 or more for commercial polymers. Figure 1.1 shows a molecular weight distribution for a typical polydisperse polymer.

$$PI = \frac{M_w}{M_n} \tag{1.4}$$

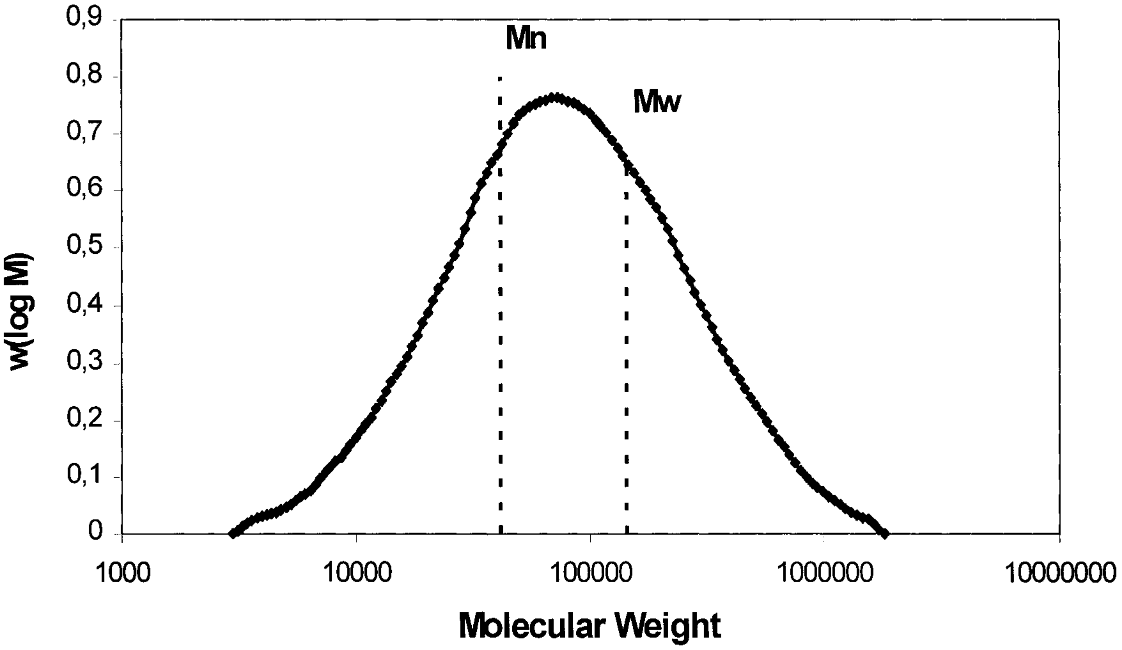

Figure 1.1 MWD for a typical polydisperse polymer

The cumulative molecular weight $W(M)$ is defined as the fraction of molecules with molecular weights less or equal to M.

$$W(M) = \int_0^M w(M')dM' \tag{1.5}$$

A common way to express a MWD is in terms of a differential molecular weight distribution defined as the derivative of the log of *W*(log *M*) with respect to *log M* (Eq.1.6).

$$w(\log M) = \frac{\mathrm{d}W(\log M)}{\mathrm{d}\log M} \tag{1.6}$$

1.2 Linear Viscoelastic Properties of Polymers

Linear viscoelastic (LVE) behavior is observed when the deformation the polymer is subjected to is sufficiently small or slow that the polymer chains are practically undisturbed from their equilibrium state. The relaxation modulus *G(t)* of a melt comes from a stress relaxation experiment. In this experiment a step strain is applied to a sample and the stress response with time is quantified. *G(t)* is then defined as the ratio of the stress response to the strain applied.

$$G(t,\gamma_o) \equiv \sigma(t)/\gamma_o \tag{1.7}$$

If the strain is small enough so that linear behavior is observed, the relaxation modulus is independent of the strain applied, and $G(t) = \sigma(t)/\gamma_o$.

However, the experiment that is most widely used to determine linear viscoelastic properties of melts is small amplitude oscillatory shear. This experiment consists of a sinusoidal shearing deformation so that the strain is given by:

$$\gamma(t) = \gamma_o \sin(\omega t) \tag{1.8}$$

where γ_o is the strain amplitude, and ω is the frequency. If the behavior is linear, i.e., if γ_o is sufficiently small, the stress response to this deformation is also sinusoidal in time and has the same frequency as the strain.

$$\sigma(t) = \sigma_o \sin(\omega t + \delta) \tag{1.9}$$

In Eq.1.9 σ_o is the stress amplitude, and δ is the phase shift between the stress and the strain. It is customary to make use of a trigonometric identity to write the stress as a linear combination of sine and cosine functions, as shown by Eq.1.10.

$$\sigma(t) = \gamma_o[G'(\omega)\sin(\omega t) + G''(\omega)\cos(\omega t)] \tag{1.10}$$

In Eq.1.10, *G'(ω)* and *G''(ω)* are the storage and loss moduli. They represent the elastic energy storage and viscous dissipation respectively. These two properties are functions only of frequency as long as the deformation is in the linear region; otherwise they also depend on the strain amplitude. The relaxation modulus *G(t)* can also be expressed in terms of a relaxation spectrum function *H(λ)*, as shown by Eq.1.11.

$$G(t) = \int_{-\infty}^{+\infty} H(\lambda)\left[\exp\left(-t/\lambda\right)\right]d(\ln\lambda) \tag{1.11}$$

The zero-shear viscosity η_o, an important parameter in several MWD determination methods, can also be calculated if *G(t)* is known:

$$\eta_o = \int_0^{\infty} G(t)dt \tag{1.12}$$

The magnitude of the complex viscosity $\eta*(\omega)$ can be calculated from the storage and loss moduli as shown by Eq.1.13. A typical set of dynamic data is shown in Fig.1.2 for a HDPE sample, using a *log-log* scale.

$$|\eta^*(\omega)| = \frac{\sqrt{G'(\omega) + G''(\omega)}}{\omega} \tag{1.13}$$

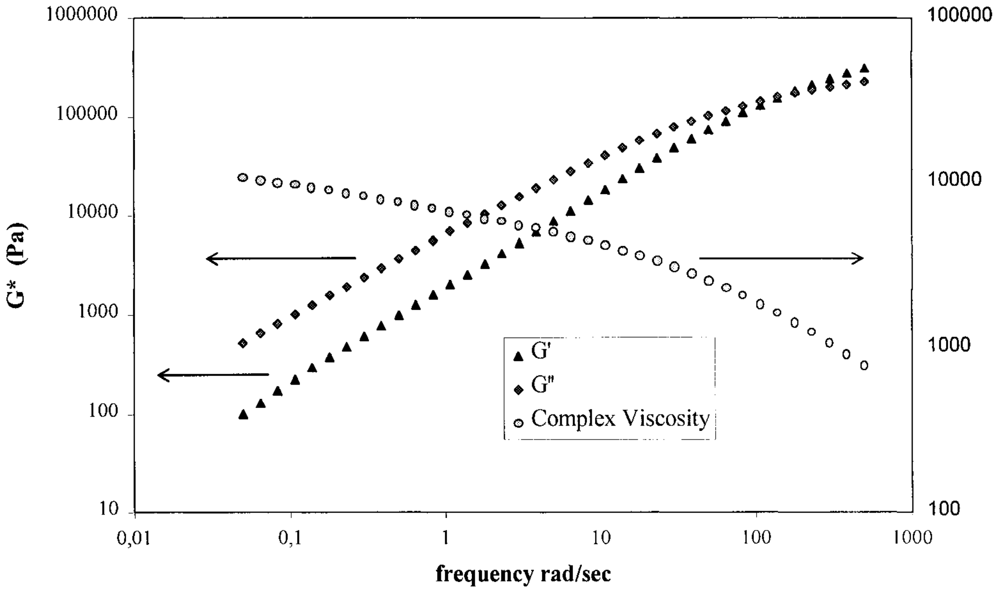

Figure 1.2 Dynamic Data for a HDPE at 170°C

1.3 MWD Determination from GPC and from Rheology

The standard experimental technique for the direct determination of MWD is gel permeation chromatography (GPC), also known as size exclusion chromatography (SEC). In this technique, the polymer is dissolved in an appropriate solvent at low concentrations. This dissolution is made at high temperatures, namely at 150 °C. Then the solution is injected in columns filled with packed organic gels which are semi-porous beads of varying pore sizes (see Fig.1.3). Polymer molecules are fractionated by their hydrodynamic volume (i.e. the sizes of polymer molecules in dilute solution). The smaller molecules are retained for a longer time in the pores than the larger ones which elute more quickly. Detectors which respond to concentration changes, viscosity changes of particle size are located at the outlet of the SEC apparatus. Calibration of retention times and detector response are generally achieved using narrow MWD standards. For linear molecules the molecular weight is proportional to its hydrodynamic volume, therefore GPC results can reflect the MWD of linear polymers.

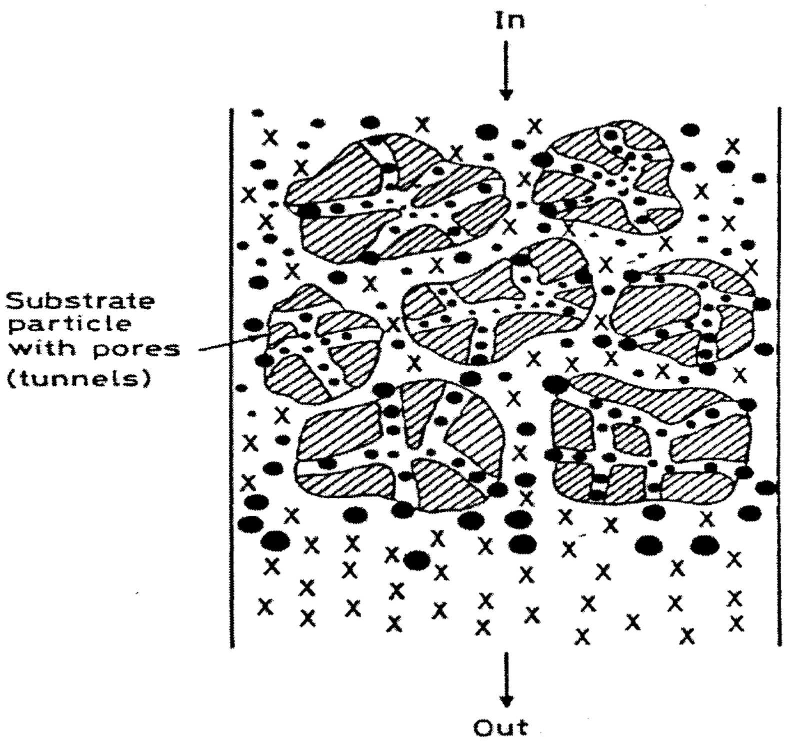

Figure 1.3 Gel permeation chromatography column. The black dots represent polymer molecules and the Xs represent the solvent.

As with any analytical technique, GPC presents a number of disadvantages which should be taken into account. First of all, many commercial polymers do not dissolve very well in the solvents normally used, so that the chromatography column must be operated at higher temperatures, increasing the cost of operation, or is not an option at all. Calibration checks of GPC columns have to be regularly performed because of their continuous degradation. Moreover, GPC tests depend strongly on the skill of the operator, are very time-consuming, and often fail to detect small amounts of high molecular weight polymer which has a very important effect on the rheological properties and processing of a polymer.

Rheological properties of polymers on the other hand are much more sensitive to high molecular weight fractions because of the strong dependency of rheological properties on molecular weight, and are also easier to measure than GPC curves. Rheological techniques are applicable to insoluble polymers, so that no solvent is involved and no solids have to be filtered. This offers the opportunity for real-time, on-line process quality control in industry, and this is not possible for any other analytical technique. However, limitations in the accessible range of shear rate or frequency for some polymers and the nature of computations may introduce some barriers to the applicability of rheological techniques in certain cases.

1.4 Linear Polyethylene

Commercially, polyethylene is produced from ethylene, and until the mid-1950s all commercial polyethylene was produced by a high-pressure process. These materials were somewhat branched materials with moderate number average molecular weights, generally less than 50,000. However, about 1954 two other polymerization processes were developed, one using metal-oxide catalysts (e.g. Phillips process) and the other aluminum alkyl or similar materials (the Ziegler process). By these processes polymers could be prepared at lower temperatures and pressures that contained few, if any, branches. As a result of this linear structure, these polymers had a higher crystallinity and density and were harder and had higher softening points. These materials are known as high-density polyethylenes (HDPE), while the high-pressure materials are known as low-density polyethylenes (LDPE). There are two main classes of HDPE now on the market:

(1) High molecular weight, broad MWD polymer – used primarily for blow molding and pipe.
(2) Low molecular weight, narrow MWD polymer – used widely for injection molding and rotational molding.

High molecular weight components confer impact strength, toughness, stiffness and good environmental stress cracking resistance, while a lower molecular weight reduces the viscosity and thus improves flow behavior.

At the end of the 1970s there was considerable interest in the so-called linear low-density polyethylenes (LLDPE), which are intermediate in properties and structure between the high pressure (LDPE) and the low pressure materials (HDPE). LLDPEs have short branches, produced by including small amounts of propene, but-1-ene, hex-1-ene, or oct-1-ene into the monomer feed. LLDPEs have lower crystallinities than HDPE and have found rapid acceptance because of their high, tensile strength, elongation at break and puncture resistance, as compared to LDPE materials of similar melt flow index and density.

1.5 Polypropylene

Polypropylene is another linear hydrocarbon polymer containing little or no unsaturation. It is therefore not surprising that polypropylene and polyethylene have many similarities in their properties. In spite of the many similarities, however, the presence of methyl groups attached to alternate carbon atoms along the backbone alters the properties of the polymer in a number of ways. For example, it can cause a slight stiffening of the chain and interfere with the molecular symmetry. In the case of the most regular polypropylenes the net effect is a melting point some 50°C higher than that of the most regular polyethylenes. The methyl side groups can also influence some aspects of chemical behavior. For example, the tertiary carbon provides a site for oxidation so that the polymer is less stable than polyethylene to the influences of high temperature and oxygen

2. OVERVIEW OF RHEOLOGICAL METHODS FOR DETERMINING MWD

There are two main types of method for inferring the MWD from rheological data. The first one involves empirical transformations that lead directly to a molecular weight distribution, whereas the second type involves the inversion of an integral that gives the relaxation modulus *G(t)* of a polydisperse polymer in terms of its molecular weight distribution.

2.1 Empirical Transformations

In this category we can distinguish two types: viscosity methods and methods based on the elastic modulus.

2.1.1 Viscosity Methods

Bruce Bersted[2,3] proposed in 1975 a model for calculating the rheological properties of a linear polymer from its MWD. The basic idea was that each size of molecule makes a contribution to the bulk viscosity equal to its zero-shear viscosity, but as the shear-rate increases, the maximum length of molecule that makes such a contribution decreases. This maximum length is called M_c, and all molecules with $M>M_c$ contribute as if they had size M_c. At a given shear rate, M_c is the molecular weight of a monodisperse sample that is just starting to exhibit a decrease in its viscosity below its zero-shear value. Bersted and Slee[4] found that for polystyrene at 190°C this relationship is given by:

$$M_c = 3.5x10^5 \dot{\gamma}^{-0.26} \tag{2.1}$$

The zero-shear viscosity is assumed to be related to the molecular weight of a monodisperse polymer as follows:

$$\eta_o = K(T)M^\alpha \tag{2.2}$$

This relationship is generally assumed to be valid for a polydisperse system if M is replaced by M_w. Thus, for a blend the zero-shear viscosity is given by the following mixing rule:

$$\eta_{o,blend} = K(T)M_w^{\alpha} = \left(\sum w_i \eta_{o,i}^{1/\alpha}\right)^{\alpha} \qquad (2.3)$$

In Eq.2.3, w_i is the weight fraction of component i, and $\eta_{o,i}$ is the zero-shear viscosity of the corresponding monodisperse polymer. The exponent α is associated with the dependence of the zero-shear viscosity on the weight average molecular weight and independent of temperature. The constant K has a fixed value for a particular polymer at a given temperature.

Malkin and Teishev[20,21] developed an analytical method using this mixing rule. They proposed that the viscosity curve of a monodisperse polymer be represented as two straight-line segments on a *log-log* plot, as shown in Fig 2.1 and Eq.2.4.

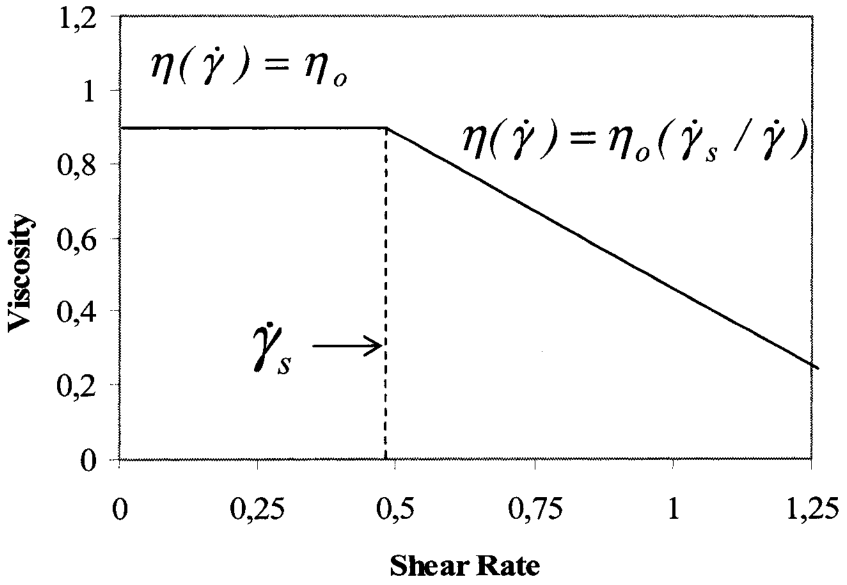

Figure 2.1 Viscosity curve for a monodisperse polymer (log-log scale)

$$\begin{array}{ll} \eta(\dot{\gamma}) = \eta_o & \dot{\gamma} \le \dot{\gamma}_s \\ \eta(\dot{\gamma}) = \eta_o(\dot{\gamma}_s / \dot{\gamma}) & \dot{\gamma} > \dot{\gamma}_s \end{array} \tag{2.4}$$

where $\dot{\gamma}_s = \dot{\gamma}_s(M)$ is the critical shear rate separating the constant viscosity range from the power law regions for a monodisperse polymer. The corresponding expression for the viscosity of a blend of M_1 and M_2, with $M_1 > M_2$ is then:

$$\begin{array}{ll} \eta(\dot{\gamma}) = \eta_{0,blend} & \dot{\gamma} \le \dot{\gamma}_s(M_1) \\ \eta(\dot{\gamma}) = \left\{ w_1 \left[\eta_0(M_1) \dfrac{\dot{\gamma}_s(M_1)}{\dot{\gamma}} \right]^{1/\alpha} + w_2 \left[\eta_0(M_2) \right]^{1/\alpha} \right\}^{\alpha} & \dot{\gamma}_s(M_1) < \dot{\gamma} \le \dot{\gamma}_s(M_2) \\ \eta(\dot{\gamma}) = \eta_0(M_2) \dot{\gamma}_s(M_2) / \dot{\gamma} & \dot{\gamma} > \dot{\gamma}_s(M_2) \end{array} \tag{2.5}$$

Equation 2.5 can be generalized for a continuous distribution of molecular weights to give:

$$\eta(\dot{\gamma}) = \left[\int_0^{M(\dot{\gamma})} \left[\eta_0(M) \right]^{1/\alpha} w(M) dM + \left[\eta_0(M_w) \frac{\dot{\gamma}_c(M_w)}{\dot{\gamma}} \right]^{1/\alpha} \int_{M(\dot{\gamma})}^{\infty} w(M) dM \right]^{\alpha} \tag{2.6}$$

where:

$$M(\dot{\gamma}) = M_w \left(\frac{\dot{\gamma}_c}{\dot{\gamma}} \right)^{1/\alpha} \tag{2.7}$$

In Eq.2.6, *w(M)* is the weight fraction MWD function, and $\dot{\gamma}_c$ is the value of $\dot{\gamma}_s$ for the polydisperse system when extrapolating the straight lines resulting from the power law region and the plateau region. In the limit of very high shear rate the viscosity obeys a power law with slope $-\nu$:

$$\eta(\dot{\gamma}) = \eta_0 \left(\frac{\dot{\gamma}}{\dot{\gamma}_c} \right)^{-v} \qquad (2.8)$$

Malkin and Teishev[20,21] defined dimensionless variables as follows:

$$Y \equiv \left(\eta / \eta_0 \right)^{1/\alpha} \qquad (2.9)$$

$$X \equiv \left(\dot{\gamma} / \dot{\gamma}_c \right)^{v/\alpha} = 1/m \qquad (2.10)$$

$$m \equiv m(\dot{\gamma}) \equiv M(\dot{\gamma}) / M_w = \left(\dot{\gamma}_c / \dot{\gamma} \right)^{v/\alpha} \qquad (2.11)$$

They also generated a solution for *w(M)* by substituting these dimensionless variables in Eq.2.6, and used differential calculus to obtain Eq.2.12.

$$w(m) = -\frac{1}{m^2 v^2} \left(\frac{\eta}{\eta_0} \right)^{1/\alpha} \left[\alpha \frac{\mathrm{d}^2 \ln \eta}{\mathrm{d} \ln \dot{\gamma}^2} + v \frac{d \ln \eta}{\mathrm{d} \ln \dot{\gamma}} + \left(\frac{\mathrm{d} \ln \eta}{d \ln \dot{\gamma}} \right)^2 \right] \qquad (2.12)$$

In Eq.2.12, each point on the viscosity curve corresponds to a relative molecular weight *m*, and *w(m)* is the reduced weight fraction MWD function. The cumulative molecular weight distribution is given by Eq.2.13.

$$F(m) = \int_0^m w(m) dm = 1 + \frac{1}{v} \left\{ \left[\frac{\eta(\dot{\gamma})}{\eta_0} \right]^{1/\alpha} \left(\frac{\dot{\gamma}}{\dot{\gamma}_c} \right)^{v/\alpha} \left(\frac{d \ln \eta}{d \ln \dot{\gamma}} \right) \right\} \qquad (2.13)$$

This original viscosity transform developed by Shaw and Tuminello[26] was modified by Wood-Adams[31] and was one of the methods chosen for this study. Unless we have specific data about the polymer studied, α is taken as 3.4[32]. Wood-Adams and Dealy[32] found that $\nu=1$ gave the best agreement with GPC results. The Cox-Merz rule states that curves of $\eta(\dot{\gamma})$ are often nearly identical to curves of complex viscosity $|\eta^*|$ versus frequency[7]. This is a very useful relationship, since it is easier to determine $|\eta^*|$ over a wide range of frequencies than it is to determine $\eta(\dot{\gamma})$ over a wide range of shear rates.

2.1.2 Empirical Correlations based on the elastic modulus

Several researchers have found similarities between dynamic modulus curves and cumulative molecular weight distributions (CMWD). Wu[35] noted a similarity between the curve of $[G'(\omega)/G_N^o]$ versus ω and that of the CMWD in the plateau and terminal zones for a series of monodisperse and polydisperse polystyrenes. While good results were obtained for polydisperse systems, the method did not predict very well bimodal distributions. Tuminello[27] found the CMWD to be similar to a plot of $[G'(\omega)/G_N^0]^{0.5}$ versus frequency in the plateau and terminal regions, explaining that all chains that have relaxed at a certain frequency will act as a non-entangling solvent for all the longer chains that are unrelaxed. He also assumed that each molecular weight fraction of molecular weight M_i has a single relaxation frequency ω_i, below which it makes no contribution to the modulus. Since the plateau modulus is known to decrease with the square of polymer concentration in concentrated solutions, the weight fraction of unrelaxed chains can be represented by

$$W_U = [G'(\omega)/G_N^0]^{0.5} \tag{2.14}$$

Tuminello further assumed that the frequency at which a chain undergoes a terminal zone relaxation is related to the molecular weight of that chain by:

$$\frac{1}{\omega} \propto MW_{3.4} \tag{2.15}$$

Therefore, plotting $1-[G'(\omega)/G_N^0]^{0.5}$ versus frequency should give a good estimate of the CMWD. For polystyrene samples, again bimodal distributions were not well described. McGrory and Tuminello[22] demonstrated that a reasonable approximation to the MWD can be obtained using *G(t)* data in the terminal relaxation zone. They assumed that ω is equivalent to *1/t*, and plotted $[G(t)/G_N^o]^{0.5}$ versus *log(1/ t)*. Using polystyrene samples, the shape of the distributions predicted are similar to SEC results for broad distribution polymers and for those with bimodal distributions, but false bimodal distributions are obtained for nearly monodisperse samples.

2.2 Modulus Methods

2.2.1 Double Reptation

For a monodisperse polymer at a given temperature, in the plateau and terminal zones the relaxation modulus *G(t)* can be represented as:

$$G(t) = G_N^o F(t, M) \tag{2.16}$$

where *F(t,M)* is a kernel relaxation function and G_N^o is the plateau modulus, which does not depend on the molecular weight. For a polydisperse polymer, the Doi-Edwards tube model can be extended by use of a linear mixing rule according to which each molecular weight makes its independent contribution to the overall relaxation process, as shown by Eq.2.17.

$$G(t) = G_N^o \int_{M_e}^{\infty} w(M)F(t,M)dM = G_N^o \int_{\ln M_e}^{\infty} w(\ln M)F(t,M)d\ln M \tag{2.17}$$

Here M_e is the molecular weight between entanglements. However, Eq.2.17 is not correct for a polydisperse system, since some of the molecules making up the tube have a much lower MW than the longest molecules in the system, thereby changing the identity of the tube during the relaxation process (tube renewal). The double reptation (both the chain and dynamical constraints are allowed to reptate while the chain keeps its identity) modification of the Doi-Edwards theory suggests that the modulus can be represented by:

$$\frac{G(t)}{G_N^o} = \left(\int_{\ln M_e}^{\infty} w(M) F^{1/2}(t, M) d \ln M \right)^2 \tag{2.18}$$

If *G(t)* were known and the integral could be inverted, the molecular weight distribution could be determined. However, to accomplish this:

1. The relaxation modulus, once obtained experimentally, must be fitted to an equation.
2. The relaxation function for monodisperse material, *F(t,M),* must be specified (see Appendix A).

Equation 2.18 is of a form that often arises in applied physics and is called a Fredholm integral equation of the first kind. It is an example of an ill-posed problem, which means that it is necessary to incorporate additional information in order to invert the integral. For this case, random errors or incompleteness in the *G(t)* data result in a system that has no unique solution for *w(M)*.

Mead[23] used a step function for *F(t,M)* in Eq.2.18 and found an analytical solution to the inversion problem that provided a fair first estimate for a continuous MWD. He then used a single exponential function and advanced mathematical transformations to deal with the integral inversion problem using a software called CONTIN, designed specifically to address such problems, to obtain a solution.

Wasserman[30] also proposed a method based on the double reptation model, but instead of solving the integral he used discrete variables and solved using linear regression with regularization. For commercial polystyrenes of moderate polydispersity (M_w/M_n from 2 to 4), the rheological MWD agreed well with the MWD from SEC. Leonardi *et al*[17], proposed a method that incorporates a detailed modeling of all the relevant relaxation processes, including Rouse fast and longitudinal modes and glassy relaxation. To invert the relaxation modulus they assumed that a GEX function can describe a MWD. Although they demonstrated that tube length fluctuations and tube renewal have important effects on the quality of the MWD, good results were not obtained for HDPE samples.

Ruymbeke *et al*[28], addressed the direct problem of predicting the linear viscoelastic response of polymers from their MWD using a suitable model also inspired by reptation theory. They found that a modified time-dependent diffusion reptation model proposed by des Cloizeaux is capable of quantitative predictions. They used this modified des Cloizeaux model to address the inverse problem, but instead of using a GEX function to describe the MWD, they use a double GEX (DGEX) function. In particular, this methodology was able to resolve small amounts of short chains in bimodal blends containing large amounts of long chains. Good predictions were obtained for PS and PC samples. For HDPE samples, the quality of the DGEX inverse predictions was satisfactory.

3. OBJECTIVE OF THIS STUDY

The objective of this project was to compare the predictions of several rheological techniques for obtaining molecular weight distributions with distributions determined by GPC. The polymers used in the comparison were linear polyethylenes and polypropylenes having polydispersities in the range of two to six and varying weight average molecular weights.

The methods compared were:

1. Modified viscosity transform
2. Modified modulus transform
3. Wasserman's discrete MWD Approach
4. Double reptation time-dependent diffusion model.

4. EXPERIMENTAL ASPECTS

4.1 Experimental Materials

To meet the objective of this project, linear polymers with narrow and broad molecular weight distributions and varying weight average molecular weights were chosen for comparison. The materials selected make up three groups. The first one includes 2 traditional linear low-density polyethylenes and 2 polypropylenes, all with broad MWDs; the second one includes two metallocene HDPEs with very high and very low $M_{w,}$ both with narrow distributions, and the third group consists of one mLDPE and one mHDPE, all with narrow distributions and typical values of M_w. Key parameters of these polymers are shown in Table 4.1. The samples and the data in Table 4.1 were provided by The Dow Chemical Company. Molecular weight distributions were determined by gel permeation chromatography.

Table 4.1 Characteristics of the polymers studied from GPC

Resin	M_w	M_w/M_n
LLDPE1	158 000	4.54
LLDPE2	145 500	3.5
PP1	184 000	3.6
PP2	366 000	6.43
HDL2	41 900	1.90
HDL4	359 000	2.08
LDL1	118 400	2.30
HDL1	100 900	2.08

4.2 Experimental Methods

Dynamic viscosity data for all the polyethylenes included in this study were collected using a Rheometrics Dynamic Analizer II (RDA II), which is a controlled strain instrument. Parallel plate fixtures with a 25-*mm* diameter were used with a gap of 1 *mm*. This instrument has a spring torque transducer with a range of 2-2000 *gmf cm*, and a torque level above 5 *gmf cm* was assumed to be reliable. The viscosity plateau region was reached within this torque range so that the use of a more precise rheometer was not necessary. Experiments were conducted under a nitrogen atmosphere to prevent degradation, and resin stability under testing conditions was verified. Strain sweeps were performed to establish the limiting strain for linear behavior at each frequency. Finally, frequency sweeps were carried out as explained to obtain the rheological data required [33]. The experimental temperature was 150°C for all the polyethylene samples except LDL1, for which the experimental temperature was 130°C.

Linear viscoelastic measurements for polypropylene samples PP1 and PP2 were performed using a Rheometric Scientific *SR 5000* stress controlled rheometer with 25-mm parallel plates and a gap between plates of 1 mm. The stress is applied by means of a torque head, the shaft of which is positioned by a precision air bearing. Calculation of material properties is performed by analysis of is the applied stress and the measured strain. The torque range is 0.01 to 500 *gmf cm*, small enough to reach the viscosity plateau region, and the angular resolution of the rotary encoder is 4.2 *μrad.* The experimental temperature for compression molding and dynamic experiments is restricted from below by the melting point and from above by the thermal stability of the polymer. The temperature used for the polypropylene samples was 180°C. Details of the experimental procedures for these polypropylenes can be found in reference 12.

5. CALCULATION OF MOLECULAR WEIGHT DISTRIBUTIONS

5.1. Modified Viscosity Transform Method

Shaw and Tuminello[26] developed a numerical approach for inferring MWDs from shear or complex viscosity data using an equation proposed by Malkin and Teishev (Eq.2.12 in section 2.1.1) and calculating numerically the values of the derivatives and the final distribution function. This equation, which relates viscosity data $\eta(\dot{\gamma})$ or complex viscosity data $\eta^*(\omega)$ to the MWD is given by Eq.5.1, where *w(log m),* the differential MWD, is obtained by taking the derivative of Eq.2.13 with respect to *log m.*

$$w(\log m) = \left[\frac{-\ln(10)}{m v^2}\right]\left[\frac{\eta}{\eta_0}\right]^{1/\alpha}\left[\alpha\frac{d^2\ln\eta}{d\ln\omega^2} + v\frac{d\ln\eta}{d\ln\omega} + \left(\frac{d\ln\eta}{d\ln\omega}\right)^2\right] \tag{5.1}$$

In this equation, each molecular weight m is associated with a frequency as follows:

$$\omega = \omega_c m^{-\alpha/v} \tag{5.2}$$

For commercial polymers, data often do not extend into the Newtonian and power law regions, so that extrapolation at both ends is necessary before calculating the derivatives and the distribution function. All calculations, including the extrapolations at the ends, determination of the first and second derivatives, and prediction of the MWD function, were performed using a spreadsheet in Excel. The Vinogradov fluidity model was used to extrapolate at high frequencies[31] Since the slope value is established as -1 as mentioned in section 2.1.1, a sufficient number of points has to be taken into account in the model so that the slope at the high frequency end is actually -1.

$$\frac{\eta_o}{\eta^*} = \sum_{i=1}^{N} A_i \omega^{iv/N} \tag{5.3}$$

According to Wood-Adams and Dealy[32], the most important portions of the viscosity curve are those where changes in shape occur, so that maxima or minima in the second derivative are related to peaks or shoulders in the MWD. In particular, the global minimum in the second derivative is responsible for the main peak in the MWD, and other minima and maxima correspond to shoulders or secondary peaks in the distribution. Therefore, it is essential to have data around this global minimum to guarantee that the main peak will be placed correctly, and a plot of the second derivative versus frequency is useful for this purpose.

In order to extrapolate at the low frequency end, the relaxation spectrum $H(\lambda)$ was calculated from the dynamic data $G'(\omega)$ and $G''(\omega)$ based on a regularization technique developed by Honerkamp and Weese[13]. The number of relaxation times for $H(\lambda)$ was set to 40 for all the samples studied. Once the relaxation spectrum was found, the loss and storage moduli were calculated using Eqs.5.4 and 5.5, and from these the complex viscosity was calculated using Eq.1.13 of section 1.2.

$$G'(\omega) = \int_{-\infty}^{\infty} \left[H(\lambda) \frac{\omega^2 \lambda^2}{\left(1 + \omega^2 \lambda^2\right)} \right] d(\ln \lambda) \tag{5.4}$$

$$G''(\omega) = \int_{-\infty}^{\infty} \left[H(\lambda) \frac{\omega \lambda}{\left(1 + \omega^2 \lambda^2\right)} \right] d(\ln \lambda) \tag{5.5}$$

The relaxation modulus $G(t)$ was also calculated from the relaxation spectrum by use of Eq.1.11 of section 1.2. Once $G(t)$ was calculated, the zero-shear viscosity was found by integration of the relaxation modulus according to Eq.1.12 of section 1.2.

Linear regression was performed on the last 10 pairs of points on the curve of natural log of frequency versus natural log of viscosity. The slope value should be equal to the power-law slope, which is -1. The intercept was then used in Eq.5.6 to calculate the critical frequency ω_c. Finally, the polydispersity index was calculated by means of Eq.5.7

$$\omega_c = Exp\left[\frac{\ln(\eta_0) - Intercept}{Slope}\right] \tag{5.6}$$

$$\frac{M_w}{M_n} = \sum_{i=1}^{N-1} \frac{\left(\frac{w(\log m_i)}{\ln(10)m_i}\right) + \left(\frac{w(\log m_{i+1})}{\ln(10)m_{i+1}}\right)}{m_i + m_{i+1}}(m_i - m_{i+1}) \tag{5.7}$$

5.2 Modified Modulus Transform

In the method of Tuminello and McGrory[22] the *G(t)* function is transformed into *G'(ω)*, assuming equivalency between *1/t* and *ω*. The simplest transposition is to assume that *G'(ω)* is equivalent to *G(t)* plotted versus *1/t*. A plot of $1-\left[G(t)/G_N^0\right]^{0.5}$ versus *log(1/t)* is then transformed to a cumulative MWD using Eqs.2.14 and 2.15 with *ω* replaced by *1/t*. The following limitations apply to this procedure: the chains must be linear; the polymer must be in the melt state; and all chains must have molecular weights greater than the critical value M_c ($M_c=2M_e$). Values of *G(t)* are calculated from the relaxation spectrum using Eq.1.11, which is found as described in the previous section. The range of times used corresponds to the range of frequencies in the experimental dynamic data.

In the original technique, the hyperbolic tangent expression of Eq.5.8 was fitted to the $\left[G(t)/G_N^0\right]^{0.5}$ data to both resolve the terminal relaxation region and smooth the data[22].

$$F(X) = \left[\frac{G(t)}{G_N^0}\right]^{0.5} = \sum_{i=1}^{n}\left(\frac{A_i}{2}\right)\{1 + \tanh[B_i(X + C_i)]\} \tag{5.8}$$

Here, $\sum A_i = 1$, B_i is a parameter controlling curve breadth, C_i locates the curve on the *log(1/t)* axis, *X=log(1/t)*, and *n* is taken as 2. It was found, however, that for the polymers considered in this study this model was not able to fit the data, especially at long times, and this portion of the data is essential in the MWD calculation, since it corresponds to the high molecular weight part. A sigmoid function with 5 parameters was found to be more suitable for this fitting (Eq.5.9). This model was also used for the extrapolation at both ends. Using an arbitrary constant of proportionality in Eq.2.15 and scaling the absolute molecular weights to the zero-shear viscosity (Eq.2.3), the MWD was determined.

$$F(X) = y_o + \frac{a}{\left[1 + \exp\left(-\left(\frac{x - x_o}{b}\right)\right)\right]^c} \tag{5.9}$$

An important parameter in this method is the plateau modulus G_N^o. Since polydisperse materials do not exhibit a plateau in the storage modulus curve, a value of G_N^o was calculated using Eq.5.10 [10].

$$G_N^0 = \frac{4.61}{\pi} \int_{-\infty}^{+\infty} G'' d \ln \omega \tag{5.10}$$

In order to use Eq.5.10, the loss modulus must be extrapolated to $\ln\omega = \pm\infty$. For this extrapolation Tuminello and McGrory[22] used Eq.5.11, where I_i, H_i and X_{oi} are adjustable parameters. For the polymers studied here, this model lacked accuracy at high frequencies as shown in Fig.5.1a. A pseudo-Voigt function with 4 parameters (Eq.5.12) was found to provide a more accurate fitting of the loss modulus data at high frequencies, and this results in a much better estimation of the plateau modulus, as can be seen in Fig.5.1b. In Eq.5.12 $x = \log\omega$ and $y = G''(\omega)$, and a, b, c, and x_o are adjustable parameters.

$$\begin{aligned} G''(X) &= \sum_{i=1}^{2} \frac{I_i}{\left[1 + 4Z_i^2\left(2^{1/m} - 1\right)\right]^m} \\ X &= \log\omega \\ Z_i &= \frac{X - X_{oi}}{H_i} \\ m &= 20 \end{aligned} \tag{5.11}$$

$$y = a\left[c\left[\frac{1}{1+\left(\frac{x-x_o}{b}\right)^2}\right] + (1-c)e^{-0.5\left(\frac{x-x_o}{b}\right)^2}\right] \qquad (5.12)$$

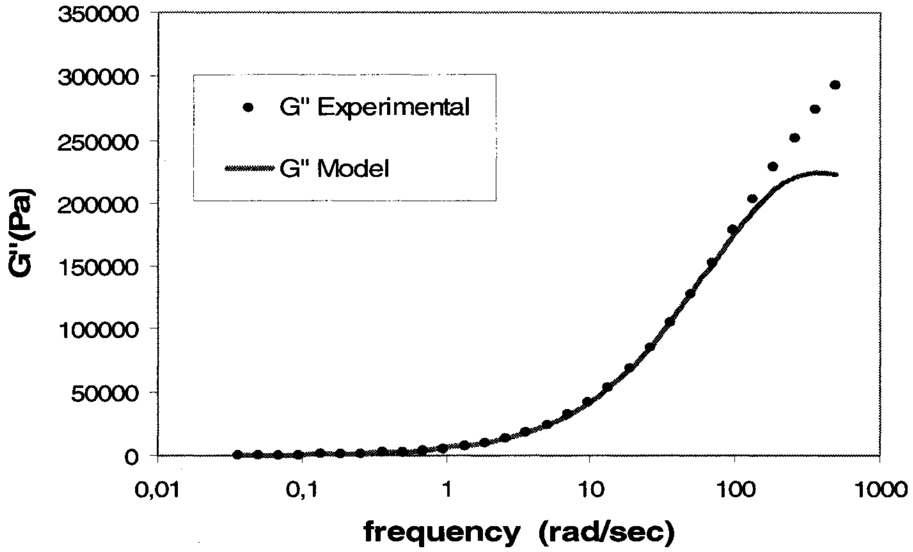

Figure 5.1a G’’ fitting for HDL1 to find G_N^0 from Eq.5.11

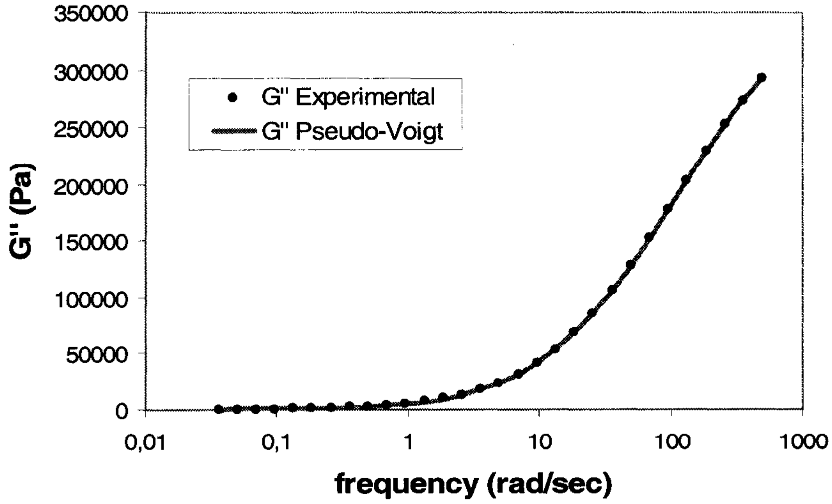

Figure 5.1b G’’ fitting for HDL1 to find G_N^0 using a pseudo-Voigt model with 4 parameters.

5.3 Wasserman's Discrete MWD Method

Wasserman's approach[30] is based on the double reptation model, in which Eq.2.18 is discretized to give Eq.5.13. This represents a linear system of equations that can be solved numerically to find the molecular weights fractions w_i.

$$\frac{G(t)}{G_N^o} = \left[\sum_{i=1}^{c} w_i F^{1/2}(t, M_i)\right]^2 \tag{5.13}$$

From the experimental data $G'(\omega)$ and $G''(\omega)$, the relaxation spectrum $H(\lambda)$ was found as explained in section 5.1.. Once the spectrum was calculated, the storage and loss moduli were calculated using Eqs.5.4 and 5.5 and compared with experimental values in order to verify that the spectrum was correct. The difference between experimental and calculated values was always less that 1% at all frequencies. Then the relaxation modulus $G(t)$ was calculated using Eq.1.11, with the range of times corresponding to the range of frequencies with ω made equivalent to $1/t$.

Equation 5.13 can be expressed in a matrix form as shown in Eq.5.14.

$$b = A \cdot x$$

$$\begin{aligned} b_j &= \left(\frac{G(t_j)}{G_N^o}\right)^{1/2}, \\ A_{j,i} &= F^{1/2}(M_i, t_j), \\ x_i &= w_i \end{aligned} \tag{5.14}$$

This system of equations was solved using a singular value decomposition technique (SVD) in MATLAB®. For the monodisperse relaxation function $F(t,M)$, Wasserman uses the BSW function (see Appendix A).

The number of molecular weights N was initially set as 150, with $M_1 = 100$ and $M_{150} = 10^6$. The lower and upper bounds on the mode times – t_1 and t_N – are governed by the frequency range of the data. In general, negative w_i values will occur if any adjacent t_i values are too close together, *i.e.*, if N is too high. The negative values of w_i are removed from the solution, and the calculation is repeated with the molecular weights corresponding to the positive w_i, until all $w_i \geq 0$. The input parameters in this method are G_N^o, α, K, the monomer molecular weight M_o and the molecular weight between entanglements M_e. The outputs are the molecular weights M_i and the corresponding weight fractions w_i, from which M_w, M_n and the polydispersity index were calculated.

5.4 TDD-DR model using a DGEX function

This method developed by Ruymbeke *et al*[29] addresses the inverse problem of computing the MWD from *G(t)* using the time-dependent diffusion model (TDD-DR) proposed by des Cloizeaux[8], with a modification to deal with short chains and Rouse relaxation processes. The generalized double reptation theory (DR) relates the relaxation modulus of an entangled linear polymer to its molecular weight distribution *w(log M)* through the following mixing rule:

$$G(t) = G_N^o\left(\int_{\log M_e}^{\infty}\left[F_{mono}(t,M)\right]^{1/\beta} w(\log M)\,d\log(M)\right)^{\beta} \qquad (5.15)$$

The original DR theory sets the mixing exponent β to a value of 2, although slightly higher values have been suggested, which could represent contributions of higher order entanglements involving more than two chains. In this method, $\beta = 2.25$. F_{mono} in Eq.5.15 is the relaxation function of the monodisperse polymer of mass M, and including constraint release effects it yields to Eq.5.16.

$$F_{mono}(t,M) = F_{sr}(t,M)^{\beta} \qquad (5.16)$$

In Eq.5.16, $F_{sr}(t,M)$ is the simple reptation relaxation function in a fixed network of entanglements. Adopting the TDD-DR reptation model:

$$F_{sr}(t,M) = \frac{8}{\pi^2} \sum_{i\,odd} \frac{1}{i^2} \exp\left(-i^2 U(t,M)\right), \tag{5.17}$$

where *U(t,M)* is given by

$$U(t,M) = \frac{t}{\tau_{rep}(M)} + \frac{M*}{M} g\left(\frac{Mt}{M*\tau_{rep}(M)}\right) \tag{5.18}$$

The function *g* in Eq.5.18 is approximated by:

$$g(x) = -x + x^{0.5}\left[x = (x\pi)^{0.5} + \pi\right]^{0.5} \tag{5.19}$$

In Eq.5.18, the reptation time is related to the molecular weight through:

$$\tau_{rept}(M) = K_{TDD} M^3 \tag{5.20}$$

In addition to the plateau modulus and M_e, the TDD-DR model has two material parameters, M^* and K_{TDD}. For systems containing a considerable fraction of short chains ($M<4M_e$), the model predicts too fast a relaxation. A simple empirical modification was found to be useful[28]; while Eq.5.15 remains valid for long chains, one uses instead $F_{mono}(t,M) = F_{sr}(t,M)$ for short chains ($M<4M_e$), and rescales the reptation time τ_{rept} to τ_{rept}/β to ensure continuity. In some cases, the solution of the inverse problem in Eq.5.18 requires inclusion of Rouse relaxation processes in the analysis. For entangled polymers, relaxation processes at times much shorter than the reptation time are dominated by the Rouse mechanism. For polyethylene samples, however, dynamic data could not be obtained at sufficiently high frequencies, and the parameters necessary to include Rouse motions could not be estimated[28]; therefore this mechanism was not incorporated into the MWD calculations. For HDPE, M^* and K_{TDD} are 1.4x10^{-17} s(mol/g)^3 and 70000 g/mol, respectively[29].

5.4.1 DGEX function and Minimization Technique

The GEX distribution is defined by Eq.5.21.

$$w_{GEX}(\log M) = C\left[\frac{M}{M_0}\right]^{a+1} \exp\left(-\left[\frac{M}{M_0}\right]^{b}\right) \tag{5.21}$$

This function involves the three parameters a, b, and M_0. The normalization constant C is such that

$$\int w_{GEX}(\log M)d\log(M) = 1 \tag{5.22}$$

The corresponding weight-average and number-average molecular weights are given by Eqs.5.23 and 5.24.

$$M_w = \int M w_{GEX}(\log M)d\log(M) = M_0\Gamma\left(\frac{a+2}{b}\right)/\Gamma\left(\frac{a+1}{b}\right) \tag{5.23}$$

$$M_n^{-1} = \int M^{-1} w_{GEX}(\log M)d\log(M) = M_0^{-1}\Gamma\left(\frac{a}{b}\right)/\Gamma\left(\frac{a+1}{b}\right) \tag{5.24}$$

The double GEX function (DGEX) is a combination of two GEX functions, as shown in Eq.5.25, where the proportion constant p is between 0 and 1. Therefore, the DGEX function depends on 7 parameters: a, b and M_0 for each GEX function plus the proportion constant p. For HDPE samples, better results were obtained using the DGEX function instead of a simple GEX function[29], and thus we used this function for all the samples studied.

$$w_{GEX}(\log M) = p w_{GEX}^{(1)}(\log M) + (1-p) w_{GEX}^{(2)}(\log M) \tag{5.26}$$

The input data is the set of experimental moduli $\{G'_{expi}, G''_{expi})$, measured at the frequency set $\{\omega_i)$ for i=1, 2,...,n_{exp}. The corresponding set of theoretical moduli calculated using the modified TDD-DR model for an assumed DGEX distribution is denoted by $\{G'_{theoi}, G''_{theoi})$. In order to find the values of the seven DGEX parameters of the distribution corresponding to the experimental data, we proceed to the minimization of the function in Eq.5.27.

$$\chi^2 = \frac{1}{2n_{\exp}}\left(\sum_{i=1}^{n_{\exp}} \frac{\left[G'_{\exp,i}-G'_{theo,i}\right]^2}{\left[G'_{\exp,i}\right]^2} + \sum_{i=1}^{n_{\exp}} \frac{\left[G''_{\exp,i}-G''_{theor,i}\right]^2}{\left[G''_{\exp,i}\right]^2}\right) \tag{5.27}$$

The minimization of this function is obtained by means of the Nelder-Mead simplex method as implemented in the function *fminsearch* in MATLAB® 6.1. A penalty term of order 10^{10} is added to Eq.5.27 when the M_0 parameters would otherwise become negative during the minimization. Therefore, for a given set of DGEX parameter values, the integral of Eq.5.15 is calculated using 25 discrete weights per decade. The theoretical values of the loss and storage moduli are computed from the theoretical relaxation function *G(t)* using the relaxation spectrum estimated from the approximation method of Schwarzl and Staverman[10], shown in Eq.5.28, where $t=2\tau$. The relaxation function *G(t)* has to be calculated for a large range of times in order to obtain a complete representation of the relaxation spectrum.

$$H(\tau) = -\frac{dG(t)}{d\ln t} + \frac{d^2G(t)}{d(\ln)^2} \tag{5.28}$$

The minimization process is very sensitive to the initial values of the seven parameters in the DGEX function. Therefore, a preliminary optimization process in two steps is necessary. First, the two GEX functions are chosen very narrow ($a^{(1)}=b^{(1)}=a^{(2)}=b^{(2)}=20$), and ten different values of the remaining parameters are tested. The combination that gives the smallest error is retained as initial $M_0^{(i)}$ and p values. Second, with these $M_0^{(i)}$ and p values the other four parameters are tested with the constraint $a^{(1)}=b^{(1)}=a^{(2)}=b^{(2)}$, and the best combination are used as initial parameters.

6. RESULTS AND DISCUSSION

This section is divided in three parts, one for each set of polymers mentioned in section 4. The first part presents the MWD predictions of all four methods for the third set mentioned in section 4, the second part for the second set and finally the third part for the first set, which is the one with the highest polydispersity indexes.

A very important parameter for the viscosity transform and the modified modulus transform is the zero-shear viscosity, which was calculated from the relaxation spectrum as explained in section 5.1. Viscosity values as well as the parameters α and K needed in Eq.2.2 for the modified modulus transform are presented in Table 6.1. The activation energies E_a are also necessary to calculate K at the experimental temperature in some cases. For the polypropylene samples, values for α and K were not available, so α was taken in this case to be 3.4, and the value of K for PP1 was estimated from the zero-shear viscosity and the M_w from GPC using Eq.2.2. This constant was also used for PP2.

Table 6.1 Parameters of materials studied

Sample	η_o **(Pa s)**	α	$K(T_a)$	T_a **(°C)**	T_{exp} **(°C)**	E_a**(kJ/mol)**
HDL1	5880.1	3.65(I)	3.9×10^{-15}(I)	150	150	27.5 (II)
LDL1	20176	3.6 (II)	6.8×10^{-15}(II)	150	130	32.9 (II)
HDL2	313.6	3.65(I)	3.9×10^{-15}(I)	150	150	27.5 (II)
HDL4	842378.5	3.65(I)	3.9×10^{-15}(I)	150	150	27.5 (II)
LLDPE1	60141	3.4 (I)	3.4×10^{-15}(I)	190	150	30 (III)
LLDPE2	43395.1	3.4 (I)	3.4×10^{-15}(I)	190	150	30 (III)
PP1	1167.9	3.4	7×10^{-17}	180	180	48 (IV)
PP2	27811.9	3.4	7×10^{-17}	180	180	48 (IV)

I. Reference 33

II. Reference 34

III Reference 18

IV. Reference 25

6.1 Narrow distributions and typical values of M_w

This set of polymers is considered first in the analysis, because the results help to show how the methods work. Narrow distributions and typical values of M_w represent the easiest case for these methods. The other two sets of polymers pose more challenges and require a closer analysis of the results.

The MWD prediction for HDL1 from the viscosity transform is shown in Fig.6.1, where there is excellent agreement with the GPC data, as is to be expected for this method for this polydispersity and M_w.

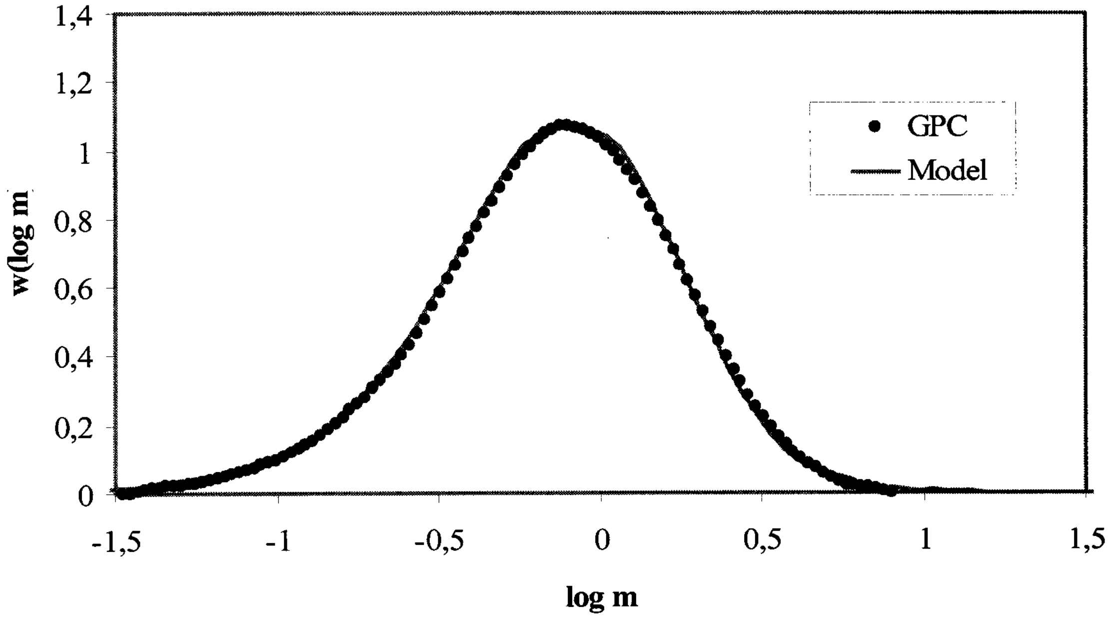

Figure 6.1 GPC and Viscosity Transform MWD for HDL1

The MWD predictions for HDL1 using the modified modulus transform and Wasserman's method are shown for comparison in Figs. 6.2 and 6.3, respectively. The location of the peak and the shape of the MWD as indicated the modulus transform are satisfactory taking into account the simplicity of the calculations required, although the method clearly underestimates the high molecular weight tail. Wasserman's method does not give good results. The regularization parameter had to be set very high (1×10^7) in order to smooth the distribution and eliminate a lot of noise, and thus the occurrence of many peaks, and this makes the interpretation of the results ambiguous. The predictions for all samples using this method were generally the smoothest MWDs and thus required very high regularization parameters.

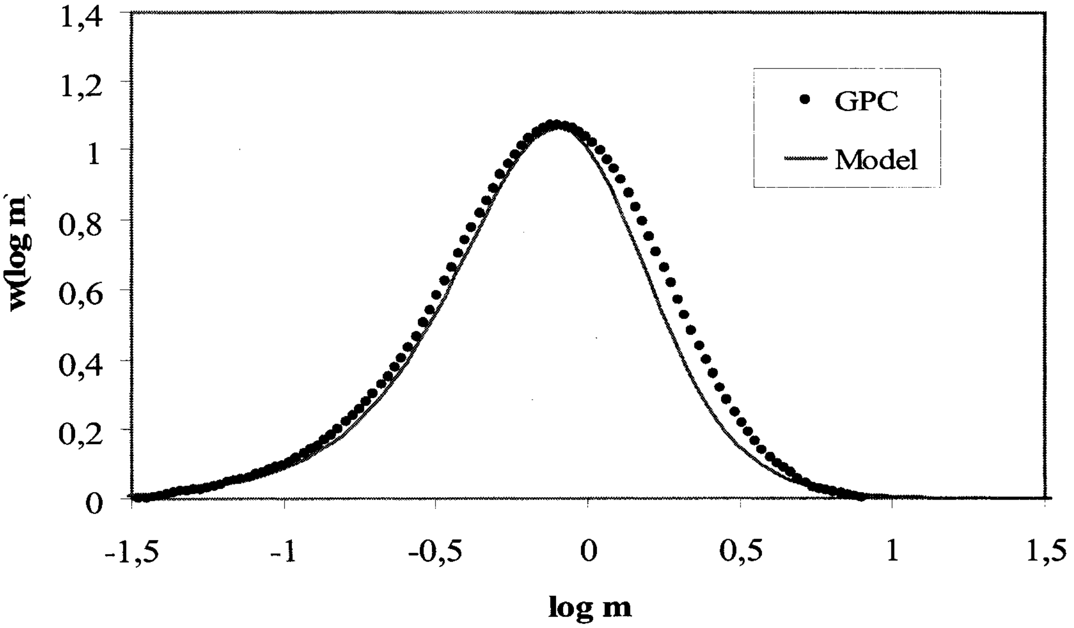

Figure 6.2 GPC and Modulus Transform for HDL1

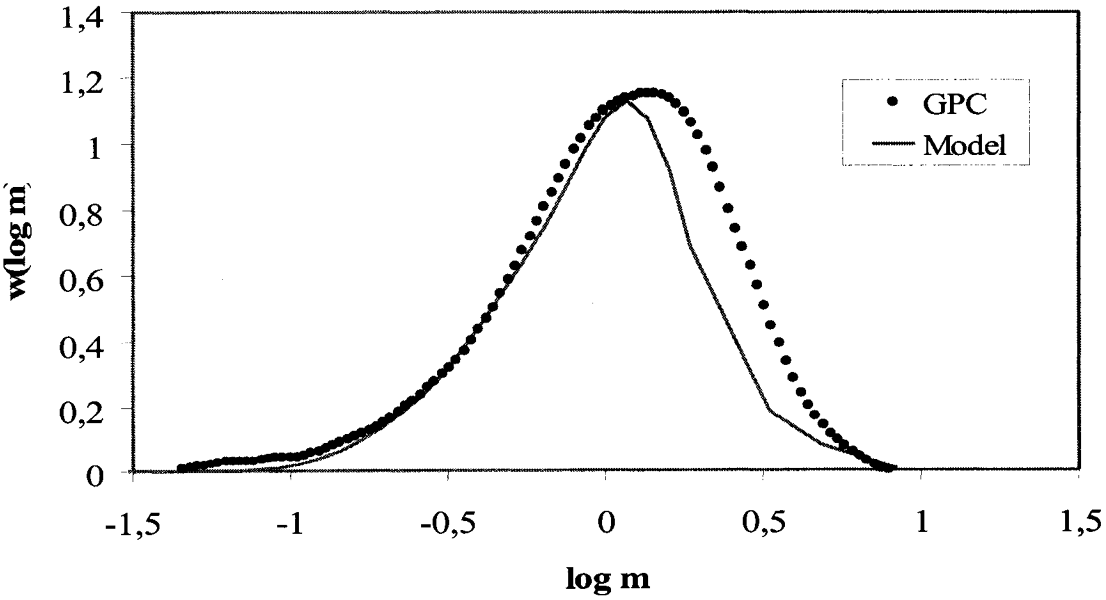

Figure 6.3 GPC and Wasserman's MWD for HDL1

The MWD predictions for LDL1 for these three methods are presented in Figs.6.4-6. Table 6.2 shows the values obtained for the plateau modulus using Eq.5.10 and the values of the parameters in the sigmoid function (Eq.5.9) used to fit *G(t)* for both HDL1 and LDL1. Again the viscosity transform MWD agrees well with GPC results but not quite as well for HDL1, predicting a small peak at the high molecular weight tail and a slight overestimation of the peak.

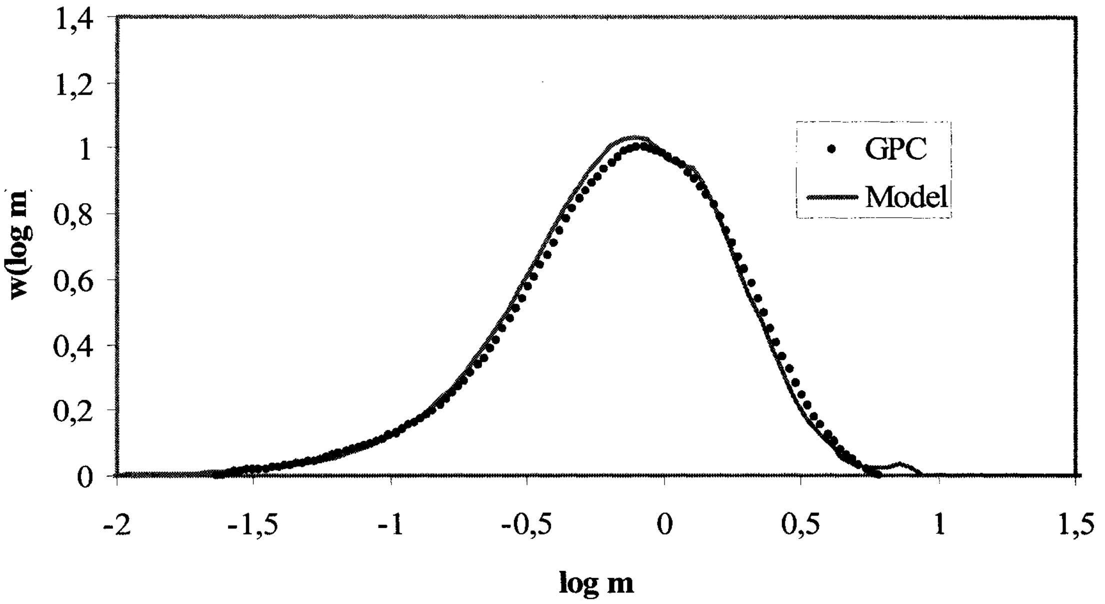

Figure 6.4 GPC and Viscosity Transform MWD for LDL1

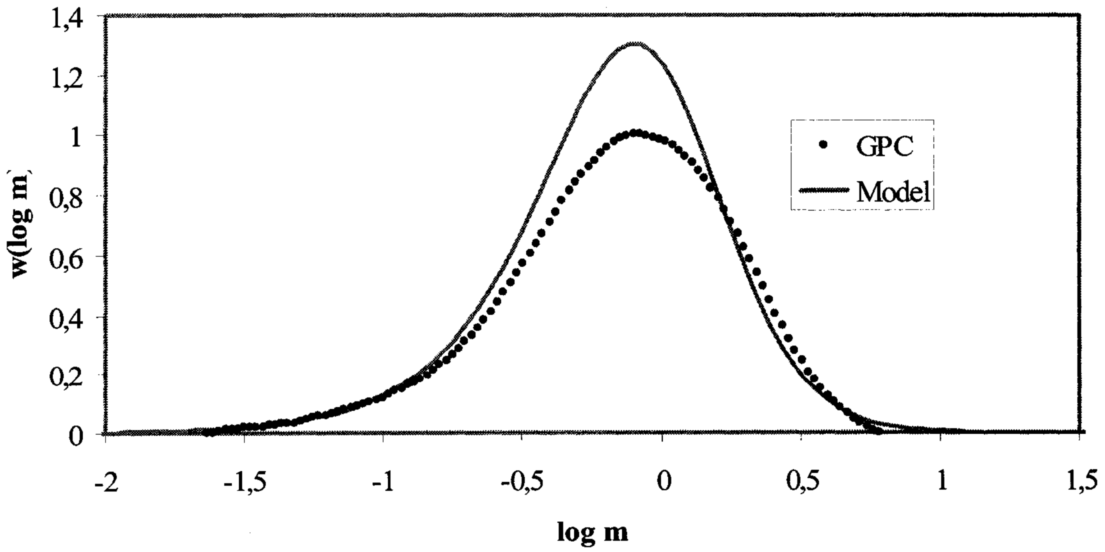

Figure 6.5 GPC and Modulus Transform MWD for LDL1

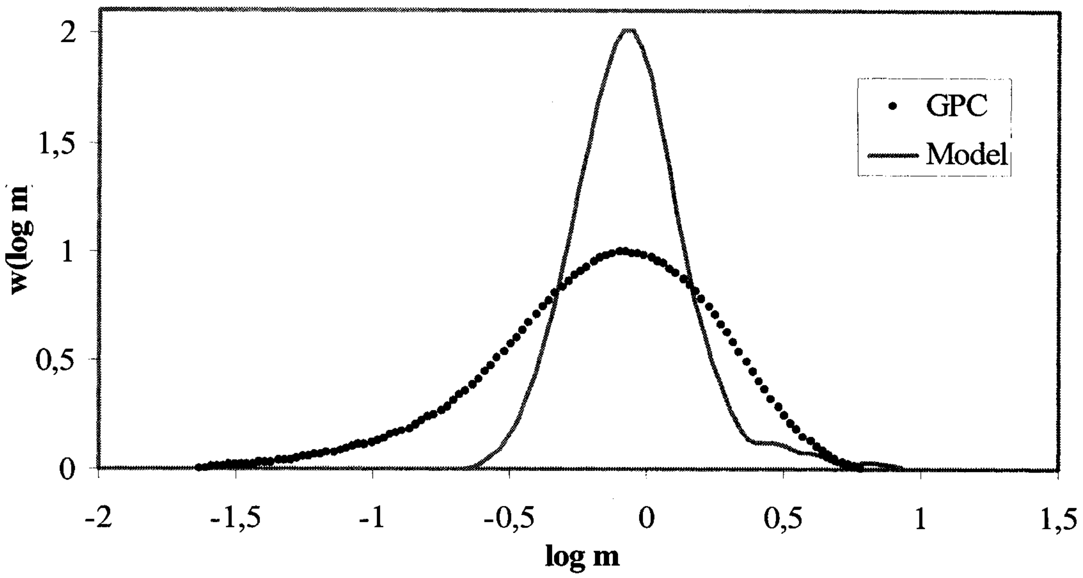

Figure 6.6 GPC and Wasserman's MWD for LDL1

There is qualitative agreement between the predicted and the GPC MWDs for LDL1 from the modulus transform, although the quantitative agreement is not as satisfactory as it is for HDL1. Wasserman's MWD for LDL1 does not predict at all a good shape of the MWD, although the location of the peak is accurate.

Table 6.2 Plateau Modulus and Sigmoid function parameters

Sample	G_N^o **(Pa)**	x_o	y_o	a	B	c
HDL1	$1.23\text{x}10^6$	1.8722	0.0005	0.8891	0.8279	1.8253
LDL1	$7.74\text{x}10^5$	1.2234	0.0015	1.1337	0.877	2.0301

The TDD-DR prediction for HDL1 is shown in Fig.6.7. The agreement between GPC and this distribution is satisfactory, although there is a slight overestimation of the low molecular weight tail, which causes a very slight shift in the peak compared to that from GPC data. The possible explanation of this overestimation can be observed in Fig.6.8, which shows the experimental dynamic data compared with those calculated from the minimization procedure used in this method.

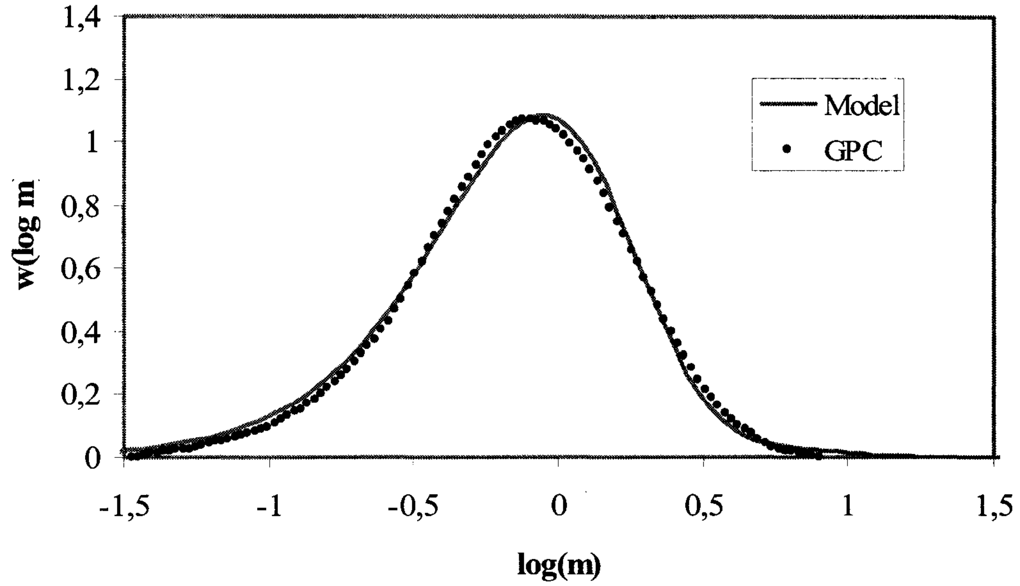

Figure 6.7 GPC and TDD-DR MWD for HDL1

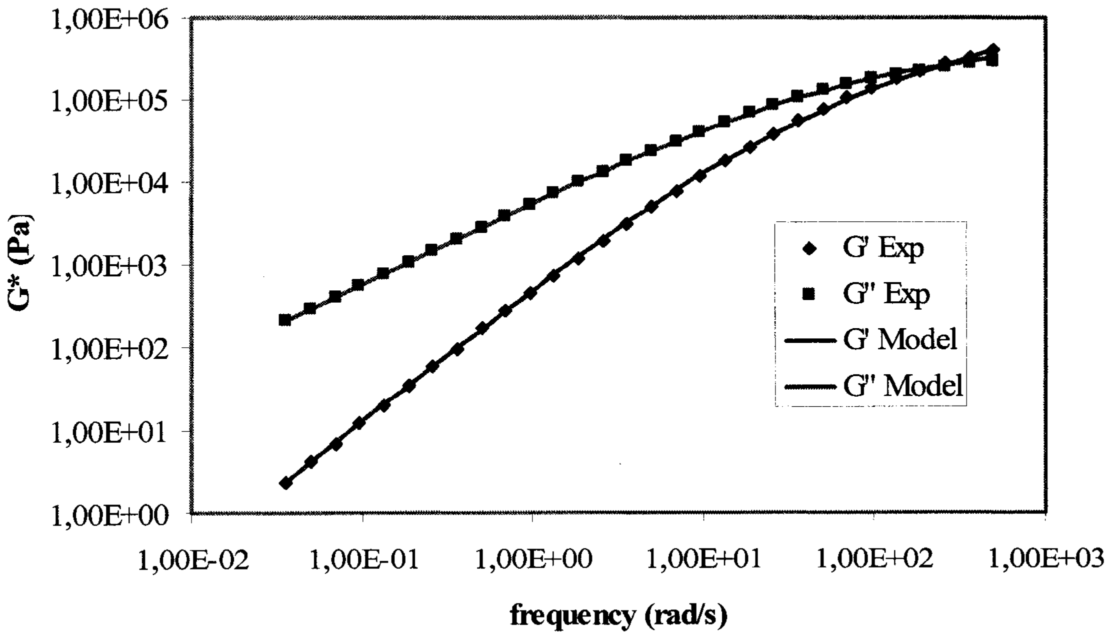

Figure 6.8 Experimental and Predicted Dynamic Data using the TDD-DR model for HDL1 at 150°C

Although the match for these two sets is excellent, there is a slight overestimation of the loss modulus at high frequencies (7-10% difference for the last two points), which probably causes the slight increase in the low MW tail. Figure 6.9 shows the evolution of the minimization procedure during the course of the Nelder-Mead iterations, where one can see that after 400 iterations convergence is reached. The TDD-DR model MWD prediction and the experimental and calculated dynamic data for LDL1 are presented in Figs.6.10 and 6.11. The relative error on the dynamic moduli and the final DGEX parameters for both HDL1 and LDL1 MWDs are presented in Table 6.3. The agreement between the predicted and GPC MWDs for LDL1 is very satisfactory although not quite as good as the result obtained for HDL1.

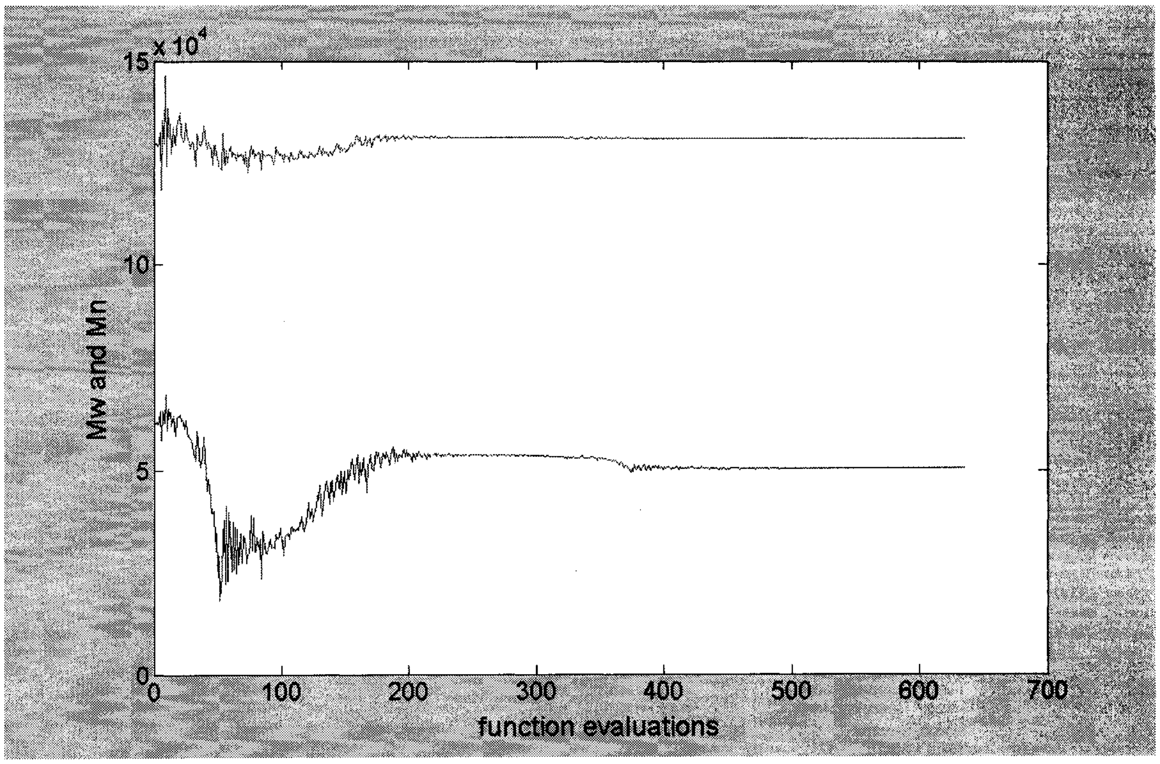

Figure 6.9 Evolution of function evaluations during Nelder-Mead iterations for HDL1

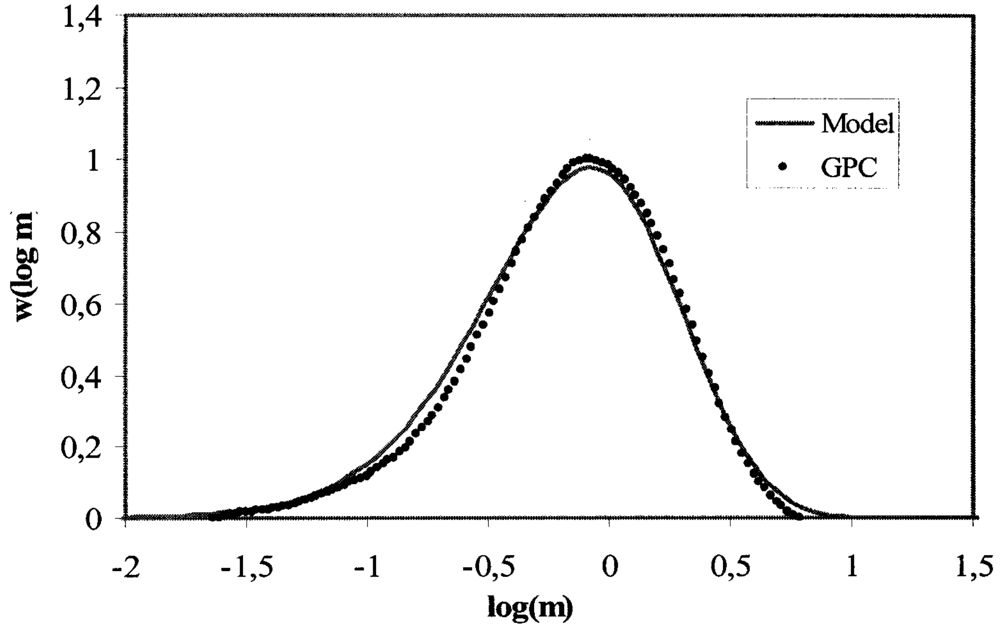

Figure 6.10 GPC and TDD-DR MWD for LDL1

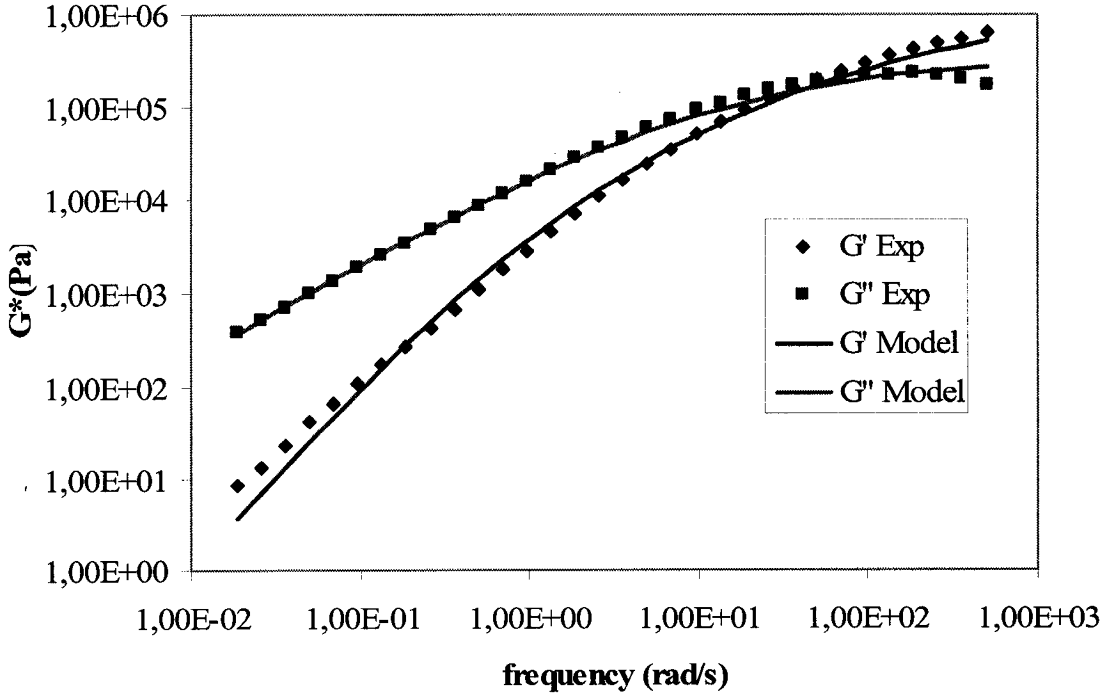

Figure 6.11 Experimental and Predicted Dynamc Data using the TDD-DR model for LDL1 at 130°C

Once more a look at the dynamic data prediction in Fig.6.11 shows that the minimization in this case is not as good as for HDL1. There was a relative error of 14.4% for this sample and this may be the cause of the discrepancies in the MWD prediction.

Table 6.3 DGEX parameters and Relative Errors on Dynamic Moduli for HDL1 and LDL1

Sample	a_1	b_1	M_{o1}	a_2	b_2	M_{o2}	p	χ %
HDL1	0.815	0.601	60,429	0.713	0.924	58,846	0.04	1.88
LDL1	0.624	0.701	53,054	0.120	0.530	11,949	0.05	14.4

The values of M_w/M_n from GPC and from each of the methods are shown in Table 6.4. Except for the Wasserman method, which produces narrower distributions, the other methods overestimate the polydispersity index.

Table 6.4 M_w/M_n values for HDL1 and LDL1

Sample	**GPC**	**Viscosity T.**	**Modulus T.**	**Wasserman**	**TDD-DR**
HDL1	2.04	2.48	2.29	1.55	2.6
LDL1	2.29	2.6	2.45	1.27	2.78

A very important aspect in the TDD-DR method is the choice for the initial parameters in the DGEX distribution function. It is suggested [29] that an optimization procedure should be used to obtain these initial parameters prior to the start of the minimization. This optimization procedure was performed for all the samples studied. For HDL1, the evolution of the MWD when starting from an optimized initial DGEX distribution is shown in Fig.6.12. It was interesting, however, to see if starting from a different DGEX distribution would yield the same convergence. As is shown in Fig.6.13, starting from a broad and clearly bimodal distribution, the procedure for this polymer converges to a good MWD prediction compared to GPC results, although the number of iterations is increased.

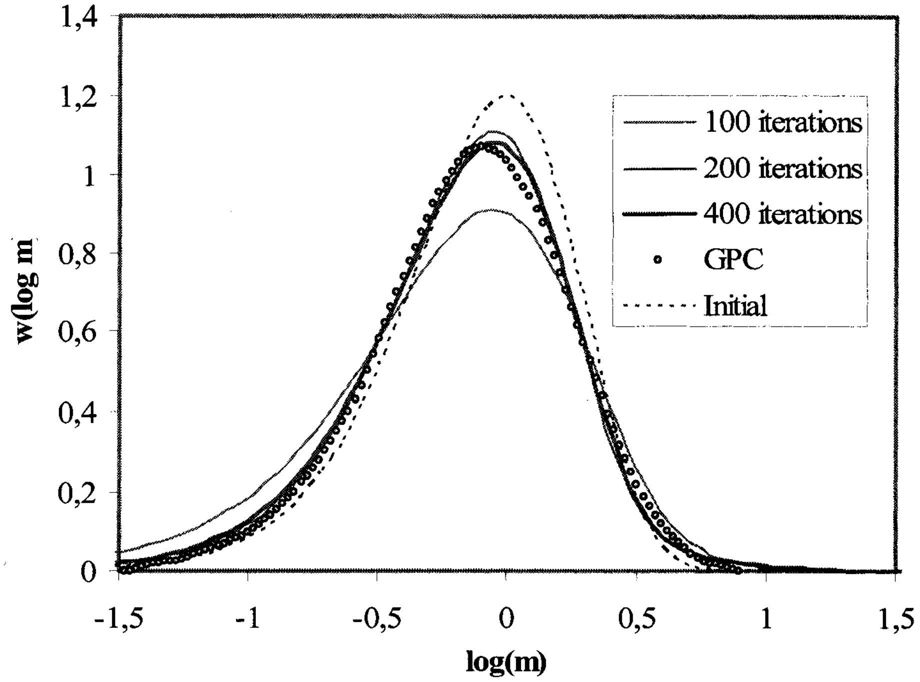

Figure 6.12 Evolution of the TDD-DR MWD predictions for HDL1 starting from optimized DGEX parameters

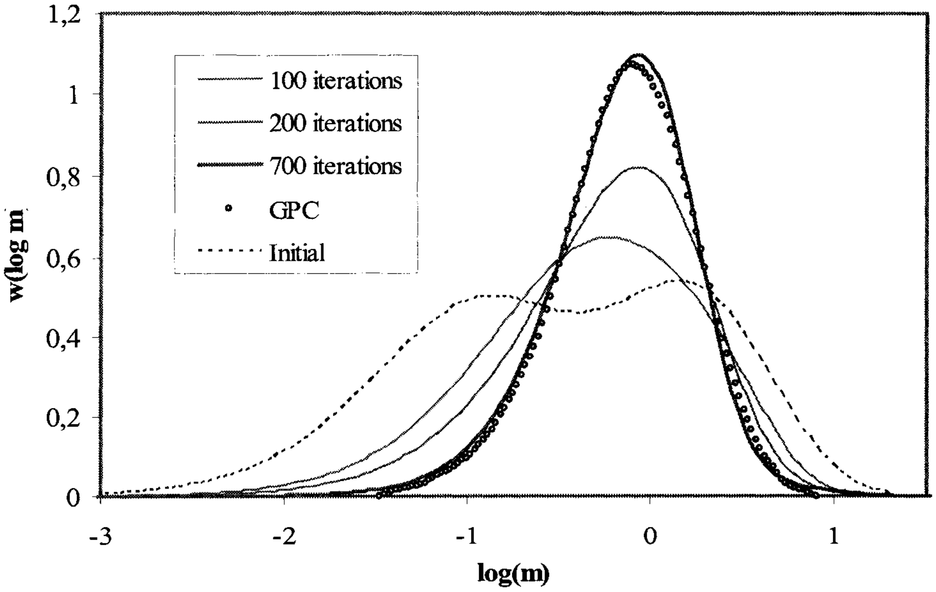

Figure 6.13 Evolution of the TDD-DR MWD predictions for HDL1 without optimization of initial DGEX parameters

6.2 Polymers with high and low molecular weight

We now consider two samples, HDL2 and HDL4, both with polydispersities close to two but very low and very high averages molecular weights, respectively. The MWD predictions for HDL2 using the viscosity transform, the modulus transform and Wasserman's method are shown in Figs.6.14-16.

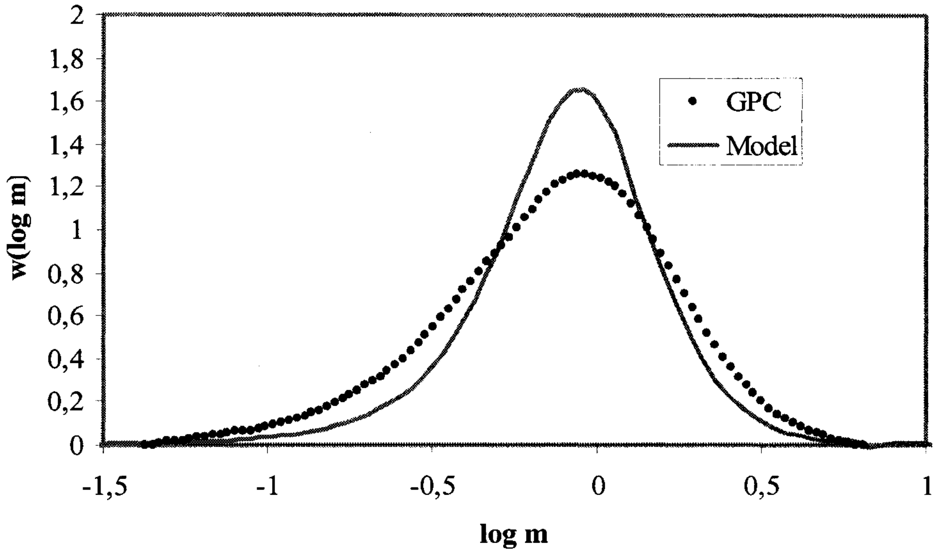

Figure 6.14 GPC and Viscosity MWD for HDL2

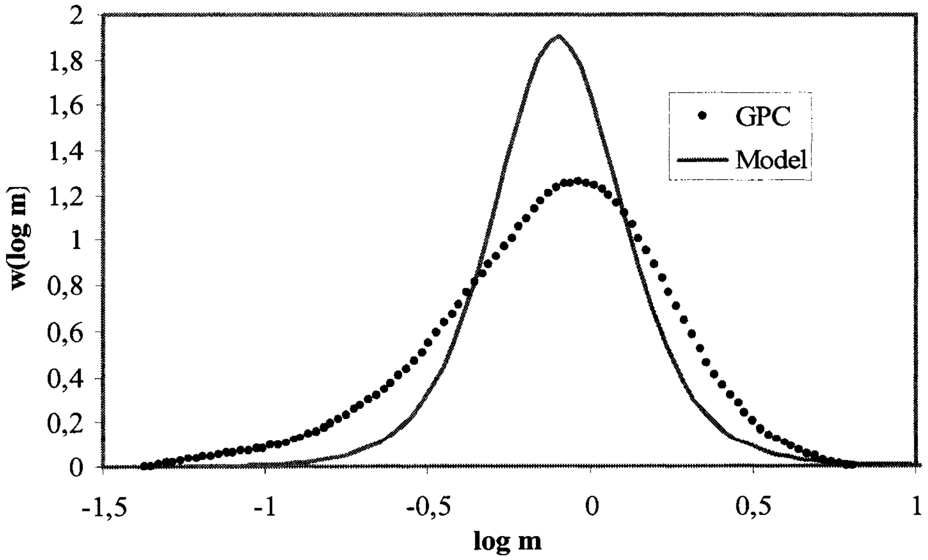

Figure 6.15 GPC and Modulus Transform MWD for HDL2

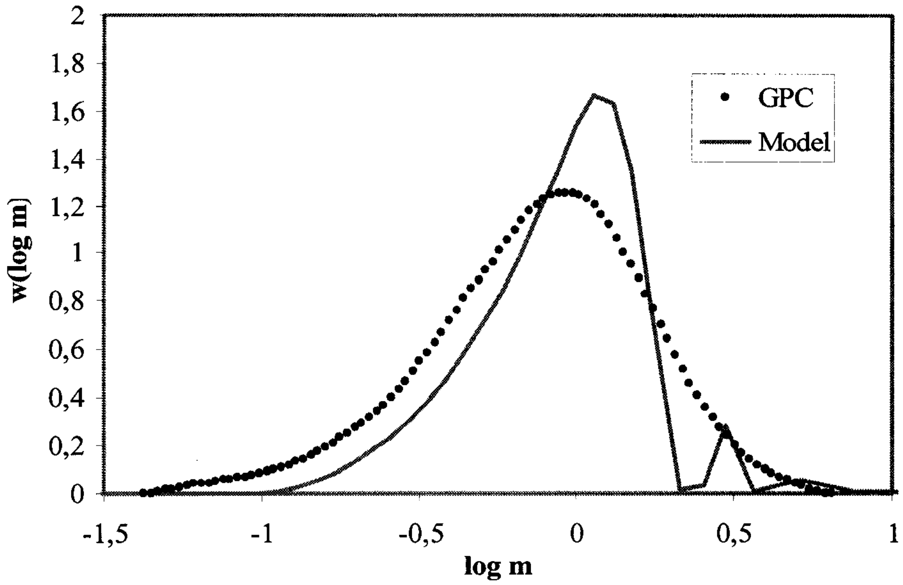

Figure 6.16 GPC and Wasserman's MWD for HDL2

Although the viscosity transform gives the best result among these three methods, none of them are able to predict an accurate MWD for the low molecular weight polymer. The TDD-DR model, however, gives a better prediction of the shape of the distribution than the other methods, as shown in Fig. 6.17.

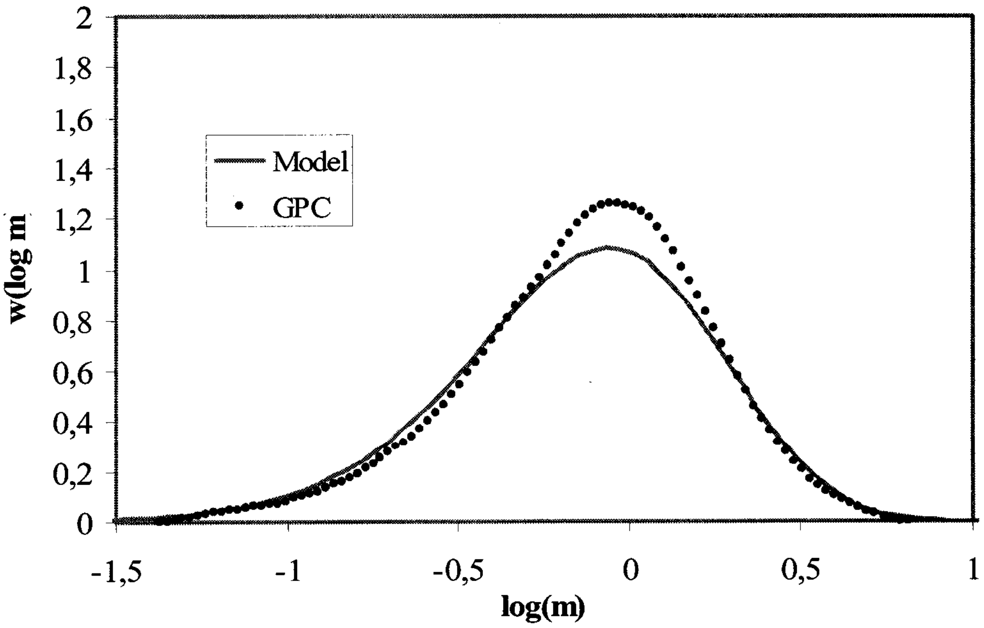

Figure 6.17 GPC and TDD-DR MWD for HDL2

The result for this method is better, especially the prediction of the high molecular weight tail, even though the relative error in the dynamic data after the minimization procedure is 14.5%. The MWD predictions for HDL4 are presented in Figs.6.18-20.

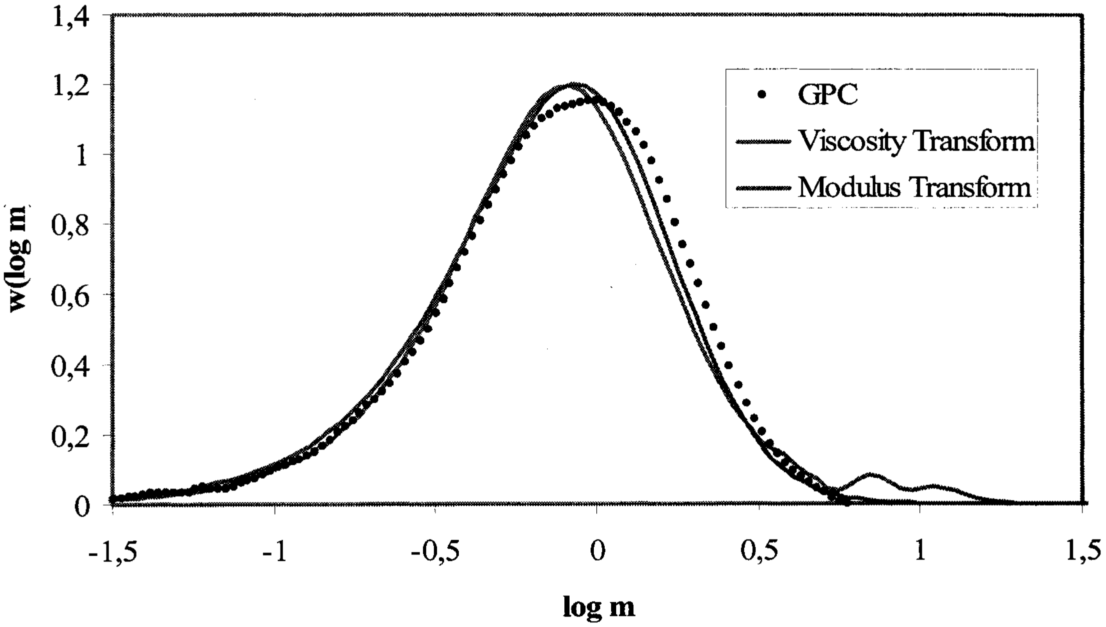

Figure 6.18 GPC, Viscosity and Modulus Transform MWD for HDL4

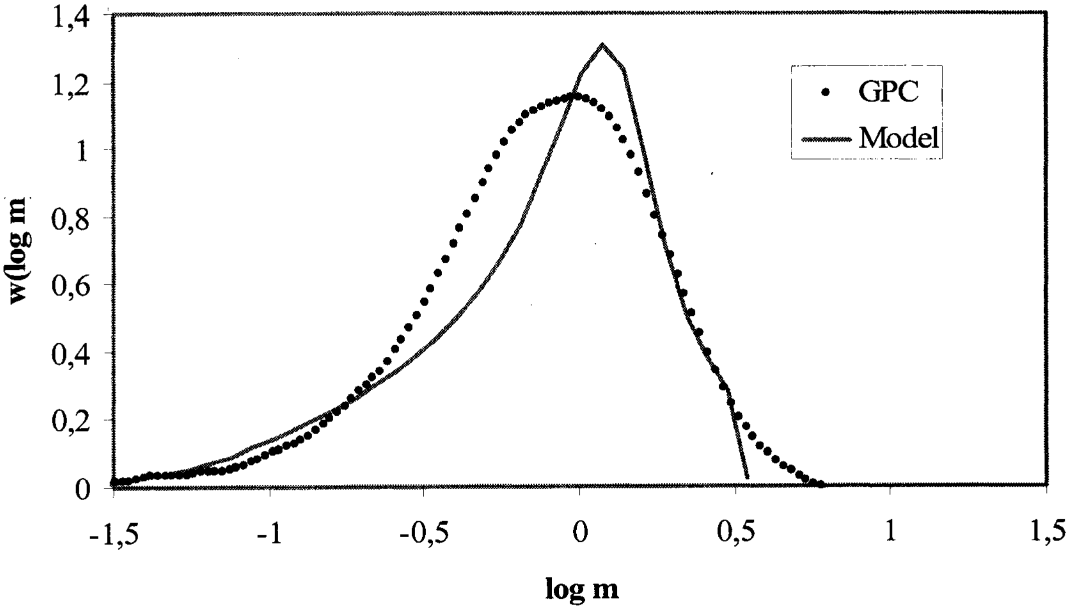

Figure 6.19 GPC and Wasserman MWD for HDL4

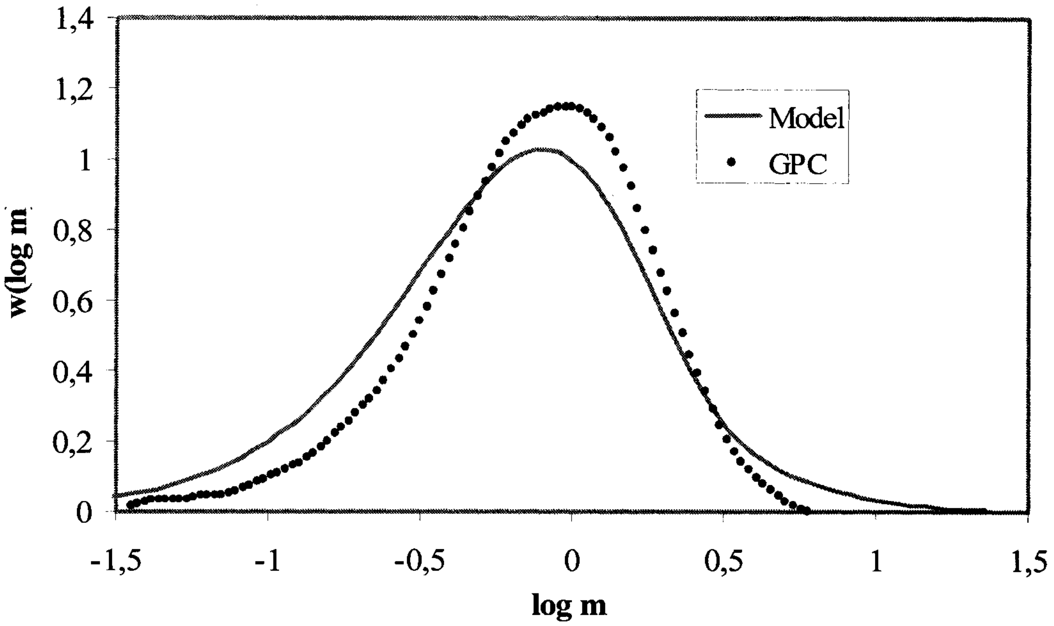

Figure 6.20 GPC and TDD-DR MWD for HDL4

For this high MW polymer the TDD-DR model predicts a MWD that is too broad, which is revealed in the M_w/M_n value reported in Table 6.5. The DGEX parameters and relative errors in the dynamic data for these two polymers are shown in Table 6.6. The best prediction for this sample is given by the modulus transform, although even for this method the location of the peak is slightly underestimated. The viscosity transform incorrectly predicts small peaks at the high molecular weight end.

Table 6.5 M_w/M_n for HDL2 and HDL4

Sample	GPC	Viscosity	Modulus	G_N^o (Pa)	Wasserman	TDD-DR
HDL2	1.90	1.66	1.45	$9.1\text{x}10^5$	1.43	2.23
HDL4	2.08	2.35	2.50	$1.42\text{x}10^6$	2.22	3.59

Table 6.6 DGEX parameters and Relative Errors on Dynamic Moduli for HDL2 and HDL4

Sample	a_1	b_1	M_{o1}	a_2	b_2	M_{o2}	p	χ %
HDL2	1.35	2.14	29,683	1.57	0.55	3,345	$5x10^{-6}$	14.51
HDL4	0.536	0.525	115,766	0.569	0.81	147,821	0.105	4.53

6.3 Polymers with broad MWD

This set of polymers comprises two LLDPEs and two polypropylenes with broad distributions (see Table 4.1). Broad distributions represent the most challenging case in predicting MWD from complex viscosity or dynamic data. The viscosity transform predictions for LLDPE1 and LLDPE2 are shown in Figs.6.21 and 6.22. Except for some noise, the distributions are very satisfactory, predicting accurately both the main peak as and the shape and breadth of the curves.

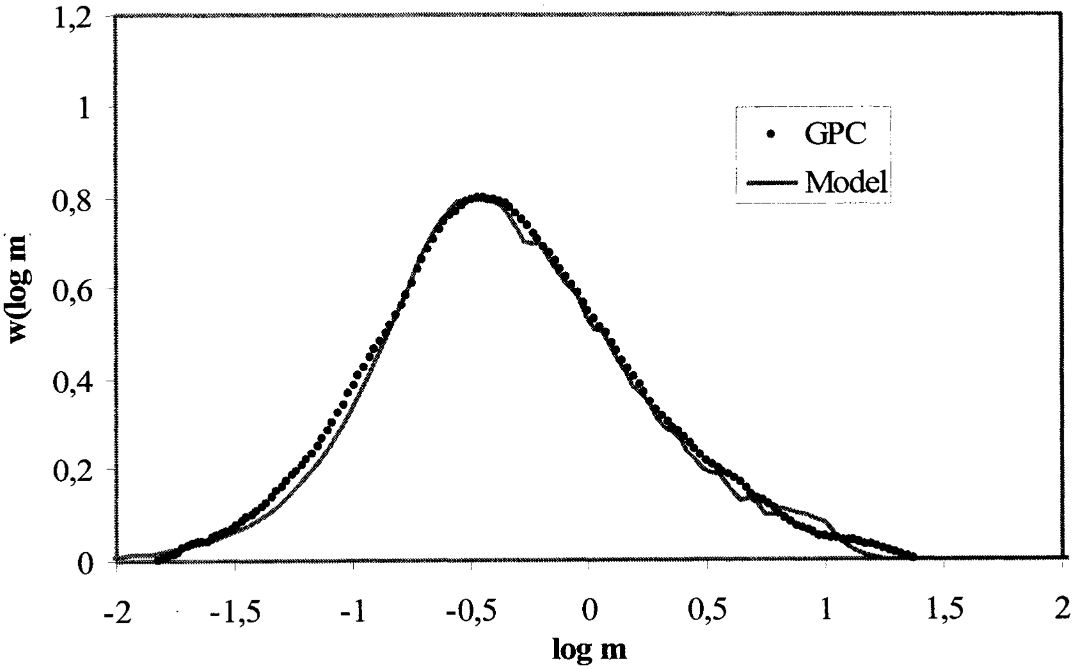

Figure 6.21 GPC and Viscosity Transform MWD for LLDPE1

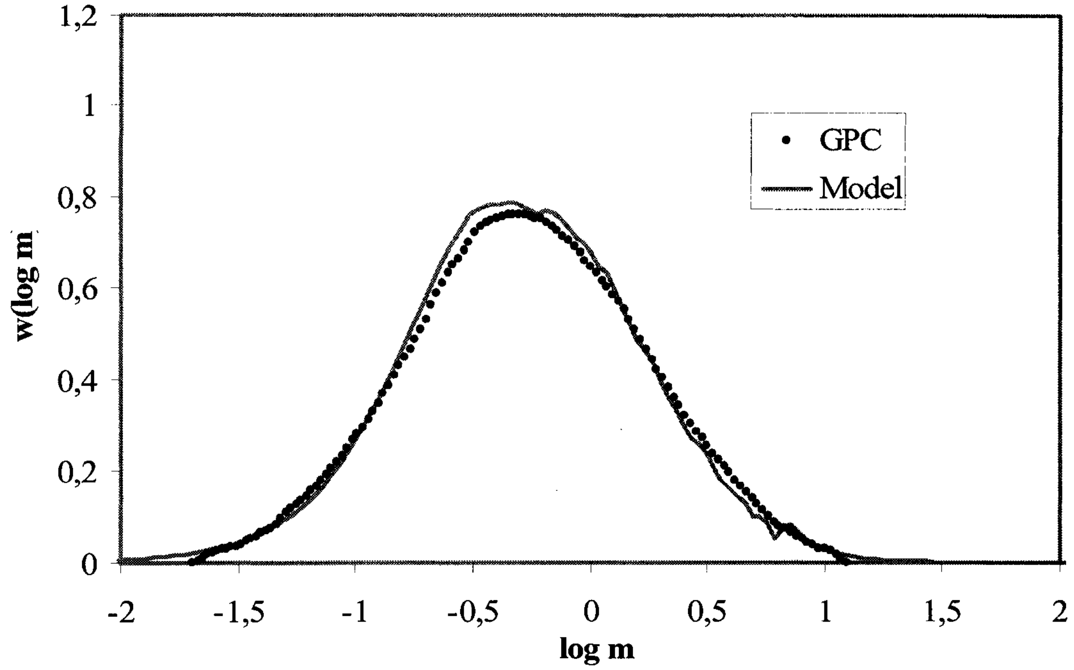

Figure 6.22 GPC and Viscosity Transform MWD for LLDPE2

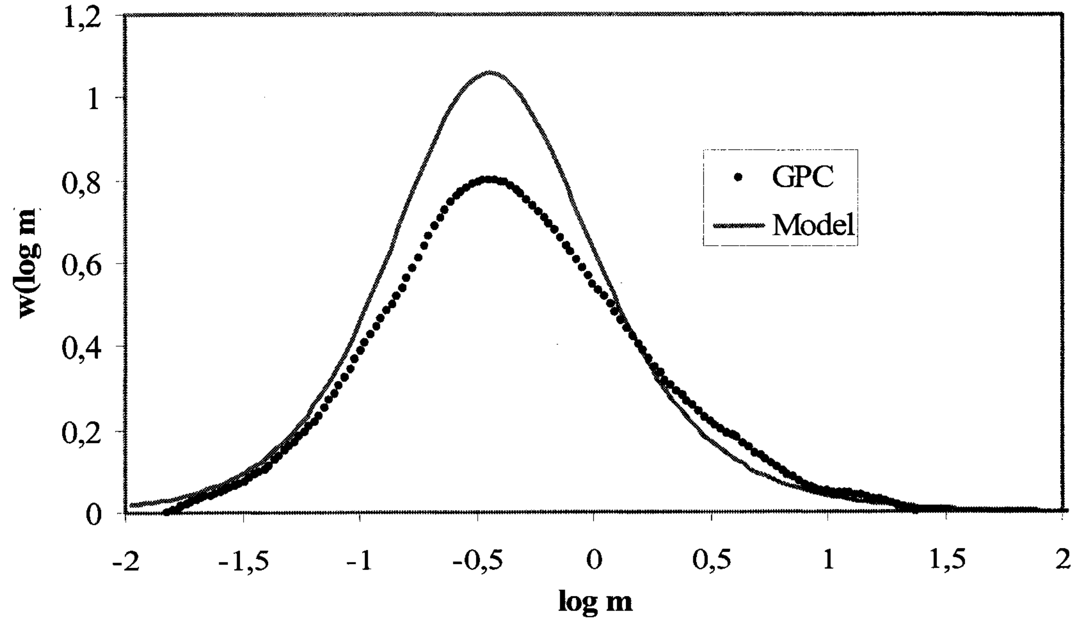

Figure 6.23 GPC and Modulus Transform MWD for LLDPE1

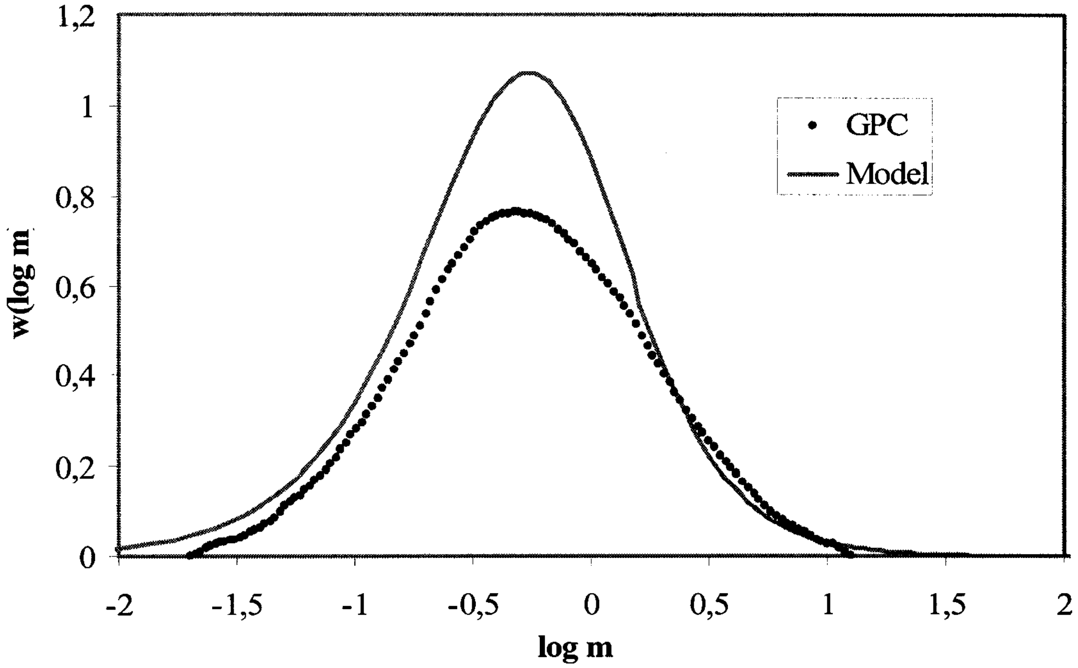

Figure 6.24 GPC and Modulus Transform MWD for LLDPE2

The predictions for these two LLDPEs using the modulus transform method are shown in Figs.6.23 and 6.24. The quantitative agreement is unsatisfactory for both of these materials and the low-molecular-weight tail is overestimated, but general shape of the distribution and the high molecular weight tail in both cases are well described. Wasserman's method (Figs.6.25 and 6.26) fails to predict the shape and the peak for these two polymers, and high regularization parameter values ($1x10^8$) were necessary in order to obtain a distribution that were at least comparable to the GPC curve.

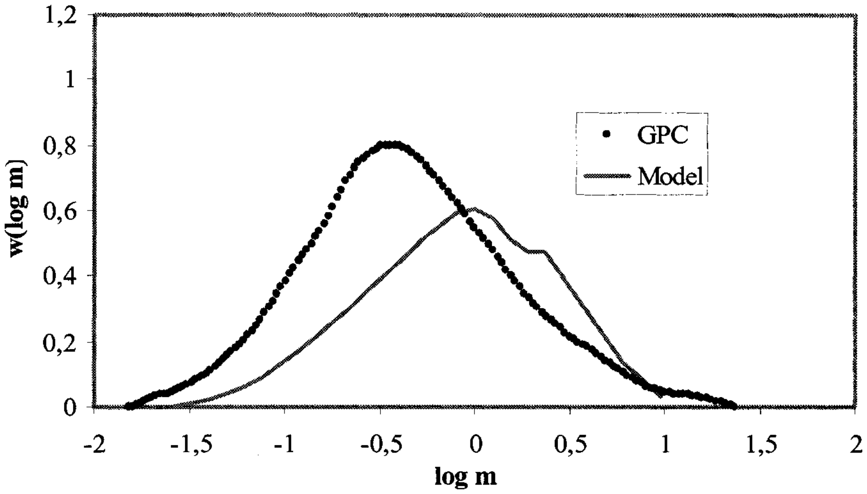

Figure 6.25 GPC and Wasserman's MWD for LLDPE1

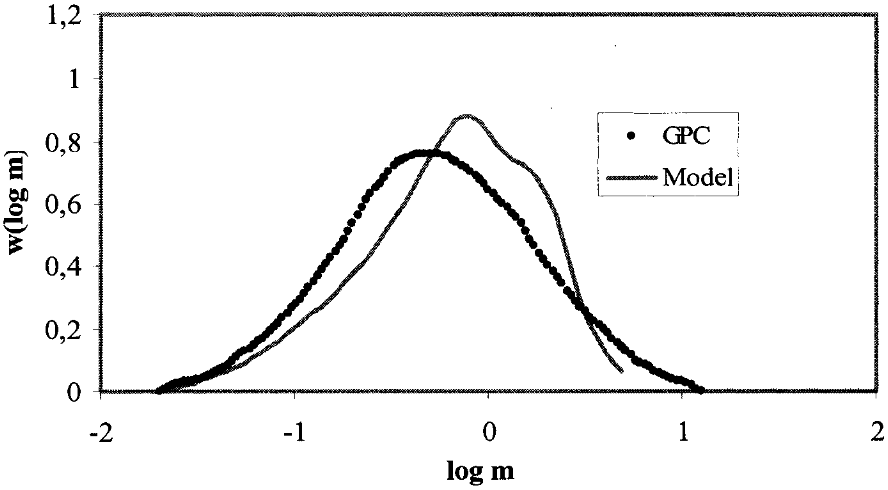

Figure 6.26 GPC and Wasserman's MWD for LLDPE2

The MWD prediction using the TDD-DR model for LLDPE1 is shown in Fig.6.27. Here we can see that the prediction is rather satisfactory, with a shape and breadth that are quite similar to the GPC results. The low molecular weight tail is overestimated and, this causes a shift to the right in the location of the peak. The calculated and experimental dynamic data for LLDPE1 are presented in Fig.6.28, where we can see that even though the match is very good, with a relative error of only 3.3%, there are some differences at the high frequencies, which might account for the overestimation of the predicted MWD in the low molecular weight tail. A similar situation was found for the LLDPE2 MWD as predicted using the TDD-DR model, as shown in Figs.6.29 and 6.30.

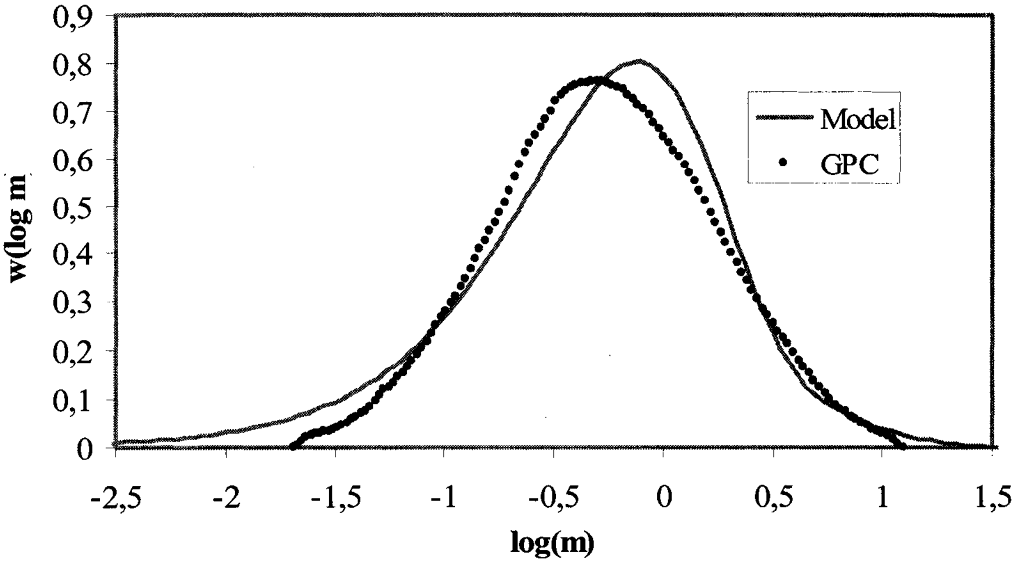

Figure 6.29 GPC and TDD-DR MWD for LLDPE2

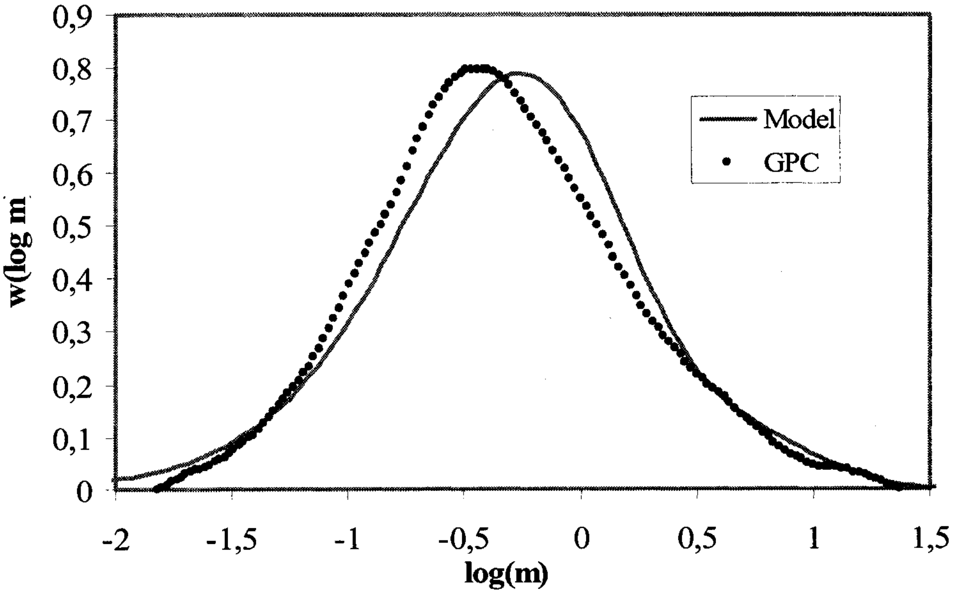

Figure 6.27 GPC and TDD-DR MWD for LLDPE1

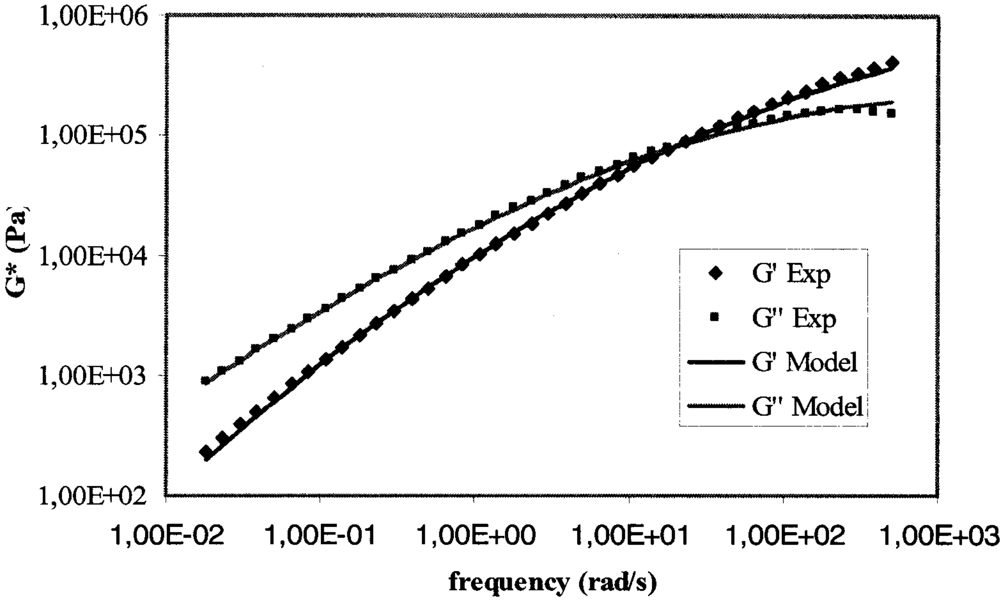

Figure 6.28 Experimental and Predicted Dynamic Data for LLDPE1 at 150°C using the TDD-DR model

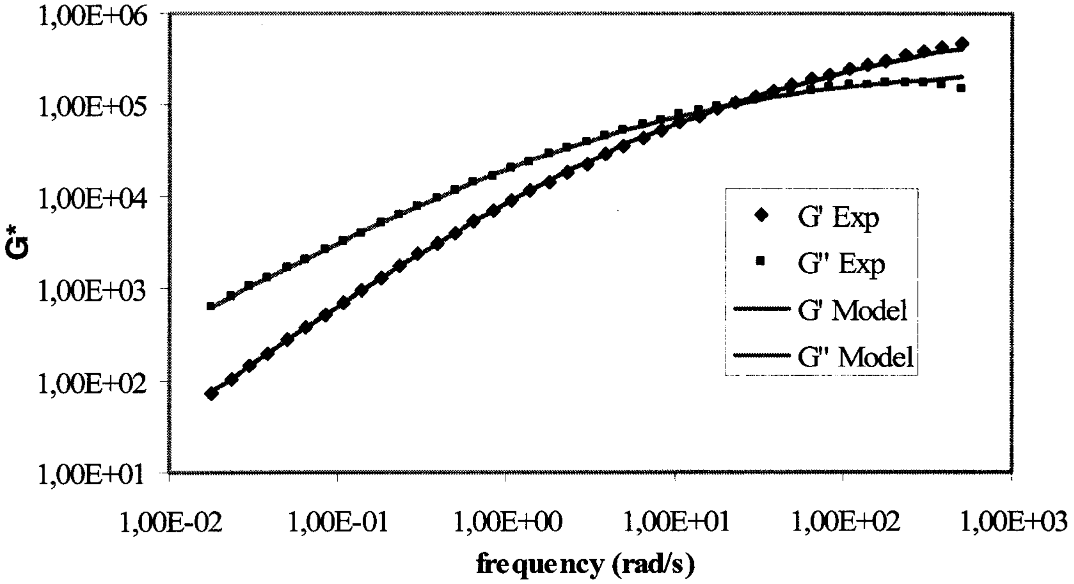

Figure 6.30 Experimental and Predicted Dynamic Data for LDDPE2 at 150°C using the TDD-DR model

In this case the overestimation of the low molecular weight tail is more pronounced as is the relative error in the dynamic data at the high frequency end compared to LLDPE1. This results in a much higher polydispersity index than that from the GPC data. The values of the DGEX parameters and the average relative error in dynamic data for these two polymers are shown in Table 6.7. Table 6.8 shows the polydispersities and plateau modulus estimations for these two polymers.

Table 6.7 DGEX parameters and Relative Errors on Dynamic Moduli for LLDPE1 and LLDPE2

Sample	a_1	b_1	M_{o1}	a_2	b_2	M_{o2}	P	χ %
LLDPE1	0.932	0.483	43,248	0.577	0.551	17,965	0.1048	3.38
LLDPE2	0.192	0.542	118,621	$2.2\text{x}10^{-6}$	0.920	156,811	0.1290	2.89

Table 6.8 M_w/M_n for LLDPE1 and LLDPE2

Sample	GPC	Viscosity	Modulus	G_N^o (Pa)	Wasserman	TDD-DR
LLDPE1	4.54	4.67	5.07	$6.63\text{x}10^5$	2.73	4.19
LLDPE2	3.50	4.08	5.68	$6.72\text{x}10^6$	2.90	6.10

The last group of polymers studied consisted of polypropylenes PP1 and PP2 having polydispersities of 3.6 and 6.43, respectively. The viscosity transform predictions for these samples are shown in Figs.6.31 and 6.32. This method works very well for PP1 but not for PP2, where the shape and location of the main peak are not well predicted, although the high molecular weight matches very well that of the GPC distribution.

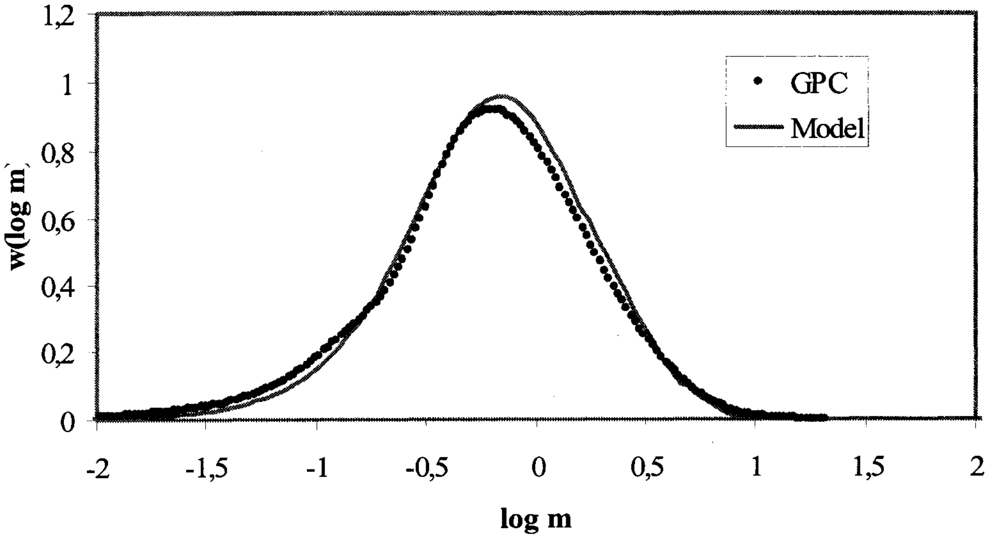

Figure 6.31 GPC and Viscosity Transform MWD for PP1

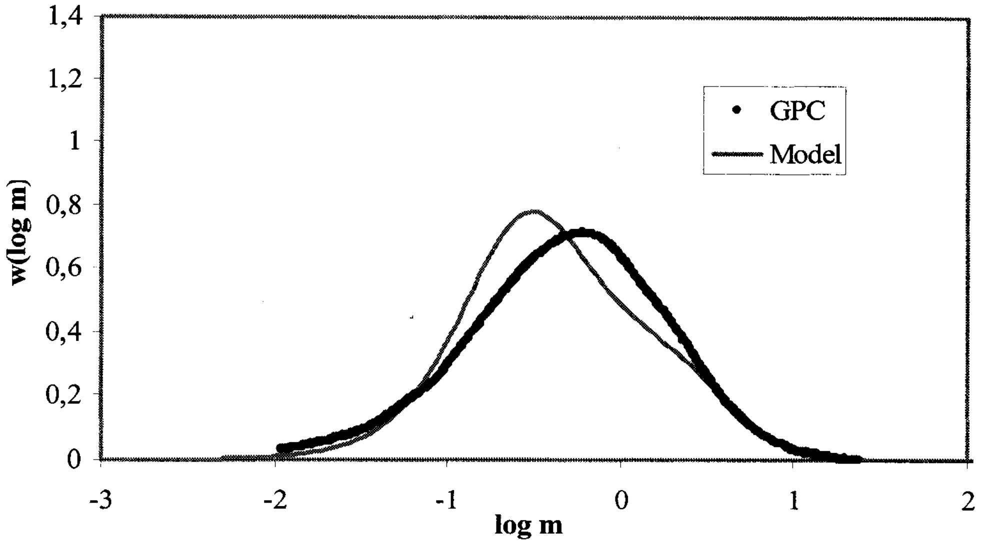

Figure 6.32 GPC and Viscosity Transform MWD for PP2

The modulus transform predictions are shown in Figs.6.33 and 6.34. The high MW tail for PP1 is well predicted, but the distribution is in general too broad; for PP2 this method fails completely, predicting a much broader distribution than GPC, although again the high molecular weight tail matches well that of the GPC curve. Wasserman's MWD predictions are too narrow and are also shifted to the right, once again because of the high values of the regularization parameters required to smooth the curves.

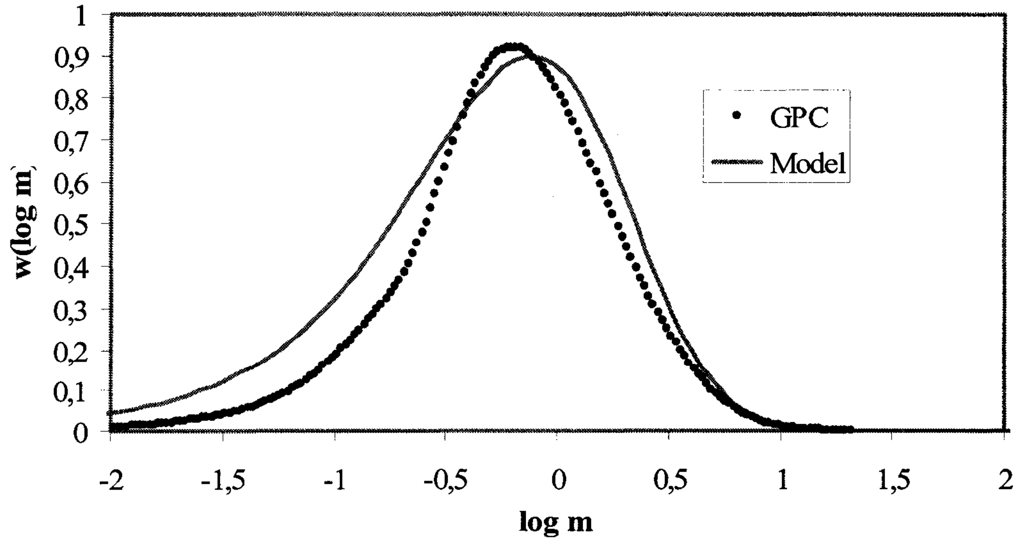

Figure 6.33 GPC and Modulus Transform MWD for PP1

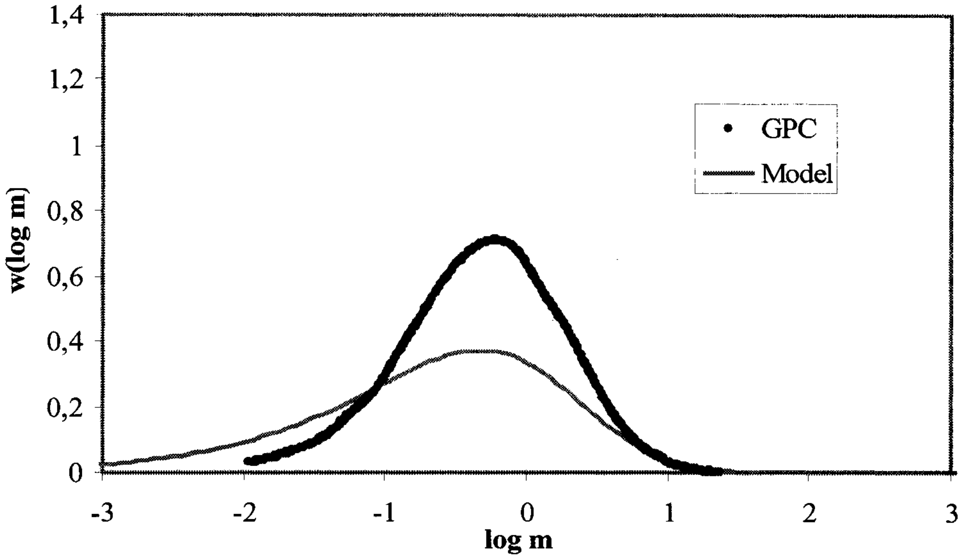

Figure 6.34 GPC and Modulus Transform MWD for PP2

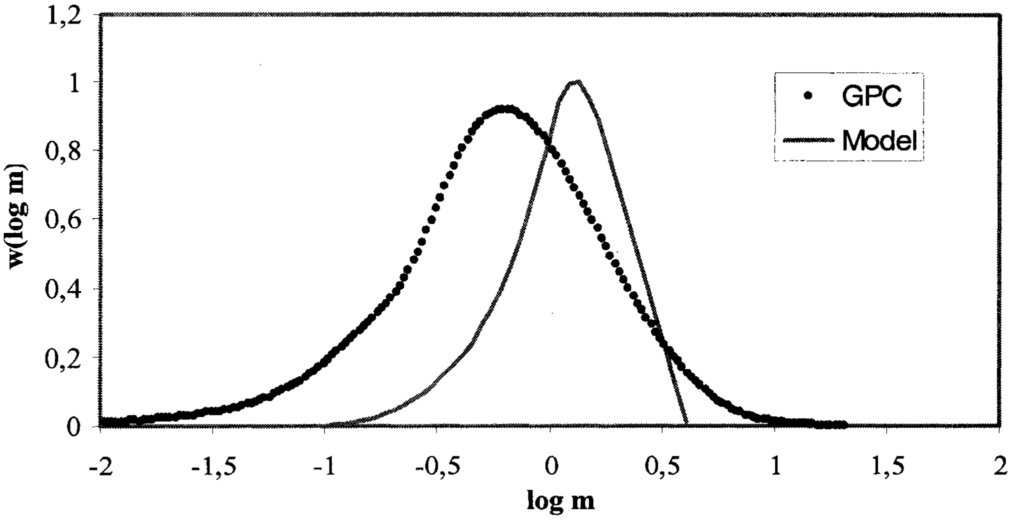

Figure 6.35 GPC and Wasserman's MWD for PP1

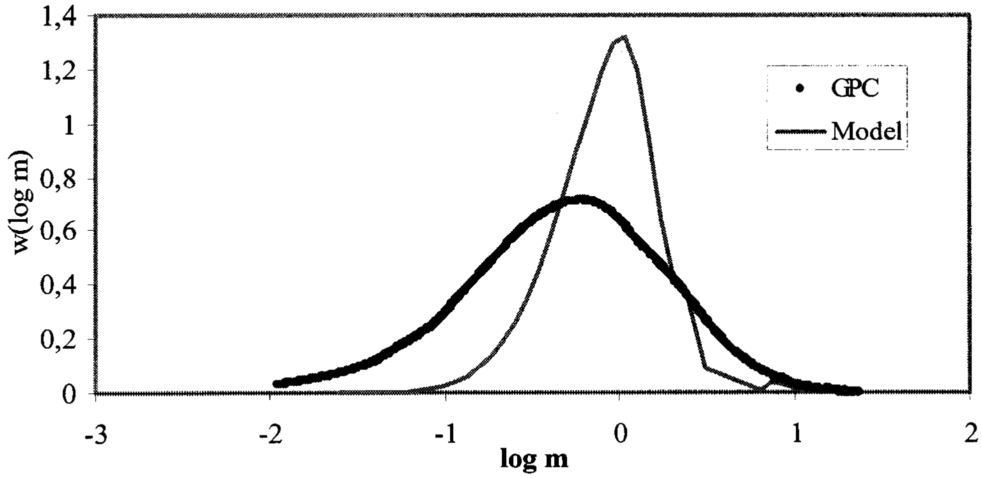

Figure 6.36 GPC and Wasserman's MWD for PP2

The TDD-DR predictions for PP1 and PP2 are shown in Figs.6.37 and 6.38. The DGEX parameters and the relative errors in dynamic moduli are presented in Table 6.9. The M_w/M_n values for PP1 and PP2 from all the methods along with the plateau modulus estimations are shown in Table 6.10. The MWD prediction for PP1 is good, with a very slight overestimation at the low molecular weight end and a polydispersity index very close to that from GPC. The high molecular weight portion this case is very well described.

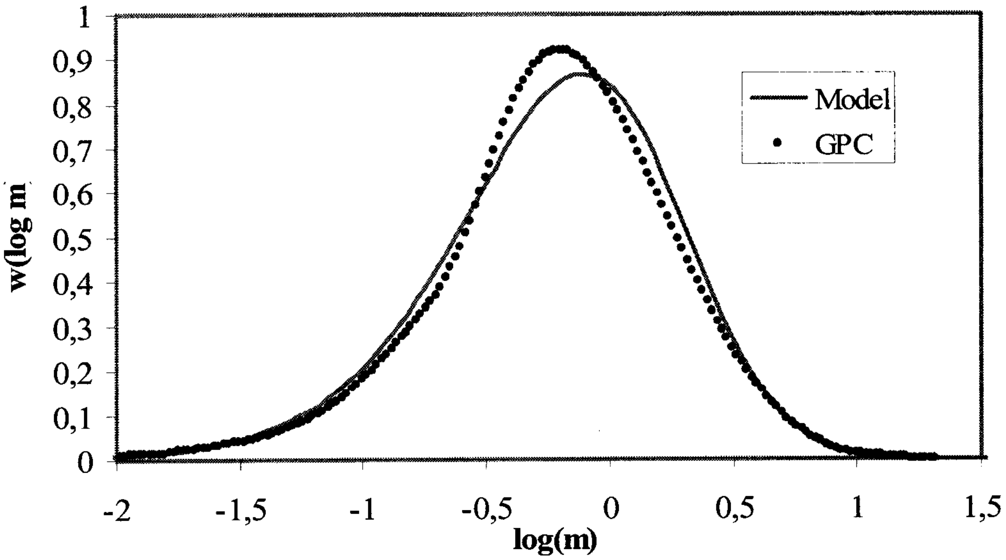

Figure 6.37 GPC and TDD-DR MWD for PP1

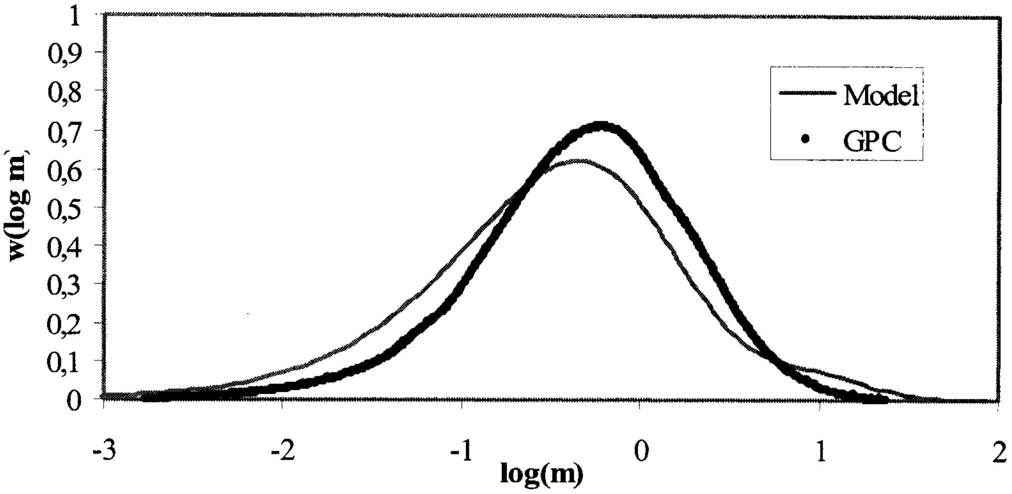

Figure 6.38 GPC and TDD-DR MWD for PP2

The PP2 prediction appears to be shifted to the right, although this method provides the best estimation of the breadth and the shape for this polymer, which has the highest polydispersity of the materials used in this study. This shift may be caused by the fact that the minimization of the dynamic data for PP2 was not as good as for PP1, with a relative error in dynamic data of 10.6% compared to less than 1% for PP1. Another explanation for this shift may be the use of polyethylene M^* and K_{TDD} parameters, since these were not available for polypropylene. The calculated and experimental dynamic data for PP1 and PP2 are presented in Figs.6.39 and 6.40. The evolution of the M_w and M_n values during the minimization procedure for PP2 (Fig.6.41) shows that the technique used is not able to minimize the objective function any further. The MWD prediction for PP2 shows that the TDD-DR model may be better able to predict MWD for samples with very broad distributions (M_w/M_n>6) than the other methods included in this study.

Table 6.9 DGEX parameters and Relative Errors on Dynamic Moduli for PP1 and PP2

Sample	a_1	b_1	M_{o1}	a_2	b_2	M_{o2}	p	χ %
PP1	0.733	0.867	158,190	0.690	0.582	15,397	0.0457	0.74
PP2	0.715	0.655	182,802	$9.9\text{x}10^{-6}$	0.552	17,417	0.054	10.67

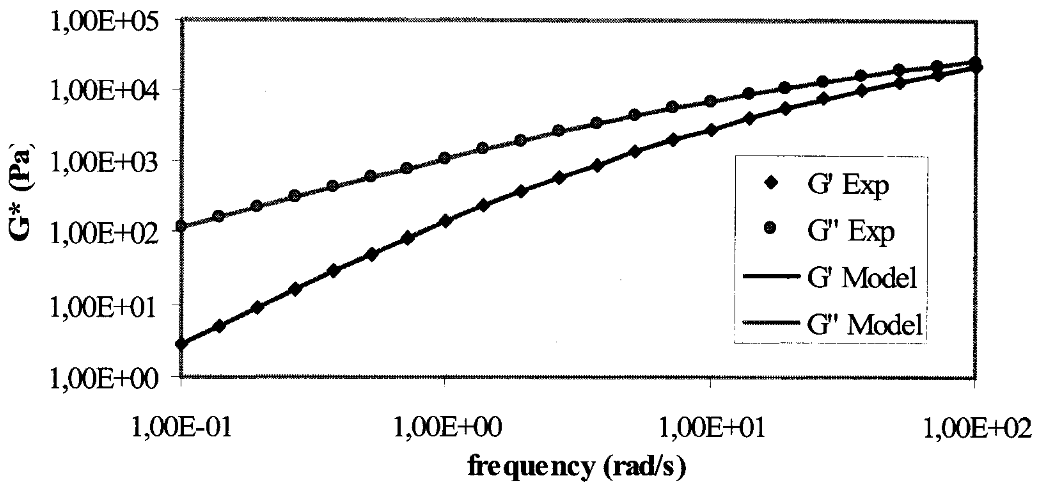

Figure 6.39 Experimental and Predicted Dynamic Data for PP1 using the TDD-DR model at 180°C

Table 6.10 M_w/M_n for PP1 and PP2

Sample	**GPC**	**Viscosity**	**Modulus**	G_N^o **(Pa)**	**Wasserman**	**TDD-DR**
PP1	3.61	2.92	8.6	$2.33\text{x}10^5$	1.30	3.56
PP2	6.43	5.19	310	$1.86\text{x}10^6$	1.58	7.70

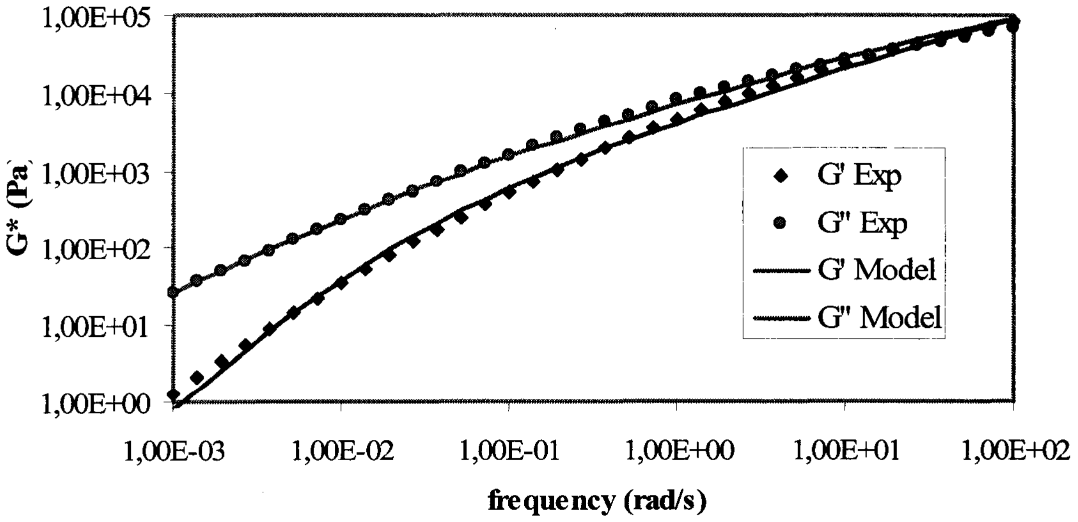

Figure 6.40 Experimental and Predicted Dynamic Data for PP2 using the TDD-DR model at 180°C

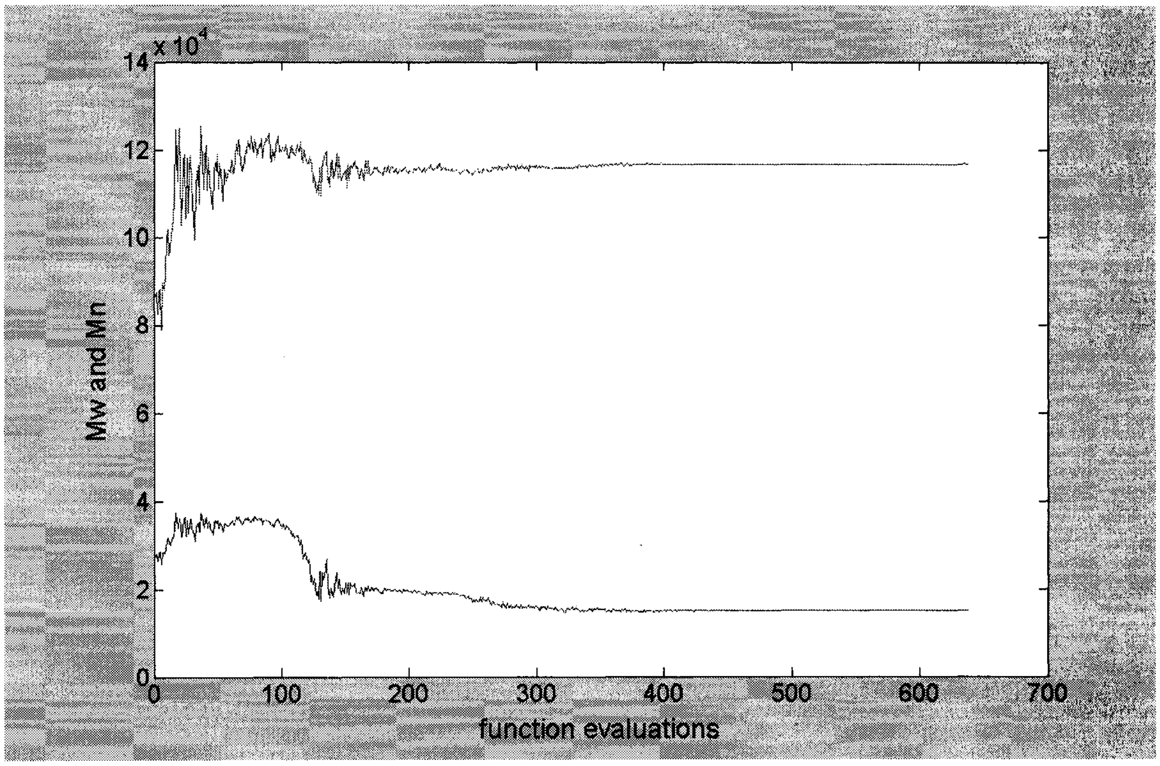

Figure 6.41 Evolution of function evaluations during Nelder-Mead iterations for PP2

7. CONCLUSIONS

Overall, the viscosity transform still represents the best rheological tool in MWD determination for linear entangled polyethylenes and polypropylenes of moderate polydispersities. This method is excellent both qualitatively and quantitatively for polydispersities up to 4.5 but fails at higher values of M_w/M_n. The modulus transform, on the other hand, is a useful technique as long as the polymer has a narrow distribution, and its accuracy is not affected by the presence of components with high molecular weights. The disadvantage of this method is the fact that the experimental data are only used to determine fitting model parameters but are not directly involved in the MWD determination. Moreover, extrapolations of the model at low and high frequencies are required, and this makes the reliability of the predictions very dependent of the range of the experimental data and the accuracy of the fitting procedures. These two methods were not able to deal with polymers with low values of weight average molecular weight, and in this case the TDD-DR model proved to be more useful. The simplicity of Wasserman's technique does not translate into good MWD predictions for any of the polymers studied, and its use depends on many parameters, especially the regularization parameter, which has an important effect on the results but whose determination is not straightforward.

The TDD-DR technique differs from the other techniques mainly in that the MWD is established *a priori* in order to solve the inversion problem. The DGEX function proved to be a good option, and the TDD-DR model appears to work well for all the polydispersities up to six. The disadvantage of this method is the sensitivity of the MWD prediction to the minimization of the objective function relating calculated and experimental dynamic data. It was found that when the minimization is good the results can be excellent, but small discrepancies can lead to inaccurate MWD predictions.

REFERENCES

1. Benallal, A., G. Marin, J-P. Montfort, and C. Derail, "Linear viscoelasticity revisited: the relaxation function of monodisperse polymer melts", Macromolecules, 26, 7229-7236 (1993).
2. Bersted, B.H. "An empirical model relating the molecular weight distribution of high density to the shear dependence of the steady shear viscosity". J. Appl. Polym. Sci., 19, 2167-2177 (1975).
3. Bersted, B.H. "A model relating the elastic properties of high density polyethylene melts to the molecular weight distribution", J. Appl. Polym. Sci., 20, 2705-2714 (1976).
4. Bersted, B.H. and J.D. Slee, "A relationship between steady state shear melt viscosity and molecular weight distribution in polystyrene", J. Appl. Polym. Sci., 21, 2631-2644 (1977).
5. Carrot, C., P. Revenu, and J. Guillet, "Rheological behavior of degraded polypropylene melts: From MWD to dynamic moduli", J. Appl. Polym. Sci., 61, 1887-1897 (1996).
6. Carrot, C. and J. Guillet, "From dynamic moduli to MWD: A study of various polydisperse linear polymers", J. Rheol., 41, 1203-1220 (1997).
7. Dealy, J.M. and K.F. Wissbrun, Melt Rheology and its Role in Plastics Processing. Kluwer Academic Publishers, 1999.
8. Des Cloizeaux, J.,"Relaxation and viscosity anomaly of melts made of entangled polymers. Time dependent reptation", Macromolecules 23(1990) 4678-4687.
9. Doi, M., "Explanation for the 3.4 power law of viscosity of polymeric liquids on the basis of the tube model", J. Poly. Sci. Lett. Ed. 19, 265-273 (1981).
10. Ferry, J.D., Viscoelastic Poperties of Polymers 3rd Ed. John Wiley & Sons Inc., 1980.
11. Graessley, W.W., "Entangled linear, branched and network polymer systems-Molecular theories", Adv. Polym. Sci. 47, 67-117 (1982).
12. He, C. and P.M. Wood-Adams, "Linear viscoelastic characterization of high-melt-strength polypropylenes over a broad range of frequencies", 2002.

13. Honerkamp, J. and J. Weese, "Determination of the relaxation spectrum by a regularization method", Macromolecules 22, 4372 (1989).
14. Leonardi, F., "Determination of the MWD of polymer melts from linear viscoelastic data", Proc. XIIIth Inter. Cong. Rheol., 1, 245-247 (2000).
15. Leonardi, F., J-C. Majeste, A. Allal and G. Marin, "Rheological models based on the double reptation mixing rule: the effects of a polydisperse environment", J. Rheol. , 44, 675-692 (2000).
16. Leonardi, F., A. Allal, and G. Marin, "On the use of molecular models to derive the molecular weight distribution of linear polymers from viscoelastic measurements", submitted to J. Rheol. (2001).
17. Leonardi, F., A. Allal, and G. Marin, "Molecular weight distribution from viscoelastic data: the importance of tube renewal and Rouse modes", J. Rheol. 46(1), 209-224 (2002).
18. Liu, G., C. B. Park, and J. A. Lefas, "Rotational molding of low-density LLDPE foams", Annual Technical Conf., Society of Plastics Eng. (1998) 56th (vol. 2), 1822-1831.
19. Maier, D., A. Eckstein, Cr. Friedrich, and J. Honerkamp, "Evaluation of models combining rheological data with the MWD", J. Rheol., 42, 1153-1173 (1998a).
20. Malkin, A.Y. and A. E. Teishev, "Can the MWD of polymers be determined uniquely from the flow curve of its melt?", Polym. Sci. USSR, 29, 2449-2455 (1988).
21. Malkin, A.Y. and A. E. Teishev, "Flow curve molecular weight distribution: is the solution of the inverse problem possible?" , Polym. Eng. Sci., 31, 1590-1596 (1991).
22. McGrory, W.J. and W.H. Tuminello, "Determining the molecular weight distribution from stress relaxation processes of a melt", J. Rheol., 34, 867-890 (1990).
23. Mead, D.W., "Determination of MWD of linear flexible polymers from linear viscoelastic material functions", J. Rheol., 38, 1797-1827 (1994).

24. Mead, D.W., “Component predictions and relaxation spectrum of the double reptation mixing rule for polydisperse linear flexible polymers”, J. Rheol., 40,33-661 (1996).
25. Mighri, F., M. A. Huneault, and A. Ajji, “Rheology of EPR/PP blends”, J. Appl. Polymer Science , vol. 82, 2113-2127 (2001).
26. Shaw, M.T. and W.H. Tuminello, “A closer look at the MWD-Viscosity transform”, Polym. Eng. Sci., 34, 159-165 (1994).
27. Tuminello, W.H., “Molecular weight and molecular weight distribution from dynamic measurements of polymer melts”, Polym. Eng. And Sci., 26, 1339-1347 (1986).
28. van Ruymbeke, E. and R. Keunings, “Evaluation of reptation models for predicting the linear viscoelastic properties of entangled linear polymers”, Macromolecules 2002, 35, 2689-2699.
29. van Ruymbeke, E., R. Keunings and C. Bailly, “Determination of molecular weight distribution of entangled linear polymers from linear viscoelastic data”, J. Non-Newtonian Fluid Mech., 105(2002) 153-175.
30. Wasserman, S.H., “Calculating the molecular weight distribution from linear viscoelastic response of polymer melts”, J. Rheol., 39, 601-625 (1995)
31. Wood-Adams, P.M., “Determination of molecular weight distribution from rheological data”. Master’s Thesis, Department of Chemical Engineering, McGill University, March 1995.
32. Wood-Adams, P.M. and J.M. Dealy, “Use of rheological measurements to estimate molecular weight distribution of linear polyethylene”, J. Rheol., 761-778 (1996).
33. Wood-Adams, P.M., “The effect of long chain branching on the rheological behavior of polyethylenes synthesized using constrained geometry and metallocene catalysts”. Master’s Thesis, Department of Chemical Engineering, McGill University, October 1998.
34. Wood-Adams, P.M. and S. Costeux, “Thermomorheological behavior of polyethylene: effects of microstructure and long chain branching”, Macromolecules 2001, 34, 6281-6290.

35. Wu, S., “Polymer Molecular Weight Distribution from Dynamic Melt Viscoelasticity”, Polym. Sci. Eng., 25,122-128 (1985).

Appendix A. Relaxation Functions for Modulus Models

1. Single Exponential Function (Tsenoglou):

$$F(t,M) = \exp\left[-t/\tau_o(M)\right]$$

2. Step Function (Tuminello):

$F(t,M) = 1$ when $t<\tau_o(M)$

$F(t,M) = 0$ when $t \geq \tau_o(M)$

3. BSW Function (Baumgaertel, Schausberger, and Winter):

$$F(t,M) = \frac{\alpha}{\lambda^{\alpha}} \int_0^{\lambda} u^{(\alpha-1)} \exp\left(-t/u\right) du$$

$$J_e^o G_N^o = \frac{(1+\alpha)^2}{\alpha(2+\alpha)}$$

$$\eta_o(M) / G_N^o = \frac{\alpha}{1+\alpha}\lambda(M)$$

Wasserman and Graessley (Effect of constraint release) assumed $J_e^o G_N^o = 1.7$, which gives $\alpha = 0.56$.

4. Des Cloizeaux Function

$$F(t,M) = \left[\frac{8}{\pi^2}\sum_{n=0}^{\infty}\frac{1}{(2n+1)^2}\exp\left\{-(2n+1)^2\left[\frac{t}{\tau}+\frac{M^*}{M}g\left(\frac{tm}{\tau M^*}\right)\right]\right\}\right]^2$$

$$g(t) = \sum_{m=0}^{\infty}\frac{1-\exp\left(-m^2 y\right)}{m^2}$$

$$\tau(M) = \frac{\eta^*}{G_N^o}\left(\frac{M}{M^*}\right)^3$$

5. Original Doi-Edwards modulus:

$$F(t,M) = \frac{8}{\pi^2}\sum_{n=1(odd)}^{\infty}\frac{e^{-t_n^2/\tau_o(M)}}{n^2}$$

Appendix B. Linear Viscoelastic Data

HDL1 Data at 150°C			
ω (rad/sec)	G' (Pa)	G" (Pa)	η (Pa-sec)
0,036	2,38	208,54	5793,02
0,050	4,36	289,10	5782,56
0,069	6,88	401,03	5773,07
0,097	12,45	554,67	5747,31
0,134	20,46	767,82	5726,21
0,186	34,68	1061,23	5696,87
0,259	58,35	1464,11	5657,86
0,360	96,97	2017,64	5613,39
0,500	170,59	2783,75	5577,96
0,695	278,90	3821,83	5515,66
0,965	456,59	5238,58	5447,20
1,341	742,63	7154,93	5362,83
1,864	1205,12	9737,47	5264,40
2,590	1944,95	13184,96	5146,36
3,598	3111,09	17757,54	5010,02
5,000	4927,41	23742,80	4849,75
6,948	7699,11	31440,48	4659,14
9,654	11845,42	41193,44	4440,10
13,414	17946,66	53364,62	4197,36
18,638	26574,80	68067,94	3920,54
25,898	38625,32	85576,72	3625,45
35,984	54862,06	105719,80	3309,98
50,000	76227,32	128241,40	2983,73
69,475	103307,60	152663,60	2653,25
96,535	136849,80	178219,60	2327,65
134,137	177005,80	203913,80	2013,04
186,383	223578,60	228891,40	1716,72
258,977	276050,80	252129,80	1443,62
359,844	333376,20	273823,40	1198,90
500,000	394078,60	293604,60	982,86

LDL1 Data at 130°C			
ω (rad/sec)	G' (Pa)	G" (Pa)	η (Pa-sec)
0,019	8,35	370,66	19861,55
0,026	13,66	511,43	19742,25
0,036	23,36	702,91	19549,98
0,050	41,76	973,43	19482,02
0,069	66,61	1339,00	19300,32
0,097	108,04	1837,43	19072,95
0,134	168,21	2518,36	18829,52
0,186	264,37	3447,92	18573,05
0,259	421,38	4719,46	18314,35
0,360	668,96	6445,46	18028,45
0,500	1094,56	8794,68	17741,67
0,695	1749,78	11913,92	17351,22
0,965	2807,47	16067,72	16916,58
1,341	4473,44	21496,06	16388,33
1,864	7055,34	28495,80	15769,45
2,590	10972,82	37313,40	15034,97
3,598	16708,80	48225,44	14199,38
5,000	24959,50	61251,70	13243,38
6,948	36253,32	76575,54	12209,22
9,654	51452,70	94024,02	11114,38
13,414	71327,20	113191,00	9983,69
18,638	96251,40	133512,80	8838,65
25,898	126906,60	154332,20	7721,31
35,984	163294,60	174662,20	6649,64
50,000	205570,20	193420,80	5648,26
69,475	253381,80	209628,60	4734,44
96,535	306310,00	221996,40	3920,95
134,137	363773,60	229448,40	3207,93
186,383	424842,40	230353,20	2594,08
258,977	488971,00	223223,40	2076,38
359,844	555279,40	206226,60	1646,74
500,000	623393,80	176536,00	1296,48

HDL2 Data at 150°C

ω (rad/sec)	G' (Pa)	G" (Pa)	η (Pa-sec)
0,695	3,05	211,78	304,87
0,965	5,14	293,25	303,84
1,341	7,94	405,69	302,51
1,864	12,21	561,62	301,42
2,590	19,65	776,33	299,88
3,000	26,21	899,32	299,91
4,168	41,40	1243,71	298,54
5,000	55,91	1488,91	298,00
6,948	91,49	2054,44	296,01
9,654	150,85	2835,91	294,19
13,414	248,63	3906,45	291,83
18,638	421,24	5368,03	288,90
25,898	708,78	7362,14	285,60
35,984	1189,85	10056,17	281,41
50,000	1994,54	13673,13	276,36
69,475	3313,69	18453,83	269,87
96,535	5460,73	24709,47	262,14
134,137	8894,71	32721,77	252,79
186,383	14278,77	42706,10	241,60
258,977	22529,57	54665,67	228,30
359,844	34905,47	68386,17	213,36
500,000	52937,13	82549,10	196,13

HDL4 Data at 150°C

ω (rad/sec)	G' (Pa)	G" (Pa)	η (Pa-sec)
0,036	4288,91	18083,06	517050,35
0,050	5961,01	24092,69	496963,71
0,069	8505,55	31900,02	475775,77
0,096	12188,13	41900,69	452602,35
0,134	17413,00	54732,10	428743,93
0,186	25046,59	71153,21	405265,77
0,259	36484,97	91547,58	381063,16
0,359	53104,13	115535,81	353864,07
0,499	75519,04	142457,22	322941,87
0,694	103992,87	172503,01	290358,07
0,964	140159,83	206413,39	258854,89
1,339	187187,23	242936,06	229001,52
1,861	246487,64	277523,49	199475,37
2,585	314666,22	305881,23	169733,45
3,592	386615,25	328953,97	141307,94
4,991	462128,10	351036,09	116268,96
6,935	545947,44	372134,63	95270,61
9,636	639813,95	385286,16	77508,30
13,389	736652,91	383961,29	62046,54
18,603	826259,25	370883,53	48685,84
25,847	906000,94	355401,40	37652,74
35,913	982229,81	342844,73	28968,48
49,899	1061820,69	328937,05	22277,11

LLDPE1 Data at 150°C			
ω (rad/sec)	G' (Pa)	G" (Pa)	η (Pa-sec)
0,018	231,76	884,73	50900,22
0,023	303,41	1092,40	48854,70
0,030	399,71	1342,98	46750,30
0,039	514,29	1644,64	44515,46
0,050	660,30	2010,36	42320,22
0,065	850,34	2452,44	40195,12
0,083	1082,37	2981,00	38025,44
0,108	1377,93	3611,40	35884,18
0,139	1745,35	4366,49	33800,52
0,180	2201,38	5265,39	31762,28
0,232	2767,62	6330,07	29770,54
0,300	3466,73	7578,08	27803,86
0,387	4326,76	9046,12	25904,44
0,500	5383,87	10769,52	24080,58
0,646	6677,05	12768,06	22312,32
0,834	8252,35	15092,64	20624,48
1,077	10149,88	17762,02	18991,76
1,391	12440,76	20828,86	17439,10
1,797	15190,34	24322,86	15959,98
2,321	18507,78	28294,00	14569,22
2,997	22425,42	32769,08	13248,62
3,871	27060,24	37765,52	12002,22
4,999	32532,36	43353,18	10841,70
6,457	38934,42	49503,20	9753,86
8,339	46410,92	56256,76	8745,29
10,771	55063,18	63608,74	7811,24
13,910	64975,76	71505,28	6945,67
17,966	76420,10	79893,16	6153,77
23,204	89471,26	88820,96	5433,31
29,968	104178,00	98061,38	4774,06
38,705	120792,80	107564,40	4178,88
49,989	139407,00	117160,80	3642,82
64,563	159992,80	126801,40	3162,02
83,385	182898,60	136038,00	2733,64
107,693	208041,20	144518,60	2352,16
139,090	235521,80	152036,40	2015,47
179,641	265652,80	157936,40	1720,41
232,012	298160,60	161518,00	1461,56
299,648	333244,80	162130,80	1236,76
387,008	370877,80	158584,60	1042,25
500,000	410466,00	149869,00	873,94

LLDPE2 Data at 150°C			
ω (rad/sec)	G' (Pa)	G" (Pa)	η (Pa-sec)
0,018	76,42	665,12	37260,06
0,023	106,74	841,24	36540,70
0,030	149,38	1065,37	35893,32
0,039	208,29	1339,04	35007,96
0,050	286,74	1678,99	34065,94
0,065	395,80	2106,33	33188,28
0,083	540,43	2628,47	32174,70
0,108	731,72	3271,50	31121,54
0,139	989,64	4062,31	30053,58
0,180	1325,94	5020,36	28898,70
0,232	1770,02	6184,92	27721,82
0,300	2347,16	7583,78	26486,98
0,387	3093,77	9261,96	25226,08
0,500	4053,15	11263,44	23941,04
0,646	5283,31	13618,88	22620,80
0,834	6832,86	16381,58	21281,62
1,077	8784,12	19608,96	19947,10
1,391	11206,46	23353,06	18618,94
1,797	14211,54	27628,64	17291,72
2,321	17910,94	32513,90	15996,12
2,997	22393,74	38029,70	14725,14
3,871	27817,10	44170,24	13485,14
4,999	34258,72	50985,24	12286,72
6,457	41953,02	58444,92	11142,10
8,339	50980,46	66535,80	10051,31
10,771	61480,04	75229,20	9020,54
13,910	73701,24	84435,64	8057,08
17,966	87519,38	94050,38	7150,94
23,204	103367,20	103994,80	6319,19
29,968	121105,20	114041,80	5550,85
38,705	140942,40	124138,80	4852,53
49,989	162899,00	134015,60	4219,74
64,563	187095,80	143464,00	3651,80
83,385	213473,80	152127,00	3143,66
107,693	242163,60	159663,40	2693,40
139,090	273023,80	165589,40	2295,75
179,641	306283,20	169490,40	1948,63
232,012	341614,00	170549,80	1645,70
299,648	378958,00	168168,60	1383,61
387,008	418649,80	161316,20	1159,29
500,000	459548,60	149212,80	966,33

PP1 Data at 180°C			
ω (rad/sec)	G' (Pa)	G" (Pa)	η (Pa-sec)
0,100	2,89	113,48	1135,14
0,139	5,18	157,72	1135,70
0,193	9,28	218,12	1130,77
0,268	16,52	301,97	1127,32
0,373	28,90	416,14	1119,05
0,518	49,72	571,17	1106,92
0,720	84,74	781,57	1092,34
1,000	140,99	1058,63	1067,98
1,390	230,43	1432,00	1043,84
1,931	370,66	1916,13	1010,85
2,683	581,22	2547,97	974,17
3,728	893,98	3349,10	929,92
5,180	1348,73	4356,10	880,42
7,197	1994,10	5598,77	825,81
10,000	2885,27	7106,80	767,02
13,895	4090,73	8917,50	706,08
19,307	5690,23	11024,67	642,59
26,827	7766,57	13461,00	579,30
37,276	10392,33	16201,67	516,37
51,795	13668,67	19265,33	456,06
71,969	17664,00	22581,67	398,36
100,000	22426,33	26075,33	343,93

PP2 Data at 180°C			
ω (rad/sec)	G' (Pa)	G" (Pa)	η (Pa-sec)
0,001	1,29	26,41	26441,75
0,001	2,15	36,34	26199,30
0,002	3,53	49,88	25901,34
0,003	5,72	68,28	25542,23
0,004	9,14	93,18	25117,53
0,005	14,43	126,72	24623,80
0,007	22,51	171,67	24058,34
0,010	34,74	231,60	23418,86
0,014	53,02	310,98	22703,89
0,019	80,01	415,45	21913,53
0,027	119,37	551,95	21050,24
0,037	176,05	729,00	20119,10
0,052	256,62	956,90	19127,59
0,072	369,79	1247,93	18085,16
0,100	526,85	1616,58	17002,66
0,139	742,34	2079,64	15891,83
0,193	1034,69	2656,22	14764,78
0,268	1426,95	3367,63	13633,56
0,373	1947,45	4237,04	12509,84
0,518	2630,46	5288,97	11404,60
0,720	3516,50	6548,49	10328,03
1,000	4652,38	8040,39	9289,37
1,389	6090,70	9788,27	8296,92
1,931	7888,96	11814,05	7357,91
2,683	10108,19	14137,97	6478,49
3,728	12811,64	16779,40	5663,52
5,179	16063,66	19758,52	4916,42
7,197	19929,31	23098,66	4239,04
10,000	24474,74	26829,08	3631,55
13,895	29768,42	30987,95	3092,48
19,307	35883,11	35625,38	2618,97
26,827	42898,31	40806,34	2206,98
37,276	50903,13	46613,77	1851,64
51,795	59999,21	53151,98	1547,58
71,969	70303,79	60550,79	1289,24
100,000	81952,82	68970,88	1071,13

HDL1 Data at 150°C		LDL1 Data at 130°C		HDL2 Data at 150°C	
H (Pa)	λ (sec)	H (Pa)	λ (sec)	H (Pa)	λ (sec)
4,276E+05	1,000E-06	1,325E+01	1,000E-06	2,860E+03	1,000E-06
3,991E+05	2,031E-06	3,162E+01	2,031E-06	3,877E+03	1,604E-06
3,725E+05	4,125E-06	7,541E+01	4,125E-06	5,254E+03	2,572E-06
3,477E+05	8,377E-06	1,799E+02	8,377E-06	7,121E+03	4,125E-06
3,245E+05	1,701E-05	4,291E+02	1,701E-05	9,651E+03	6,615E-06
3,030E+05	3,455E-05	1,023E+03	3,455E-05	1,308E+04	1,061E-05
2,830E+05	7,017E-05	2,441E+03	7,017E-05	1,771E+04	1,701E-05
2,646E+05	1,425E-04	5,821E+03	1,425E-04	2,397E+04	2,728E-05
2,476E+05	2,894E-04	1,386E+04	2,894E-04	3,237E+04	4,375E-05
2,319E+05	5,878E-04	3,280E+04	5,878E-04	4,354E+04	7,017E-05
2,164E+05	1,194E-03	7,547E+04	1,194E-03	5,803E+04	1,125E-04
1,968E+05	2,424E-03	1,550E+05	2,424E-03	7,590E+04	1,805E-04
1,642E+05	4,924E-03	2,261E+05	4,924E-03	9,550E+04	2,894E-04
1,145E+05	1,000E-02	1,985E+05	1,000E-02	1,113E+05	4,642E-04
6,392E+04	2,031E-02	1,373E+05	2,031E-02	1,128E+05	7,444E-04
2,894E+04	4,125E-02	9,199E+04	4,125E-02	9,128E+04	1,194E-03
1,095E+04	8,377E-02	5,516E+04	8,377E-02	5,525E+04	1,914E-03
3,745E+03	1,701E-01	2,571E+04	1,701E-01	2,566E+04	3,070E-03
1,252E+03	3,455E-01	8,968E+03	3,455E-01	1,030E+04	4,924E-03
4,111E+02	7,017E-01	2,602E+03	7,017E-01	4,053E+03	7,897E-03
1,271E+02	1,425E+00	7,856E+02	1,425E+00	1,677E+03	1,266E-02
3,785E+01	2,894E+00	2,949E+02	2,894E+00	7,420E+02	2,031E-02
1,151E+01	5,878E+00	1,312E+02	5,878E+00	3,461E+02	3,257E-02
3,546E+00	1,194E+01	5,180E+01	1,194E+01	1,662E+02	5,223E-02
1,068E+00	2,424E+01	1,488E+01	2,424E+01	8,065E+01	8,377E-02
3,138E-01	4,924E+01	3,538E+00	4,924E+01	3,934E+01	1,343E-01
9,118E-02	1,000E+02	7,974E-01	1,000E+02	1,945E+01	2,154E-01
2,640E-02	2,031E+02	1,775E-01	2,031E+02	9,902E+00	3,455E-01
7,633E-03	4,125E+02	3,941E-02	4,125E+02	5,229E+00	5,541E-01
2,207E-03	8,377E+02	8,745E-03	8,377E+02	2,839E+00	8,886E-01
6,379E-04	1,701E+03	1,940E-03	1,701E+03	1,557E+00	1,425E+00
1,844E-04	3,455E+03	4,304E-04	3,455E+03	8,530E-01	2,285E+00
5,330E-05	7,017E+03	9,549E-05	7,017E+03	4,656E-01	3,665E+00
1,541E-05	1,425E+04	2,119E-05	1,425E+04	2,534E-01	5,878E+00
4,454E-06	2,894E+04	4,700E-06	2,894E+04	1,377E-01	9,427E+00
1,287E-06	5,878E+04	1,043E-06	5,878E+04	7,474E-02	1,512E+01
3,722E-07	1,194E+05	2,313E-07	1,194E+05	4,055E-02	2,424E+01
1,076E-07	2,424E+05	5,132E-08	2,424E+05	2,200E-02	3,888E+01
3,110E-08	4,924E+05	1,139E-08	4,924E+05	1,193E-02	6,236E+01
8,989E-09	1,000E+06	2,526E-09	1,000E+06	6,472E-03	1,000E+02

HDL4 Data at 150°C		LLDPE1 Data at 150°C		LLDPE2 Data at 150°C	
H (Pa)	λ (sec)	H (Pa)	λ (sec)	H (Pa)	λ (sec)
89857,35	1,000E-03	1,455E+05	1,000E-03	8,043E+01	1,000E-06
141882,6	4,642E-03	1,489E+05	1,343E-03	1,628E+02	2,031E-06
220539,5	2,154E-02	1,515E+05	1,805E-03	3,294E+02	4,125E-06
302407,8	1,000E-01	1,518E+05	2,424E-03	6,667E+02	8,377E-06
209778,5	4,642E-01	1,483E+05	3,257E-03	1,349E+03	1,701E-05
54325,32	2,154E+00	1,402E+05	4,375E-03	2,731E+03	3,455E-05
6719,598	1,000E+01	1,282E+05	5,878E-03	5,525E+03	7,017E-05
1514,748	4,642E+01	1,140E+05	7,897E-03	1,117E+04	1,425E-04
415,59	2,154E+02	9,948E+04	1,061E-02	2,252E+04	2,894E-04
118,3515	1,000E+03	8,602E+04	1,425E-02	4,482E+04	5,878E-04
		7,425E+04	1,914E-02	8,523E+04	1,194E-03
		6,420E+04	2,572E-02	1,392E+05	2,424E-03
		5,560E+04	3,455E-02	1,588E+05	4,924E-03
		4,808E+04	4,642E-02	1,227E+05	1,000E-02
		4,134E+04	6,236E-02	8,582E+04	2,031E-02
		3,521E+04	8,377E-02	6,246E+04	4,125E-02
		2,963E+04	1,125E-01	4,371E+04	8,377E-02
		2,460E+04	1,512E-01	2,734E+04	1,701E-01
		2,017E+04	2,031E-01	1,549E+04	3,455E-01
		1,637E+04	2,728E-01	8,211E+03	7,017E-01
		1,318E+04	3,665E-01	4,108E+03	1,425E+00
		1,057E+04	4,924E-01	1,942E+03	2,894E+00
		8,463E+03	6,615E-01	8,705E+02	5,878E+00
		6,776E+03	8,886E-01	3,673E+02	1,194E+01
		5,423E+03	1,194E+00	1,445E+02	2,424E+01
		4,325E+03	1,604E+00	5,374E+01	4,924E+01
		3,422E+03	2,154E+00	1,936E+01	1,000E+02
		2,674E+03	2,894E+00	6,881E+00	2,031E+02
		2,056E+03	3,888E+00	2,432E+00	4,125E+02
		1,554E+03	5,223E+00	8,578E-01	8,377E+02
		1,160E+03	7,017E+00	3,023E-01	1,701E+03
		8,615E+02	9,427E+00	1,065E-01	3,455E+03
		6,446E+02	1,266E+01	3,754E-02	7,017E+03
		4,919E+02	1,701E+01	1,323E-02	1,425E+04
		3,868E+02	2,285E+01	4,660E-03	2,894E+04
		3,150E+02	3,070E+01	1,642E-03	5,878E+04
		2,656E+02	4,125E+01	5,785E-04	1,194E+05
		2,303E+02	5,541E+01	2,038E-04	2,424E+05
		2,031E+02	7,444E+01	7,181E-05	4,924E+05
		1,804E+02	1,000E+02	2,530E-05	1,000E+06

PP1 Data at 180°C		PP2 Data at 180°C	
H (Pa)	λ (sec)	H (Pa)	λ (sec)
1,196E+05	1,000E-06	1,706E+06	1,000E-06
1,060E+05	2,031E-06	1,256E+06	2,031E-06
9,385E+04	4,125E-06	9,251E+05	4,125E-06
8,312E+04	8,377E-06	6,814E+05	8,377E-06
7,359E+04	1,701E-05	5,019E+05	1,701E-05
6,511E+04	3,455E-05	3,699E+05	3,455E-05
5,751E+04	7,017E-05	2,728E+05	7,017E-05
5,066E+04	1,425E-04	2,014E+05	1,425E-04
4,438E+04	2,894E-04	1,489E+05	2,894E-04
3,849E+04	5,878E-04	1,104E+05	5,878E-04
3,279E+04	1,194E-03	8,225E+04	1,194E-03
2,707E+04	2,424E-03	6,164E+04	2,424E-03
2,120E+04	4,924E-03	4,659E+04	4,924E-03
1,528E+04	1,000E-02	3,556E+04	1,000E-02
9,826E+03	2,031E-02	2,731E+04	2,031E-02
5,548E+03	4,125E-02	2,084E+04	4,125E-02
2,762E+03	8,377E-02	1,543E+04	8,377E-02
1,211E+03	1,701E-01	1,079E+04	1,701E-01
4,553E+02	3,455E-01	7,022E+03	3,455E-01
1,416E+02	7,017E-01	4,254E+03	7,017E-01
3,656E+01	1,425E+00	2,415E+03	1,425E+00
8,297E+00	2,894E+00	1,294E+03	2,894E+00
1,777E+00	5,878E+00	6,564E+02	5,878E+00
3,743E-01	1,194E+01	3,133E+02	1,194E+01
7,858E-02	2,424E+01	1,392E+02	2,424E+01
1,649E-02	4,924E+01	5,770E+01	4,924E+01
3,458E-03	1,000E+02	2,256E+01	1,000E+02
7,255E-04	2,031E+02	8,195E+00	2,031E+02
1,522E-04	4,125E+02	2,687E+00	4,125E+02
3,192E-05	8,377E+02	8,029E-01	8,377E+02
6,697E-06	1,701E+03	2,286E-01	1,701E+03
1,405E-06	3,455E+03	6,401E-02	3,455E+03
2,947E-07	7,017E+03	1,784E-02	7,017E+03
6,182E-08	1,425E+04	4,963E-03	1,425E+04
1,297E-08	2,894E+04	1,381E-03	2,894E+04
2,720E-09	5,878E+04	3,840E-04	5,878E+04
5,706E-10	1,194E+05	1,068E-04	1,194E+05
1,197E-10	2,424E+05	2,970E-05	2,424E+05
2,511E-11	4,924E+05	8,259E-06	4,924E+05
5,267E-12	1,000E+06	2,297E-06	1,000E+06

Appendix C. Gel Permeation Chromatography Data

HDL1					
M	w(log m)	M	w(log m)	M	w(log m)
802411,23	0,0000	64991,57	1,0322	5366,02	0,0261
760305,27	0,0035	61588,98	1,0108	5095,80	0,0245
720475,14	0,0087	58363,99	0,9852	4839,49	0,0225
682791,33	0,0148	55307,88	0,9563	4596,38	0,0209
647130,70	0,0184	52411,91	0,9244	4365,73	0,0181
613373,49	0,0212	49667,58	0,8881	4146,89	0,0150
581414,69	0,0255	47067,16	0,8522	3939,25	0,0109
551151,51	0,0321	44603,30	0,8146	3742,19	0,0057
522487,61	0,0435	42268,81	0,7788	3555,16	0,0021
495336,12	0,0581	40056,96	0,7401	3377,64	0,0000
469611,80	0,0737	37961,47	0,7023		
445237,77	0,0876	35976,26	0,6627		
422137,56	0,1018	34095,50	0,6232		
400243,23	0,1202	32313,80	0,5819		
379491,45	0,1423	30626,05	0,5420		
359818,10	0,1666	29027,26	0,5034		
341167,77	0,1911	27512,75	0,4672		
323482,66	0,2184	26078,10	0,4331		
306714,99	0,2498	24719,18	0,4023		
290814,46	0,2840	23431,98	0,3760		
275736,34	0,3205	22212,68	0,3521		
261436,97	0,3584	21057,80	0,3285		
247875,73	0,3983	19963,84	0,3038		
235014,14	0,4399	18927,62	0,2804		
222815,81	0,4828	17946,10	0,2605		
211246,73	0,5281	17016,37	0,2419		
200274,20	0,5726	16135,67	0,2230		
189866,79	0,6178	15301,43	0,2030		
179996,47	0,6615	14511,16	0,1846		
170635,35	0,7066	13762,55	0,1690		
161756,97	0,7499	13053,35	0,1548		
153336,31	0,7928	12381,46	0,1429		
145350,66	0,8340	11744,97	0,1304		
137777,40	0,8744	11141,92	0,1181		
130595,44	0,9111	10570,51	0,1058		
123784,99	0,9436	10029,15	0,0963		
117326,47	0,9709	9516,14	0,0903		
111202,61	0,9959	9030,01	0,0835		
105395,97	1,0170	8569,31	0,0764		
99890,46	1,0362	8132,70	0,0682		
94670,35	1,0502	7718,89	0,0620		
89721,60	1,0612	7326,66	0,0570		
85029,96	1,0674	6954,85	0,0526		
80582,36	1,0699	6602,37	0,0478		
76366,34	1,0687	6268,20	0,0416		
72369,90	1,0617	5951,36	0,0351		
68581,82	1,0504	5650,93	0,0295		

LDL1					
M	w(log m)	M	w(log m)	M	w(log m)
720475,1	0,0000	58363,99	0,8425	4839,49	0,0281
682791,3	0,0063	55307,88	0,8122	4596,38	0,0249
647130,7	0,0163	52411,91	0,7798	4365,73	0,0226
613373,5	0,0317	49667,58	0,7450	4146,89	0,0203
581414,7	0,0467	47067,16	0,7089	3939,25	0,0187
551151,5	0,0640	44603,3	0,6739	3742,19	0,0171
522487,6	0,0820	42268,81	0,6401	3555,16	0,0156
495336,1	0,1013	40056,96	0,6069	3377,64	0,0132
469611,8	0,1235	37961,47	0,5735	3209,10	0,0100
445237,8	0,1499	35976,26	0,5404	3049,09	0,0061
422137,6	0,1801	34095,5	0,5081	2897,15	0,0026
400243,2	0,2115	32313,8	0,4761	2752,85	0,0007
379491,5	0,2450	30626,05	0,4441	2615,81	0,0000
359818,1	0,2813	29027,26	0,4125		
341167,8	0,3213	27512,75	0,3832		
323482,7	0,3627	26078,1	0,3572		
306715	0,4049	24719,18	0,3334		
290814,5	0,4486	23431,98	0,3099		
275736,3	0,4937	22212,68	0,2873		
261437	0,5396	21057,8	0,2672		
247875,7	0,5847	19963,84	0,2497		
235014,1	0,6278	18927,62	0,2330		
222815,8	0,6690	17946,1	0,2147		
211246,7	0,7086	17016,37	0,1972		
200274,2	0,7482	16135,67	0,1822		
189866,8	0,7869	15301,43	0,1707		
179996,5	0,8231	14511,16	0,1610		
170635,3	0,8535	13762,55	0,1509		
161757	0,8797	13053,35	0,1401		
153336,3	0,9029	12381,46	0,1292		
145350,7	0,9258	11744,97	0,1195		
137777,4	0,9455	11141,92	0,1120		
130595,4	0,9623	10570,51	0,1053		
123785	0,9749	10029,15	0,0981		
117326,5	0,9849	9516,144	0,0906		
111202,6	0,9927	9030,005	0,0826		
105396	0,9979	8569,313	0,0766		
99890,46	1,0012	8132,705	0,0713		
94670,35	1,0012	7718,893	0,0668		
89721,6	0,9978	7326,659	0,0618		
85029,96	0,9888	6954,854	0,0561		
80582,36	0,9751	6602,372	0,0508		
76366,34	0,9553	6268,202	0,0442		
72369,9	0,9345	5951,357	0,0400		
68581,82	0,9123	5650,931	0,0358		
64991,57	0,8924	5366,016	0,0339		
61588,98	0,8687	5095,796	0,0304		

HDL2			
M	w(log m)	M	w(log m)
270788,99	0,0000	21562,44	0,9265
256240,63	0,0030	20447,02	0,8889
242491,77	0,0087	19389,12	0,8501
229497,52	0,0180	18385,82	0,8087
217216,09	0,0298	17434,32	0,7637
205607,52	0,0421	16531,79	0,7180
194634,13	0,0564	15675,88	0,6724
184260,40	0,0690	14864,04	0,6308
174452,42	0,0856	14094,06	0,5894
165179,44	0,1014	13363,71	0,5483
156410,53	0,1208	12671,06	0,5066
148118,05	0,1420	12014,07	0,4687
140275,56	0,1695	11390,95	0,4333
132857,78	0,2029	10799,96	0,4014
125841,24	0,2403	10239,44	0,3691
119203,22	0,2795	9707,85	0,3420
112923,15	0,3187	9203,67	0,3172
106980,84	0,3598	8725,55	0,2968
101357,99	0,4073	8272,12	0,2736
96036,65	0,4605	7842,13	0,2527
91000,13	0,5204	7434,37	0,2316
86232,90	0,5802	7047,73	0,2119
81719,93	0,6425	6681,12	0,1907
77447,43	0,7038	6333,50	0,1726
73402,02	0,7686	6003,94	0,1586
69571,60	0,8310	5691,48	0,1464
65944,26	0,8926	5395,27	0,1325
62508,63	0,9499	5114,45	0,1190
59254,73	1,0078	4848,27	0,1093
56172,40	1,0639	4595,98	0,1013
53252,50	1,1179	4356,84	0,0928
50486,12	1,1638	4130,21	0,0820
47864,99	1,2008	3915,43	0,0749
45381,41	1,2263	3711,90	0,0687
43027,89	1,2437	3519,04	0,0666
40797,35	1,2526	3336,31	0,0617
38683,43	1,2569	3163,18	0,0582
36679,80	1,2553	2999,16	0,0500
34780,51	1,2482	2843,79	0,0456
32980,10	1,2328	2696,62	0,0414
31273,32	1,2088	2557,21	0,0384
29655,14	1,1760	2425,18	0,0310
28120,89	1,1379	2300,15	0,0227
26666,25	1,0964	2181,75	0,0180
25286,92	1,0532	2069,63	0,0147
23978,94	1,0088	1963,46	0,0096
22738,67	0,9660	1862,95	0,0037

HDL4					
M	w(log m)	M	w(log m)	M	w(log m)
2136825	0,0000	156410,53	0,7629	12671,06	0,0189
2022414	0,0060	148118,05	0,7202	12014,07	0,0177
1913837	0,0159	140275,56	0,6782	11390,95	0,0151
1810827	0,0297	132857,78	0,6364	10799,96	0,0088
1713141	0,0429	125841,24	0,5955	10239,44	0,0038
1620537	0,0568	119203,22	0,5533	9707,85	0,0000
1532777	0,0735	112923,15	0,5128		
1449633	0,0908	106980,84	0,4752		
1370879	0,1119	101357,99	0,4426		
1296313	0,1352	96036,65	0,4120		
1225722	0,1620	91000,13	0,3811		
1158911	0,1933	86232,90	0,3512		
1095696	0,2301	81719,93	0,3250		
1035888	0,2742	77447,43	0,3039		
979318,6	0,3229	73402,02	0,2852		
925818,8	0,3725	69571,60	0,2655		
875231,6	0,4240	65944,26	0,2457		
827402,8	0,4786	62508,63	0,2256		
782189,5	0,5353	59254,73	0,2085		
739452	0,5919	56172,40	0,1917		
699059,3	0,6442	53252,50	0,1755		
660886,7	0,6998	50486,12	0,1584		
624812,9	0,7571	47864,99	0,1441		
590728,6	0,8170	45381,41	0,1322		
558521,6	0,8734	43027,89	0,1225		
528091,3	0,9235	40797,35	0,1130		
499340,7	0,9676	38683,43	0,1050		
472179,4	1,0025	36679,80	0,0972		
446517	1,0312	34780,51	0,0881		
422273,7	1,0537	32980,10	0,0784		
399368,7	1,0709	31273,32	0,0696		
377729,6	1,0820	29655,14	0,0622		
357285,2	1,0866	28120,89	0,0556		
337970,7	1,0874	26666,25	0,0483		
319720,9	1,0841	25286,92	0,0432		
302478,1	1,0789	23978,94	0,0420		
286184,4	1,0713	22738,67	0,0443		
270789	1,0637	21562,44	0,0446		
256240,6	1,0526	20447,02	0,0395		
242491,8	1,0389	19389,12	0,0337		
229497,5	1,0175	18385,82	0,0303		
217216,1	0,9931	17434,32	0,0308		
205607,5	0,9607	16531,79	0,0324		
194634,1	0,9260	15675,88	0,0329		
184260,4	0,8857	14864,04	0,0325		
174452,4	0,8458	14094,06	0,0271		
165179,4	0,8045	13363,71	0,0228		

LLDPE1					
M	w(log m)	M	w(log m)	M	w(log m)
3634820,76	0,0000	267982,23	0,3672	21338,85	0,4999
3426951,83	0,0034	253768,08	0,3861	20257,55	0,4833
3232019,71	0,0087	240305,66	0,4033	19233,53	0,4654
3049109,35	0,0148	227557,42	0,4207	18263,63	0,4473
2877385,16	0,0194	215484,98	0,4388	17344,87	0,4270
2716070,26	0,0232	204052,07	0,4603	16474,57	0,4085
2564460,42	0,0271	193226,64	0,4806	15650,06	0,3874
2421904,42	0,0299	182975,10	0,5007	14868,87	0,3671
2287799,71	0,0324	173268,25	0,5164	14128,60	0,3450
2161583,42	0,0364	164076,36	0,5324	13427,09	0,3249
2042744,27	0,0392	155373,88	0,5486	12762,24	0,3051
1930803,16	0,0418	147134,32	0,5680	12131,96	0,2866
1825324,15	0,0412	139332,68	0,5876	11534,53	0,2687
1725885,58	0,0422	131946,84	0,6060	10968,06	0,2508
1632119,67	0,0428	124954,24	0,6234	10430,93	0,2343
1543671,90	0,0463	118334,67	0,6408	9921,52	0,2194
1460208,93	0,0504	112067,58	0,6589	9438,35	0,2066
1381427,19	0,0556	106135,34	0,6762	8980,01	0,1947
1307046,38	0,0594	100519,89	0,6913	8545,16	0,1834
1236798,64	0,0645	95203,96	0,7060	8132,50	0,1712
1170434,19	0,0711	90172,48	0,7211	7740,87	0,1597
1107732,76	0,0800	85410,05	0,7371	7369,14	0,1482
1048469,98	0,0890	80902,14	0,7522	7016,22	0,1377
992450,83	0,0981	76635,32	0,7651	6681,12	0,1249
939485,32	0,1078	72597,05	0,7761	6362,88	0,1132
889399,74	0,1168	68774,91	0,7856	6060,61	0,1035
842026,97	0,1256	65157,59	0,7919	5773,42	0,0973
797214,15	0,1332	61733,80	0,7958	5500,55	0,0908
754815,83	0,1418	58493,55	0,7968	5241,23	0,0826
714700,36	0,1531	55426,82	0,7989	4994,71	0,0744
676735,56	0,1656	52524,39	0,7984	4760,34	0,0667
640803,68	0,1770	49777,49	0,7956	4537,48	0,0623
606793,61	0,1841	47177,83	0,7891	4325,51	0,0572
574600,50	0,1911	44717,34	0,7802	4123,85	0,0529
544120,39	0,1987	42388,50	0,7708	3931,98	0,0463
515264,24	0,2079	40184,45	0,7593	3749,37	0,0416
487942,90	0,2158	38098,34	0,7454	3575,53	0,0394
462073,43	0,2277	36123,85	0,7281	3410,03	0,0377
437575,50	0,2416	34254,92	0,7074	3252,42	0,0351
414378,30	0,2571	32485,91	0,6877	3102,29	0,0292
392410,84	0,2683	30811,37	0,6642	2959,24	0,0247
371607,10	0,2795	29226,18	0,6397	2822,94	0,0190
351904,65	0,2906	27725,60	0,6104	2693,01	0,0138
333246,81	0,3045	26304,92	0,5847	2569,15	0,0068
315576,02	0,3166	24959,91	0,5605	2451,03	0,0025
298840,88	0,3315	23686,45	0,5393	2338,36	0,0000
282991,90	0,3475	22480,66	0,5186		

GPC Data for LLDPE2					
M	w(log m)	M	w(log m)	M	w(log m)
1825324	0,0000	139332,68	0,6609	11534,53	0,2052
1725886	0,0075	131946,84	0,6752	10968,06	0,1929
1632120	0,0163	124954,24	0,6895	10430,93	0,1802
1543672	0,0261	118334,67	0,7020	9921,52	0,1687
1460209	0,0289	112067,58	0,7134	9438,35	0,1569
1381427	0,0320	106135,34	0,7233	8980,01	0,1457
1307046	0,0376	100519,89	0,7343	8545,16	0,1357
1236799	0,0444	95203,96	0,7432	8132,50	0,1276
1170434	0,0514	90172,48	0,7501	7740,87	0,1193
1107733	0,0577	85410,05	0,7533	7369,14	0,1099
1048470	0,0648	80902,14	0,7565	7016,22	0,0969
992450,8	0,0735	76635,32	0,7602	6681,12	0,0855
939485,3	0,0804	72597,05	0,7626	6362,88	0,0759
889399,7	0,0891	68774,91	0,7624	6060,61	0,0701
842027	0,0989	65157,59	0,7597	5773,42	0,0642
797214,2	0,1123	61733,80	0,7567	5500,55	0,0580
754815,8	0,1263	58493,55	0,7521	5241,23	0,0519
714700,4	0,1394	55426,82	0,7474	4994,71	0,0463
676735,6	0,1533	52524,39	0,7410	4760,34	0,0409
640803,7	0,1658	49777,49	0,7328	4537,48	0,0368
606793,6	0,1821	47177,83	0,7193	4325,51	0,0337
574600,5	0,1968	44717,34	0,7007	4123,85	0,0321
544120,4	0,2119	42388,50	0,6815	3931,98	0,0303
515264,2	0,2244	40184,45	0,6636	3749,37	0,0278
487942,9	0,2387	38098,34	0,6490	3575,53	0,0234
462073,4	0,2547	36123,85	0,6317	3410,03	0,0189
437575,5	0,2706	34254,92	0,6127	3252,42	0,0108
414378,3	0,2866	32485,91	0,5879	3102,29	0,0050
392410,8	0,3035	30811,37	0,5612	2959,24	0,0000
371607,1	0,3223	29226,18	0,5335		
351904,6	0,3417	27725,60	0,5083		
333246,8	0,3612	26304,92	0,4863		
315576	0,3821	24959,91	0,4665		
298840,9	0,4023	23686,45	0,4483		
282991,9	0,4226	22480,66	0,4288		
267982,2	0,4419	21338,85	0,4091		
253768,1	0,4643	20257,55	0,3883		
240305,7	0,4875	19233,53	0,3686		
227557,4	0,5116	18263,63	0,3488		
215485	0,5331	17344,87	0,3297		
204052,1	0,5527	16474,57	0,3113		
193226,6	0,5705	15650,06	0,2955		
182975,1	0,5856	14868,87	0,2813		
173268,3	0,6010	14128,60	0,2669		
164076,4	0,6152	13427,09	0,2510		
155373,9	0,6313	12762,24	0,2342		
147134,3	0,6457	12131,96	0,2194		

GPC Data for PP1									
M	w(log m)	M	w(log m)	M	w(log m)	M	w(log m)	M	w(log m)
602,56	0,0000	5248,04	0,0358	45708,45	0,4772	398103,1	0,4218	3467326	0,0010
630,95	0,0006	5495,38	0,0383	47862,62	0,5048	416865,2	0,3984	3630736	0,0010
660,69	0,0006	5754,36	0,0401	50118,32	0,5347	436511,4	0,3752	3801847	0,0006
691,83	0,0011	6025,56	0,0421	52480,32	0,5677	457083,5	0,3536		
724,43	0,0016	6309,53	0,0438	54953,64	0,5995	478625,2	0,3317		
758,57	0,0025	6606,89	0,0461	57543,52	0,6317	501182,1	0,3116		
794,32	0,0031	6918,27	0,0487	60255,46	0,6643	524802	0,2916		
831,76	0,0028	7244,31	0,0525	63095,21	0,6959	549535,2	0,2719		
870,96	0,0029	7585,73	0,0554	66068,79	0,7278	575433,9	0,2521		
912,01	0,0030	7943,23	0,0592	69182,51	0,7565	602553,3	0,2350		
954,99	0,0030	8317,58	0,0631	72442,98	0,7855	630950,7	0,2178		
1000,00	0,0031	8709,58	0,0663	75857,11	0,8104	660686,5	0,2003		
1047,12	0,0039	9120,05	0,0713	79432,14	0,8333	691823,6	0,1844		
1096,47	0,0044	9549,86	0,0759	83175,66	0,8540	724428,2	0,1691		
1148,15	0,0044	9999,93	0,0802	87095,61	0,8714	758569,4	0,1550		
1202,26	0,0044	10471,22	0,0849	91200,29	0,8862	794319,7	0,1409		
1258,92	0,0049	10964,71	0,0908	95498,42	0,8988	831754,8	0,1276		
1318,25	0,0049	11481,46	0,0972	99999,12	0,9088	870954,1	0,1144		
1380,38	0,0053	12022,56	0,1032	104711,93	0,9155	912000,9	0,1026		
1445,43	0,0062	12589,17	0,1094	109646,85	0,9194	954982,1	0,0915		
1513,55	0,0066	13182,48	0,1170	114814,34	0,9205	999989	0,0826		
1584,89	0,0069	13803,75	0,1236	120225,37	0,9192	1047117	0,0729		
1659,58	0,0078	14454,30	0,1317	125891,41	0,9171	1096466	0,0654		
1737,79	0,0081	15135,51	0,1410	131824,48	0,9115	1148141	0,0574		
1819,69	0,0085	15848,82	0,1500	138037,17	0,9037	1202251	0,0497		
1905,45	0,0098	16595,75	0,1606	144542,66	0,8949	1258911	0,0434		
1995,25	0,0108	17377,88	0,1705	151354,74	0,8843	1318242	0,0384		
2089,29	0,0118	18196,88	0,1818	158487,86	0,8708	1380369	0,0314		
2187,75	0,0118	19054,47	0,1921	165957,15	0,8560	1445423	0,0273		
2290,86	0,0123	19952,48	0,2039	173778,46	0,8405	1513544	0,0235		
2398,82	0,0135	20892,81	0,2151	181968,38	0,8231	1584875	0,0195		
2511,87	0,0150	21877,46	0,2272	190544,28	0,8033	1659568	0,0174		
2630,25	0,0155	22908,51	0,2382	199524,35	0,7835	1737781	0,0156		
2754,21	0,0146	23988,15	0,2505	208927,63	0,7619	1819680	0,0137		
2884,02	0,0152	25118,68	0,2630	218774,08	0,7401	1905439	0,0115		
3019,94	0,0174	26302,48	0,2758	229084,57	0,7160	1995239	0,0099		
3162,26	0,0189	27542,08	0,2869	239880,98	0,6912	2089272	0,0081		
3311,29	0,0205	28840,10	0,2992	251186,22	0,6669	2187736	0,0069		
3467,35	0,0213	30199,29	0,3118	263024,25	0,6429	2290841	0,0070		
3630,76	0,0219	31622,53	0,3251	275420,19	0,6210	2398805	0,0052		
3801,87	0,0236	33112,86	0,3386	288400,33	0,5951	2511857	0,0037		
3981,05	0,0253	34673,42	0,3527	301992,20	0,5712	2630237	0,0038		
4168,67	0,0269	36307,52	0,3695	316224,64	0,5443	2754196	0,0034		
4365,13	0,0283	38018,64	0,3869	331127,83	0,5194	2883997	0,0023		
4570,86	0,0299	39810,40	0,4060	346733,39	0,4941	3019915	0,0020		
4786,27	0,0318	41686,61	0,4283	363074,42	0,4693	3162239	0,0016		
5011,84	0,0339	43651,23	0,4525	380185,57	0,4445	3311271	0,0013		

GPC Data for PP2									
M	w(log m)	M	w(log m)	M	w(log m)	M	w(log m)	M	w(log m)
8689796	0,0007	4613819	0,0177	2449692,81	0,0764	1304267,24	0,2264	686428,73	0,4501
8573528	0,0010	4552088	0,0184	2416916,51	0,0783	1280472,48	0,2311	675028,74	0,4562
8458817	0,0009	4491182	0,0194	2384578,76	0,0809	1261979,37	0,2361	667180,46	0,4598
8345640	0,0013	4431091	0,0209	2352673,67	0,0837	1246210,05	0,2407	657890,04	0,4635
8233977	0,0017	4371804	0,0234	2321195,47	0,0861	1237542,55	0,2445	653264,85	0,4669
8123808	0,0026	4313310	0,0215	2290138,44	0,0878	1228125,30	0,2479	642547,70	0,4705
8015114	0,0008	4255599	0,0206	2259496,95	0,0891	1205707,27	0,2529	632416,01	0,4747
7907874	0,0004	4198660	0,0230	2229265,43	0,0915	1189188,27	0,2577	624785,74	0,4773
7802068	0,0001	4142483	0,0248	2199438,40	0,0951	1177051,18	0,2612	619206,84	0,4810
7697678	0,0014	4087058	0,0244	2170010,45	0,0970	1154708,63	0,2670	612309,92	0,4847
7594685	0,0014	4032374	0,0253	2140976,23	0,0996	1142913,69	0,2716	605082,94	0,4874
7493070	0,0014	3978422	0,0259	2112330,49	0,1032	1127527,58	0,2766	600028,58	0,4905
7392815	0,0026	3925192	0,0263	2084068,02	0,1048	1110745,70	0,2819	591153,03	0,4953
7293901	0,0034	3872673	0,0274	2056183,70	0,1060	1096502,85	0,2871	579071,16	0,5007
7196310	0,0041	3820858	0,0284	2028672,46	0,1095	1080887,63	0,2919	571742,76	0,5041
7100025	0,0006	3769736	0,0286	2001529,32	0,1126	1067399,13	0,2960	568383,19	0,5055
7005029	0,0009	3719298	0,0303	1974749,34	0,1161	1050050,17	0,3014	562295,91	0,5070
6911303	0,0023	3669534	0,0306	1948327,68	0,1199	1036262,98	0,3059	557052,92	0,5108
6818831	0,0022	3620437	0,0314	1922259,53	0,1220	1022380,51	0,3111	550040,13	0,5155
6727597	0,0021	3571996	0,0330	1896540,16	0,1245	1008498,19	0,3166	542810,15	0,5194
6637584	0,0030	3524204	0,0358	1871164,92	0,1274	990978,85	0,3223	537143,06	0,5222
6548774	0,0040	3477051	0,0395	1846129,19	0,1299	981021,20	0,3272	528645,48	0,5251
6461153	0,0044	3430529	0,0405	1821428,43	0,1330	969711,01	0,3306	521049,32	0,5287
6374705	0,0047	3384629	0,0405	1797058,16	0,1363	954961,66	0,3357	515448,84	0,5328
6289413	0,0046	3339344	0,0420	1773013,96	0,1389	938871,99	0,3421	511882,54	0,5357
6205262	0,0052	3294664	0,0425	1749291,46	0,1439	927620,00	0,3470	506527,10	0,5381
6122237	0,0054	3250582	0,0445	1725886,37	0,1459	914891,70	0,3518	502240,53	0,5397
6040323	0,0055	3207090	0,0480	1702794,43	0,1483	902598,05	0,3571	496788,03	0,5444
5959505	0,0074	3164180	0,0498	1680011,45	0,1525	900999,23	0,3598	488525,88	0,5518
5879768	0,0099	3121844	0,0498	1657533,31	0,1567	882441,78	0,3658	482549,25	0,5524
5801098	0,0126	3080075	0,0497	1635355,91	0,1593	862878,67	0,3725	480911,29	0,5533
5723481	0,0133	3038864	0,0527	1613475,25	0,1629	851620,38	0,3769	475559,07	0,5585
5646902	0,0124	2998205	0,0538	1591887,34	0,1669	842184,33	0,3814	468459,38	0,5629
5571348	0,0108	2958090	0,0531	1570588,28	0,1700	832158,58	0,3856	463358,73	0,5669
5496805	0,0104	2918511	0,0528	1549574,19	0,1734	814948,37	0,3933	458972,94	0,5693
5423259	0,0099	2879462	0,0552	1528841,26	0,1771	804816,18	0,3976	454100,78	0,5725
5350697	0,0097	2840936	0,0580	1508385,74	0,1816	796617,62	0,4014	447876,12	0,5762
5279106	0,0095	2802925	0,0601	1488203,90	0,1857	781803,74	0,4076	443169,41	0,5796
5208473	0,0100	2765422	0,0619	1468292,10	0,1891	771916,70	0,4109	438356,45	0,5834
5138785	0,0112	2728421	0,0633	1448646,71	0,1938	763716,13	0,4152	432866,93	0,5882
5070029	0,0151	2691916	0,0650	1429264,17	0,1975	753739,54	0,4203	429251,36	0,5915
5002193	0,0164	2655899	0,0666	1410140,96	0,2025	744189,34	0,4249	424287,89	0,5956
4935265	0,0165	2620363	0,0680	1391273,62	0,2059	735259,02	0,4295	420016,57	0,5996
4869232	0,0153	2585304	0,0709	1372658,71	0,2089	727526,29	0,4333	415692,10	0,6015
4804083	0,0159	2550713	0,0727	1354292,87	0,2144	716271,78	0,4375	409961,61	0,6041
4739806	0,0159	2516585	0,0751	1336172,77	0,2183	701708,29	0,4427	405862,48	0,6086
4676388	0,0160	2482914	0,0755	1318295,10	0,2223	692447,47	0,4467	400207,20	0,6147

M	w(log m)	M	w(log m)	M	w(log m)	M	w(log m)	M	w(log m)
395839,66	0,6177	222783,93	0,7122	121955,25	0,6452	66961,54	0,4804	36451,48	0,2915
393969,41	0,6193	222531,01	0,7129	119670,72	0,6434	66100,70	0,4753	35982,87	0,2858
388411,81	0,6237	218676,68	0,7126	117804,83	0,6420	65250,93	0,4700	35520,29	0,2825
382717,74	0,6270	216030,00	0,7125	118316,08	0,6381	64412,08	0,4673	35063,65	0,2798
379841,19	0,6315	214554,77	0,7112	118254,02	0,6339	63584,02	0,4633	34612,88	0,2761
372469,96	0,6358	211605,31	0,7105	115302,53	0,6305	62766,60	0,4590	34167,91	0,2718
368714,38	0,6387	207128,88	0,7110	113820,23	0,6287	61959,69	0,4548	33728,65	0,2686
364799,32	0,6417	204565,76	0,7109	112356,99	0,6261	61163,15	0,4511	33295,05	0,2640
361252,68	0,6448	204462,52	0,7102	110912,56	0,6235	60376,86	0,4469	32867,02	0,2615
358438,57	0,6473	201671,64	0,7102	109486,70	0,6184	59600,67	0,4440	32444,49	0,2579
355202,24	0,6510	197868,82	0,7092	108079,17	0,6161	58834,46	0,4420	32027,39	0,2555
349300,65	0,6563	196500,41	0,7080	106689,73	0,6133	58078,10	0,4361	31615,66	0,2530
345652,87	0,6583	193983,50	0,7071	105318,16	0,6112	57331,47	0,4301	31209,21	0,2483
339971,28	0,6612	190096,24	0,7056	103964,22	0,6075	56594,43	0,4254	30808,00	0,2455
335205,65	0,6645	187075,86	0,7051	102627,68	0,6041	55866,87	0,4232	30411,94	0,2410
333740,50	0,6668	187342,05	0,7046	101308,33	0,6008	55148,66	0,4204	30020,97	0,2388
329469,34	0,6694	184841,16	0,7041	100005,94	0,5967	54439,68	0,4173	29635,03	0,2381
324575,47	0,6734	181016,49	0,7022	98720,29	0,5940	53739,82	0,4129	29254,05	0,2348
321580,50	0,6760	178853,27	0,7014	97451,17	0,5911	53048,96	0,4063	28877,97	0,2312
315075,28	0,6787	175869,64	0,7010	96198,37	0,5873	52366,97	0,4041	28506,72	0,2294
312205,64	0,6803	172585,22	0,7000	94961,67	0,5837	51693,76	0,4003	28140,25	0,2271
309588,87	0,6814	172019,75	0,6971	93740,87	0,5795	51029,20	0,3965	27778,48	0,2235
306404,79	0,6831	170996,00	0,6958	92535,76	0,5768	50373,18	0,3940	27421,37	0,2216
303141,67	0,6865	168685,13	0,6950	91346,15	0,5729	49725,60	0,3906	27068,85	0,2204
299095,46	0,6890	165104,85	0,6936	90171,83	0,5684	49086,34	0,3858	26720,86	0,2164
295715,37	0,6908	163570,01	0,6929	89012,60	0,5655	48455,30	0,3787	26377,34	0,2133
290897,60	0,6935	161629,60	0,6920	87868,28	0,5628	47832,37	0,3759	26038,24	0,2121
288307,64	0,6946	157303,39	0,6902	86738,67	0,5597	47217,45	0,3734	25703,50	0,2100
282847,48	0,6969	155596,07	0,6868	85623,58	0,5558	46610,44	0,3694	25373,07	0,2083
280559,30	0,6982	155039,14	0,6849	84522,83	0,5522	46011,23	0,3663	25046,88	0,2055
279234,03	0,6991	154235,10	0,6828	83436,23	0,5474	45419,72	0,3611	24724,88	0,2020
273975,06	0,7013	151675,08	0,6813	82363,60	0,5432	44835,82	0,3572	24407,03	0,2018
271031,59	0,7024	149295,45	0,6803	81304,75	0,5397	44259,42	0,3524	24093,26	0,2009
267122,90	0,7033	147620,84	0,6783	80259,52	0,5338	43690,43	0,3493	23783,52	0,1959
264498,92	0,7049	144127,18	0,6756	79227,73	0,5311	43128,76	0,3447	23477,77	0,1938
259778,73	0,7055	144018,41	0,6751	78209,20	0,5291	42574,31	0,3412	23175,94	0,1924
256537,79	0,7080	142402,51	0,6732	77203,76	0,5245	42026,99	0,3375	22878,00	0,1896
255441,00	0,7080	140826,93	0,6694	76211,25	0,5183	41486,70	0,3312	22583,89	0,1882
251469,89	0,7091	138999,72	0,6678	75231,50	0,5148	40953,36	0,3283	22293,55	0,1874
247496,23	0,7090	137411,53	0,6640	74264,35	0,5113	40426,87	0,3253	22006,95	0,1837
246223,74	0,7089	134548,15	0,6615	73309,63	0,5073	39907,16	0,3186	21724,04	0,1818
243258,20	0,7108	131808,16	0,6600	72367,18	0,5027	39394,12	0,3163	21444,76	0,1808
238208,49	0,7108	130491,45	0,6578	71436,85	0,4989	38887,68	0,3120	21169,07	0,1774
236581,53	0,7114	129863,01	0,6560	70518,47	0,4967	38387,75	0,3078	20896,93	0,1758
234550,51	0,7110	128648,71	0,6538	69611,91	0,4910	37894,25	0,3041	20628,28	0,1740
231441,17	0,7113	128310,30	0,6502	68717,00	0,4873	37407,09	0,2996	20363,09	0,1711
226427,05	0,7114	125742,86	0,6473	67833,59	0,4834	36926,20	0,2962	20101,31	0,1683

M	w(log m)	M	w(log m)	M	w(log m)	M	w(log m)	M	w(log m)
19842,89	0,1699	10801,77	0,0822	5880,10	0,0457	3200,92	0,0231	1742,47	0,0111
19587,80	0,1649	10662,90	0,0814	5804,51	0,0451	3159,77	0,0240	1720,06	0,0109
19335,98	0,1624	10525,82	0,0810	5729,88	0,0450	3119,15	0,0230	1697,95	0,0083
19087,41	0,1579	10390,51	0,0802	5656,22	0,0431	3079,05	0,0215	1676,12	0,0092
18842,02	0,1567	10256,93	0,0799	5583,51	0,0433	3039,46	0,0209	1654,58	0,0122
18599,80	0,1548	10125,07	0,0789	5511,73	0,0424	3000,39	0,0208	1633,30	0,0102
18360,68	0,1527	9994,90	0,0771	5440,87	0,0426	2961,82	0,0197	1612,31	0,0094
18124,64	0,1524	9866,41	0,0762	5370,92	0,0408	2923,74	0,0197	1591,58	0,0086
17891,64	0,1513	9739,57	0,0759	5301,88	0,0406	2886,15	0,0215	1571,12	0,0084
17661,63	0,1488	9614,36	0,0752	5233,72	0,0405	2849,05	0,0216	1550,92	0,0099
17434,57	0,1414	9490,76	0,0750	5166,43	0,0398	2812,42	0,0195	1530,98	0,0103
17210,44	0,1395	9368,75	0,0728	5100,02	0,0399	2776,27	0,0196	1511,30	0,0115
16989,19	0,1380	9248,31	0,0730	5034,45	0,0377	2740,58	0,0194	1491,87	0,0064
16770,78	0,1384	9129,42	0,0742	4969,73	0,0370	2705,34	0,0192	1472,69	0,0059
16555,18	0,1363	9012,05	0,0708	4905,84	0,0368	2670,57	0,0192	1453,76	0,0101
16342,35	0,1331	8896,19	0,0699	4842,77	0,0376	2636,23	0,0202	1435,07	0,0094
16132,26	0,1319	8781,83	0,0689	4780,52	0,0391	2602,34	0,0200	1416,62	0,0067
15924,87	0,1289	8668,93	0,0682	4719,06	0,0352	2568,89	0,0180	1398,41	0,0075
15720,14	0,1276	8557,49	0,0677	4658,39	0,0353	2535,86	0,0182	1380,43	0,0076
15518,05	0,1249	8447,47	0,0671	4598,50	0,0358	2503,26	0,0169	1362,69	0,0075
15318,55	0,1223	8338,87	0,0669	4539,39	0,0347	2471,08	0,0182	1345,17	0,0079
15121,62	0,1209	8231,67	0,0665	4481,03	0,0327	2439,31	0,0191	1327,88	0,0077
14927,22	0,1197	8125,85	0,0650	4423,42	0,0331	2407,95	0,0170	1310,80	0,0078
14735,32	0,1172	8021,38	0,0629	4366,56	0,0326	2377,00	0,0159	1293,95	0,0074
14545,89	0,1149	7918,26	0,0630	4310,42	0,0320	2346,44	0,0157	1277,32	0,0076
14358,89	0,1137	7816,47	0,0619	4255,01	0,0309	2316,28	0,0147	1260,90	0,0078
14174,30	0,1114	7715,98	0,0593	4200,31	0,0305	2286,50	0,0141	1244,69	0,0075
13992,07	0,1112	7616,79	0,0585	4146,31	0,0304	2257,10	0,0146	1228,69	0,0074
13812,20	0,1092	7518,87	0,0587	4093,01	0,0304	2228,09	0,0142	1212,89	0,0061
13634,63	0,1058	7422,21	0,0591	4040,39	0,0303	2199,44	0,0142	1197,30	0,0061
13459,35	0,1048	7326,79	0,0579	3988,44	0,0300	2171,17	0,0151	1181,91	0,0069
13286,32	0,1038	7232,60	0,0575	3937,17	0,0285	2143,26	0,0150	1166,71	0,0064
13115,51	0,1030	7139,62	0,0576	3886,56	0,0288	2115,70	0,0140	1151,71	0,0049
12946,90	0,1021	7047,83	0,0544	3836,59	0,0286	2088,50	0,0126	1136,91	0,0048
12780,46	0,0984	6957,23	0,0544	3787,27	0,0284	2061,65	0,0108	1122,29	0,0039
12616,16	0,0974	6867,79	0,0531	3738,58	0,0275	2035,15	0,0113	1107,86	0,0034
12453,97	0,0968	6779,50	0,0528	3690,52	0,0274	2008,99	0,0124	1093,62	0,0093
12293,87	0,0948	6692,34	0,0545	3643,07	0,0254	1983,16	0,0135	1079,56	0,0071
12135,82	0,0941	6606,31	0,0557	3596,24	0,0251	1957,67	0,0141	1065,68	0,0031
11979,80	0,0942	6521,38	0,0521	3550,01	0,0257	1932,50	0,0127	1051,98	0,0030
11825,79	0,0942	6437,54	0,0500	3504,37	0,0262	1907,65	0,0131	1038,46	0,0042
11673,77	0,0887	6354,78	0,0505	3459,32	0,0258	1883,13	0,0092	1025,11	0,0044
11523,69	0,0869	6273,09	0,0490	3414,85	0,0246	1858,92	0,0100	1011,93	0,0047
11375,55	0,0868	6192,44	0,0460	3370,95	0,0241	1835,02	0,0120	998,92	0,0043
11229,30	0,0868	6112,83	0,0464	3327,61	0,0240	1811,43	0,0124	986,08	0,0047
11084,94	0,0864	6034,25	0,0483	3284,83	0,0233	1788,15	0,0105	973,40	0,0048
10942,44	0,0833	5956,68	0,0457	3242,60	0,0234	1765,16	0,0112	960,89	0,0044

M	w(log m)
948,54	0,0036
936,34	0,0038
924,30	0,0037
912,42	0,0038
900,69	0,0040
889,11	0,0038
877,68	0,0028
866,40	0,0028
855,26	0,0035
844,27	0,0029
833,41	0,0024
822,70	0,0021
812,12	0,0021
801,68	0,0029
791,38	0,0023
781,20	0,0036
771,16	0,0038
761,25	0,0020
751,46	0,0024
741,80	0,0016
732,26	0,0020
722,85	0,0019
713,56	0,0020
704,38	0,0020
695,33	0,0018
686,39	0,0012
677,56	0,0014
668,85	0,0015
660,25	0,0003
651,77	0,0000
643,39	0,0014
635,12	0,0016
626,95	0,0018